Supporting Information

Cuproussiloxane of Self-Assemblies $Cu_{20}O_{20}Si_{10}Me_{10}R_{10}$ and $Cu_{24}O_{24}Si_{12}Me_{12}R_{12}$ and the Catalytic Property

Wenjun Jiang, Jinjin Wang, Yilin Chen, Zhikang Chen, Jiancheng Li, Liuyin Jiang,* Yanbo Peng, Hongping Zhu*

State Key Laboratory of Physical Chemistry of Solid Surfaces, National Engineering Laboratory for Green Chemical Productions of Alcohols, Ethers and Esters, College of Chemistry and Chemical Engineering , Xiamen University, Xiamen, Fujian, 361005, China.

Contents:

1. Experimental Section

Materials and Methods All manipulations were carried out under dry argon or nitrogen atmosphere by using Schlenk line and glovebox techniques. Organic solvents as toluene, benzene, and *n*-hexane were dried by refluxing with sodium/potassium benzophenone under N_2 prior to use. Dichloromethane was dried over CaH_2 under N_2 prior to use. NMR (^1H, ^{13}C, ^{29}Si, and ^{31}P) spectra were recorded on Bruker Avance II 400 or 500 spectrometers. The melting point of the compound was measured in a sealed glass tube using the Büchi-540 instrument. Elemental analysis was performed on a Thermo Quest Italia SPA EA 1110 instrument. Commercial reagents were purchased from *J&K* Chemical Co. and used as received. Compounds $R(Me)Si(OH)_2$ (R = $N(SiMe_3)(2,6\text{-}iPr_2C_6H_3)$)[S1] and $(CuMes)_4$ (Mes = $2,4,6\text{-}Me_3C_6H_2$) [S2] were prepared according to literature procedures.

Synthesis of Cuproussiloxane (1): At room temperature a solution of $(CuMes)_4$ (0.731 g, 1 mmol) in toluene (30 mL) was added dropwise to a stirring solution of $R(Me)Si(OH)_2$ (0.651 g, 2 mmol) in toluene (20 mL). After addition, the mixture was reacted for 12 h to give a light yellow solution. The solution was concentrated (to ca. 5 mL), and to it *n*-hexane (30 mL) was added. The mixture was kept at –20 ℃ for 24 h, giving a light yellow solid of **1** that was collected by filtration and dried under vacuum for 10 h to remove the volatiles. Yield: 0.82 g (91%). Mp: 256 ℃ (dec.). Recrystallization of **1** (0.2 g) was performed in *n*-hexane (10 mL) at −20 °C for 7 d to give x-ray quality colorless single-crystals of $[(CuO)_2Si(Me)R]_{12}\cdot 8C_6H_{14}$ (**1a**$\cdot 8C_6H_{14}$). When this recrystallization (0.2 g, in toluene/*n*-hexane (1 mL/10 mL)) was conducted by slow evaporation at room temperature under Ar atmosphere, X-ray quality light-yellow single-crystals of $[(CuO)_2Si(Me)R]_{10}\cdot 7C_7H_8$ (**1b**$\cdot 7C_7H_8$) were yielded in two weeks. Similarly, an addition of one drop C_6H_6 and one drop CH_2Cl_2 into the toluene/*n*-hexane (1 mL/10 mL) solution of **1** (0.2 g) followed by a slow evaporation at room temperature under Ar for two weeks led to X-ray quality light-yellow single-crystals of $[(CuO)_2Si(Me)R]_{10}\cdot C_6H_6\cdot C_6H_{14}\cdot 0.5CH_2Cl_2$ (**1b**$\cdot C_6H_6\cdot C_6H_{14}\cdot 0.5CH_2Cl_2$). ^1H NMR (using the dried sample **1**, 400 MHz, $CDCl_3$, 298 K, ppm, based on the $(CuO)_2Si(Me)R$ unit): δ = 0.07 (s) and 0.08 (s) (9 H, Si*Me*$_3$), 0.12 (s) and 0.13 (s) (3 H, Si*Me*), 1.08 (d, $^3J_{HH}$ = 10.0 Hz) and 1.11 (d, $^3J_{HH}$ = 10.0 Hz) (12 H, CH*Me*$_2$), 3.36 (sept, 2 H, $^3J_{HH}$ = 10.0 Hz, C*H*Me$_2$), 6.95 (m) and 7.25 (m) (3 H, C_6H_3). ^{13}C NMR (100 MHz, $CDCl_3$, 298 K, ppm): δ = 0.99 (Si*Me*), 3.18 (Si*Me*$_3$), 25.68, 27.25 (CH*Me*$_2$), 31.57 (*C*HMe$_2$), 123.88, 124.78, 139.86, 147.22 (C_6H_3). ^{29}Si NMR (99 MHz, $CDCl_3$, 298 K, ppm): δ = –28.33 (*Si*MeO$_2$), 4.87 (*Si*Me$_3$). IR (Nujol mull, KBr plate): ν = 442.8 (w), 540.7 (w), 587.3 (w), 637.2 (w), 724.0 (m), 784.7 (w), 801.9 (m), 837.7 (m), 919.1 (s), 966.3 (w), 1041.6 (w), 1104.5 (w), 1177.1 (m), 1247.2 (m), 1257.7 (m), 1312.8 (w), 1377.1 (s), 1460.0 (vs). Anal. calcd for $C_{16}H_{25}Cu_2NO_2Si_2$ (using the dried sample **1**, based on the $(CuO)_2Si(Me)R$ unit, M_r = 446.64): C, 43.03; H, 5.64; N, 3.14. Found: C, 43.08; H, 5.62; N, 3.12.

Reference

[S1] V. Chandrasekhar, S. Nagendran and R. J. Butcher, *Organometallics* 1999, **18**, 4488−4492.

[S2] H. Eriksson and M. Håkansson, *Organometallics* 1997, **16**, 4243–4244.

II. X-Ray crystallographic details and crystal structures

Crystallographic data for compounds **1b**·$7C_7H_8$, and **1b**·C_6H_6·C_6H_{14}·$0.5CH_2Cl_2$ were collected on an Oxford Gemini S Ultra system. During measurements graphite monochromatic Mo-Kα radiation (λ = 0.71073 Å) was used. The structures were solved by direct methods (SHELXS-96)[S3] and refined against F^2 using SHELXL-97.[S4] The data for **1a**·$8C_6H_{14}$ (note: the structure solution gives solvents as $5.5C_6H_8$ and $2.5C_6H_8$ probably due to geometry restriction of the *n*-hexane molecules, and therefore the formula is written as **1a**·$8C_6H_8$ based on the structure determination. The actrual molecular formula is **1a**·$8C_6H_{14}$) was collected on XtaLAB Synergy, Dualflex, HyPix diffractometer (Cu-Kα radiation, λ = 1.54184 Å). The structure was solved with the ShelXS-97[S3] solution program using direct methods and by using Olex2 1.5-dev[S5] as the graphical interface. The model was refined with ShelXL 2018/3[S6-S9] using full matrix least squares minimisation on F^2. Absorption corrections were all applied using the spherical harmonics program (multi-scan type). In general, the non-hydrogen atoms were located by difference Fourier synthesis and refined anisotropically, and hydrogen atoms were included using a riding model with U_{iso} tied to the U_{iso} of the parent atoms unless otherwise specified. In **1a**·$8C_6H_8$, a half moiety of **1a**, that is $[(CuO)_2Si(Me)R]_6$, was disclosed, and a whole molecule is obtained through a symmetric operation. *Two B alerts by "High wR2 Value (i.e. > 0.25) of 0.39" and "Low Bond Precision on C-C Bonds by 0.02694 Å" are caused mostly due to the crystal quality.* In **1b**·$7C_7H_8$, all the toluene molecules were refined isotropically. Final refinements gave toluenes as C(131)C(132)C(133)C(134)C(135)C(136)C(137) (0.5), C(141)C(142)C(143)C(144)C(145)C(146)C(147) (1.0), C(181)C(182)C(183)C(184)C(185)C(186)-C(187) (0.5), C(191)C(192)C(193)C(194)C(195)C(196)C(197) (1.0), C(201)C(202)C(203)C(204)C(205)-C(206)C(207) (0.5), respectively. For disordered toluene molecules, the PART method was applied and final refinements gave C(151)C(152)C(153)C(154)C(155)C(156)C(157) (0.65) and C(51a)C(52a)C(53a)-C(54a)C(55a)C(56a)C(57a) (0.35), C(171)C(172)C(173)C(174)C(175)C(176)C(177) (0.5) and C(71a)C(72a)C(73a)C(74a)C(75a)C(76a)C(77a) (0.5), and C(241)C(242)C(243)C(244)C(245)C(246)-C(247) (0.5) and C(41a)C(42a)C(43a)C(44a)C(45a)C(46a)C(47a) (0.5). Seriously disordered toluene molecules C(211)C(212)C(213)C(214)C(215) (0.25) and C(231)C(232)C(233)C(234)C(235) (0.25) were finally determined where hydrogen geometric addition was not able to perform. In **1b**·C_6H_6·C_6H_{14}·$0.5CH_2Cl_2$, two $SiMe_3$ groups were disordered and treated by the PART method, and final refinements gave Si(15)C(57)C(58)C(59) (0.40589) and Si(5a)C(57a)C(58a)C(59a) (0.59411) and Si(20)C(107)C(108)C(109) (0.39973) and Si(2a)C(107a)C(108a)C(109a) (0.60027). All of the solvent molecules were refined isotropically. Two *n*-hexane molecules as C(11a)C(12a)C(13a)C(14a)C(15a)-C(16a) (0.5) and C(21a)C(22a)C(23a)C(24a)C(25a)C(26a) (0.5) were refined. One benzene was disordered and treated by the PART method, and final refinements gave C(1a)C(2a)C(3a)C(4a)C(5a)C(6a) (0.5) and C(1b)C(2b)C(3b)C(4b)C(5b)C(6b) (0.5). The dichloromethane molecule was also disordered and treated by the PART method, and final refinements gave C(1)Cl(1)Cl(2) (0.25) and C(1)Cl(1a)Cl(2a) (0.25). *The cif check reports alert **B** as "*U*nit cell contains solvent accessible VOIDS of 133 Å^3" for both **1b**·$7C_7H_8$ and **1b**·C_6H_6·C_6H_{14}·$0.5CH_2Cl_2$. We run the PLATON/SQUEEZE program to gain the .spf files. The recovered number of single electrons is 4 for the former, implying almost no non-hydrogen atom left to locate. The number of single electrons is 10 for the latter. This implies possibly one non-hydrogen atom like O or N was to locate. But we were not succeeded in determining the suitable atom.* A summary of cell parameters, data collection, and structure solution and refinements is given in Table S1.

Reference

[S3] G. M. Sheldrick, SHELXS-90, Program for Structure Solution; *Acta Crystallogr., Sect. A* 1990, **46**, 467–473.
[S4] G. M. Sheldrick, SHELXL-97, Program for Crystal Structure Refinement; University of Göttingen: Göttingen, Germany, 1997.
[S5] O.V. Dolomanov, L.J. Bourhis, R. J. Gildea, J. A. K. Howard, and H. Puschmann, Olex2: A Complete Structure Solution, Refinement and Analysis program, *J. Appl. Cryst.*, 2009, **42**, 339–341.
[S6] G. M. Sheldrick, Crystal Structure Refinement with ShelXL, *Acta Cryst.*, 2015, **C71**, 3–8.
[S7] G. M. Sheldrick, A Short History of ShelX, *Acta Cryst.*, 2008, **A64**, 339-341.
[S8] CrysAlisPro (Rigaku, V1.171.41.110a), 2021.
[S9] CrysAlisPro (ROD), Rigaku Oxford Diffraction, Poland, 2015.

Table S1. Crystal data and refinements[a]

	1a·8C_6H_8	**1b**·7C_7H_8	**1b**·C_6H_6·C_6H_{14}·0.5CH_2Cl_2
CCDC number	2192322	2119775	2119776
formula	$C_{240}H_{412}Cu_{24}N_{12}O_{24}Si_{24}$	$C_{209}H_{346}Cu_{20}N_{10}O_{20}Si_{20}$	$C_{172.5}H_{311}ClCu_{20}N_{10}O_{20}Si_{20}$
formula weight	6048.91	5151.56	4713.36
crystal system	Triclinic	Triclinic	Monoclinic
space group	*P*–1	*P*–1	*P*2(1)/*n*
a/Å	18.0648(5)	21.1659(3)	17.9559(4)
b/Å	20.5162(6)	26.5516(3)	34.2763(8)
c/Å	23.1502(8)	26.8313(4)	39.5595(10)
α/deg	112.836(3)	90.1630(10)	
β/deg	100.175(3)	106.3980(10)	101.029(2)
γ/deg	101.388(3)	112.0060(10)	
V/Å^3	7440.9(4)	13314.4(3)	23897.1(10)
Z	1	2	4
ρ_{calcd}/g·cm^{-3}	1.263	1.435	1.310
μ/mm^{-1}	3.107	1.710	1.900
F(000)	2944	5980	9812
crystal size/mm^3	0.20x0.10x0.10	0.26x0.22x0.20	0.30x0.27x0.18
θ range/deg	2.44–64.92	2.70–26.00	2.69–26.00
Max. and min. transmission	0.7464 and 0.5754	0.7272 and 0.6660	0.6000 and 0.7260
index ranges	$-20 \le h \le 20$	$-26 \le h \le 25$	$-22 \le h \le 22$
	$-23 \le k \le 23$	$-31 \le k \le 32$	$-42 \le k \le 38$
	$-26 \le l \le 25$	$-33 \le l \le 33$	$-42 \le l \le 48$
collected data	70498	132972	132717
unique data	24414	52238	46888
	(R_{int} = 0.0691)	(R_{int} = 0.0595)	(R_{int} = 0.0763)
completeness to *θ*	96.5%	99.8%	99.8%
data/restraints/parameters	24414/1131/1291	52238/7/2364	46888/410/2241
GOF on F^2	1.044	1.027	1.015
final *R* indices [*I*>2 (*I*)]	R_1 = 0.1228	R_1 = 0.0688	R_1 = 0.0585
	wR_2 = 0.3293	wR_2 = 0.1491	wR_2 = 0.1217
R indices (all data)	R_1 = 0.1520	R_1 = 0.1069	R_1 = 0.1065
	wR_2 = 0.3559	wR_2 = 0.1639	wR_2 = 0.1389
Largest diff peak/hole (e·Å^{-3})	1.721/–1.075	1.091/–0.629	1.262/–0.687

[a]Data were collected at 173(2) K for **1b**·7C_7H_8 and **1b**·C_6H_6·C_6H_{14}·0.5CH_2Cl_2 and at 100(2) K for **1a**·8C_6H_8 (note: **1a**·8C_6H_8 was determined by the structure solution, but the actural formula is **1a**·8C_6H_{14}). $R_1 = \sum(||F_o|-|F_c||)/\sum|F_o|$, $wR_2 = \{\sum[w(F_o^2-F_c^2)^2/\sum[w(F_o^2)^2]\}^2\}^{1/2}$, GOF = $\{\sum[w(F_o^2-F_c^2)^2]/(N_o-N_p)\}^{1/2}$.

Crystal structures with or without selected bond parameters

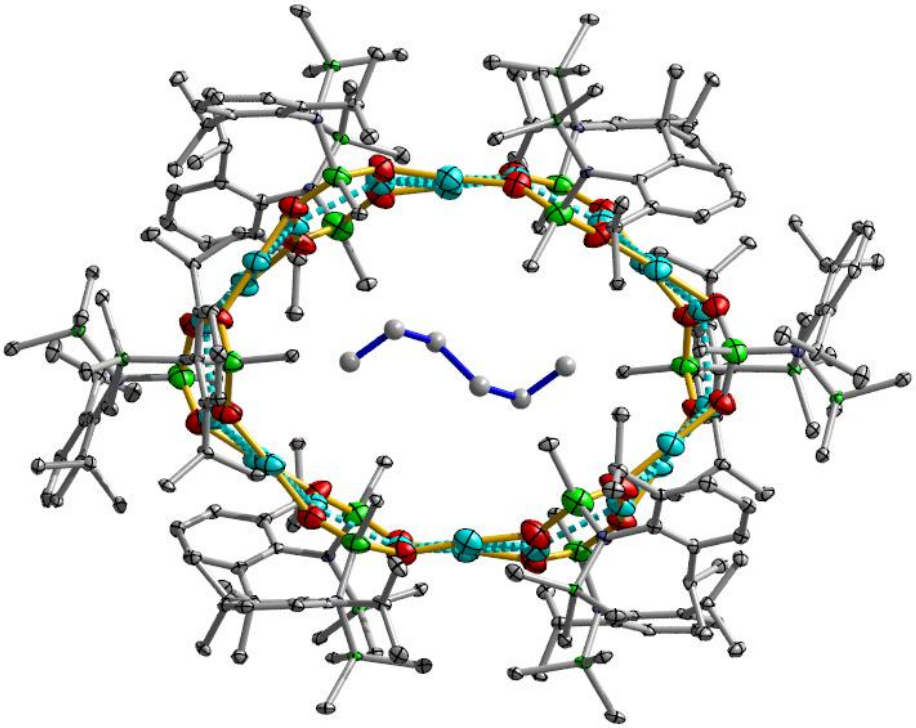

Figure S3 Crystal structure of **1a** in **1a**·8C_6H_{14} with one *n*-hexane molecule embedded in the prism core (viewed in the bc-plane direction).

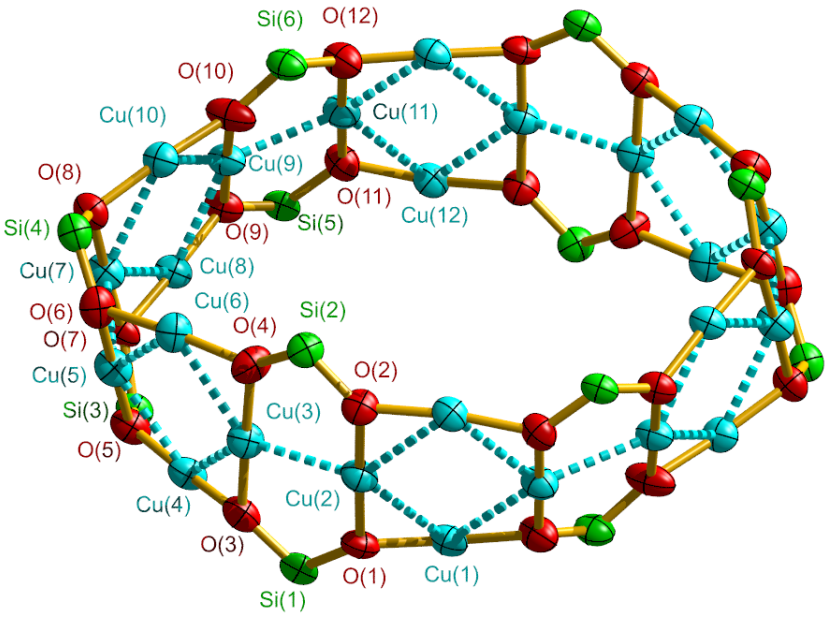

Figure S4 Crystal structure of the $Cu_{24}O_{24}Si_{12}$ core of **1a** in **1a**·8C_6H_{14} at 50% thermal ellipsoid level. Selected bond distances (Å) and angles (°): Cu(1)–O(1) 1.836(9), Cu(1)–O(12A) 1.837(10), Cu(2)–O(1) 1.851(8), Cu(2)–O(2) 1.847(7), Cu(3)–O(3) 1.851(8), Cu(3)–O(4) 1.876(8), Cu(4)–O(3) 1.843(8), Cu(4)–O(5) 1.839(8), Cu(5)–O(5) 1.871(8), Cu(5)–O(6) 1.887(9), Cu(6)–O(4) 1.856(8), Cu(6)–O(6) 1.890(8), Cu(7)–O(7) 1.859(7), Cu(7)–O(8) 1.869(8), Cu(8)–O(7) 1.840(7), Cu(8)–O(9) 1.849(8),

Cu(9)–O(9) 1.843(8), Cu(9)–O(10) 1.861(9), Cu(10)–O(8) 1.853(8), Cu(10)–O(9) 1.861(9), Cu(11)–O(11) 1.846(8), Cu(11)–O(12) 1.866(9), Cu(12)–O(11) 1.848(9), Cu(12)–O(2A) 1.851(8), Si(1)–O(1) 1.628(8), Si(1)–O(3) 1.626(9), Si(2)–O(2) 1.619(9), Si(2)–O(4) 1.598(8), Si(3)–O(5) 1.640(8), Si(3)–O(7) 1.626(8), Si(4)–O(6) 1.610(10), Si(4)–O(8) 1.610(8), Si(5)–O(9) 1.623(8), Si(5)–O(11) 1.633(9), Si(6)–O(10) 1.605(10), Si(6)–O(12) 1.614(10), Cu(1)··Cu(2) 2.725(3), Cu(1)··Cu(11A) 2.619(3), Cu(2)··Cu(3) 2.614(2), Cu(2)··Cu(12A) 2.620(3), Cu(3)··Cu(4) 2.674(3), Cu(3)··Cu(6) 2.665(3), Cu(4)··Cu(5) 2.665(3), Cu(5)··Cu(6) 2.714(3), Cu(5)··Cu(7) 2.616(2), Cu(7)··Cu(8) 2.662(3), Cu(7)··Cu(10) 2.688(3), Cu(8)··Cu(9) 2.663(3), Cu(9)··Cu(10) 2.666(3), Cu(9)··Cu(11) 2.614(3), Cu(11)··Cu(1A) 2.621(2), Cu(11)··Cu(12) 2.727(3), Cu(12)··Cu(2A) 2.620(3); O(1)–Cu(1)–O(12A) 173.5(4), O(1)–Cu(2)–O(2) 178.7(4), O(3)–Cu(3)–O(4) 178.4(4), O(3)–Cu(4)–O(5) 172.8(4), O(5)–Cu(5)–O(6) 179.0(4), O(4)–Cu(6)–O(6), 172.4(4), O(7)–Cu(7)–O(8) 178.4(4), O(7)–Cu(8)–O(9) 174.0(3), O(9)–Cu(10)–O(10) 178.1(4), O(8)–Cu(10)–O(10) 173.3(4), O(11)–Cu(11)–O(12) 178.6(4), O(11)–Cu(12)–O(2A) 172.3(4), O(1)–Si(1)–O(3) 108.2(4), O(2)–Si(2)–O(4) 109.5(4), O(5)–Si(3)–O(7) 105.3(4), O(6)–Si(4)–O(8) 109.5(5), O(9)–Si(5)–O(11) 108.0(4), O(10)–Si(6)–O(12), 110.0(5).

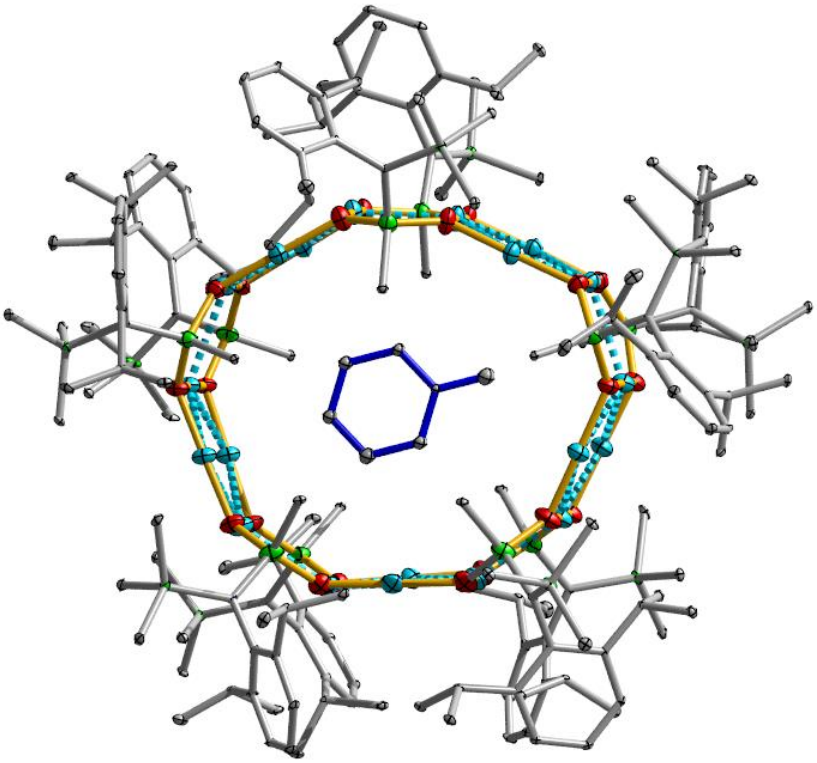

Figure S5 Crystal structure of **1b** in **1b**·7C_7H_8 with one toluene molecule embedded in the prism core (viewed in the ab-plane direction).

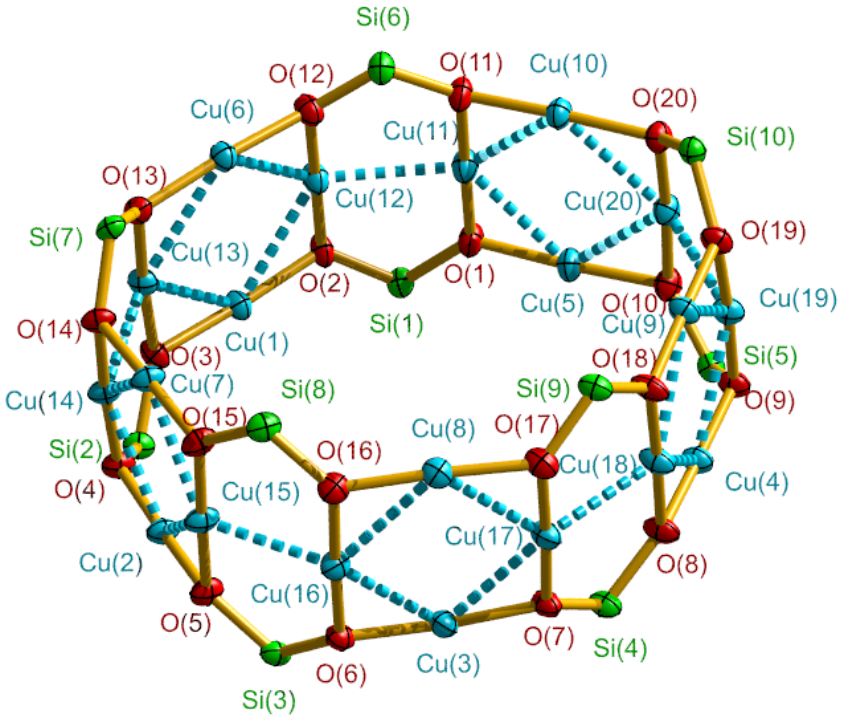

Figure S6 Crystal structure of the $Cu_{24}O_{24}Si_{12}$ core of **1b** in **1b**·$7C_7H_8$ at 50% thermal ellipsoid level. Selected bond distances (Å) and angles (°): Cu(1)–O(2) 1.844(4), Cu(1)–O(3) 1.842(3), Cu(2)–O(4) 1.841(3), Cu(2)–O(5) 1.839(3), Cu(3)–O(6) 1.843(4), Cu(3)–O(7) 1.838(4), Cu(4)–O(8) 1.834(3), Cu(4)–O(9) 1.838(3), Cu(5) –O(1) 1.829(4), Cu(5)–O(10) 1.846(4), Cu(6)–O(12) 1.838(4), Cu(6)–O(13) 1.848(4), Cu(7)–O(14) 1.845(3), Cu(7)–O(15) 1.840(3), Cu(8)–O(16) 1.837(4), Cu(8)–O(17) 1.839(4), Cu(9)–O(18) 1.830(3), Cu(9)–O(19) 1.835(3), Cu(10)–O(11) 1.838(4), Cu(10)–O(20) 1.844(4), Cu(11)–O(11) 1.844(4), Cu(11)–O(1) 1.846(4), Cu(12)–O(2) 1.850(4), Cu(12)–O(12) 1.867(4), Cu(13)–O(3) 1.858(4), Cu(13)–O(13) 1.852(4), Cu(14)–O(4) 1.858(4), Cu(14)–O(14) 1.846(4), Cu(15)–O(5) 1.852(4), Cu(15)–O(15) 1.852(4), Cu(16)–O(6) 1.846(4), Cu(16)–O(16) 1.856(4), Cu(17)–O(7) 1.858(4), Cu(17)–O(17) 1.860(4), Cu(18)–O(8) 1.844(4), Cu(18)–O(18) 1.846(4), Cu(19)–O(9) 1.859(4), Cu(19)–O(19) 1.847(4), Cu(20)–O(10) 1.849(4), Cu(20)−O(20) 1.868(4), Si(1)–O(1) 1.631(4), Si(1)–O(2) 1.632(4), Si(2)–O(3) 1.632(4), Si(2)–O(4) 1.629(3), Si(3)–O(5) 1.631(4), Si(3)–O(6) 1.635(4), Si(4)–O(7) 1.624(4), Si(4)–O(8) 1.634(4), Si(5) –O(9) 1.634(4), Si(5)–O(10) 1.630(4), Si(6)–O(11) 1.638(4), Si(6)–O(12) 1.627(4), Si(7)–O(13) 1.639(3), Si(7)–O(14) 1.634(4), Si(8)–O(15) 1.634(4), Si(8)–O(16) 1.631(4), Si(9)–O(17) 1.628(4), Si(9)–O(18) 1.630(4), Si(10)–O(19) 1.630(4), Si(10)–O(20) 1.631(4), Cu(1) ··Cu(12) 2.7054(10), Cu(1) ··Cu(13) 2.6903(9), Cu(2) ··Cu(14) 2.6469(9), Cu(2) ··Cu(15) 2.7508(9), Cu(3) ··Cu(16) 2.6799(10), Cu(3) ··Cu(17) 2.7047(9), Cu(4) ··Cu(18) 2.6981(9), Cu(4) ··Cu(19) 2.6743(10), Cu(5) ··Cu(11) 2.6813(10), Cu(5) ··Cu(20) 2.7111(9), Cu(6) ··Cu(12) 2.6838(9), Cu(6) ··Cu(13) 2.7176(9), Cu(7) ··Cu(14) 2.7437(9), Cu(7) ··Cu(15) 2.6356(9), Cu(8) ··Cu(16) 2.7147(10), Cu(9) ··Cu(18) 2.6713(10), Cu(9) ··Cu(19) 2.7142(9), Cu(10) ··Cu(11) 2.6772(9), Cu(10) ··Cu(20) 2.6875(10), Cu(11) ··Cu(12) 2.6825(10), Cu(13) ··Cu(14) 2.6584(9), Cu(15) ··Cu(16) 2.6551(10), Cu(17) ··Cu(18) 2.6268(9), Cu(19) ··Cu(20) 2.6598(9); O(2)–Cu(1)–O(3) 174.74(17), O(4)–Cu(2)–O(5) 175.53(17), O(6)–Cu(3)–O(7) 174.53(17), O(8)–Cu(4)–O(9) 174.96(17), O(1)–Cu(5)–O(10) 173.98(16), O(12)–Cu(6)–O(13), 174.81(17), O(14)–Cu(7)–O(15) 175.95(17), O(16)–Cu(8)–O(17) 174.42(16), O(18)–Cu(9)–O(19) 173.98(17), O(11)–Cu(10)–O(20) 175.83(17), O(1)–Cu(11)–O(11) 177.78(17), O(2)–Cu(12)–O(12) 176.59(16),

O(3)–Cu(13)–O(13) 175.95(16), O(4)–Cu(14)–O(14), 175.75(17), O(5)–Cu(15)–O(15) 175.66(16), O(6)–Cu(16)–O(16) 176.03(16), O(7)–Cu(17)–O(17) 176.90(18), O(8)–Cu(18)–O(18) 176.97(18), O(9)–Cu(19)–O(19) 176.46(17), O(10)–Cu(20)–O(20) 176.11(17), O(1)–Si(1)–O(2) 106.7(2), O(3)–Si(2)–O(4) 110.54(19), O(5)–Si(3)–O(6) 108.8(2), O(7)–Si(4)–O(8) 109.3(2), O(9)–Si(5)–O(10) 108.9(2), O(11)–Si(6)–O(12) 109.8(2), O(13)–Si(7)–O(14) 108.68(19), O(15)–Si(8)–O(16) 110.64(2), O(17)–Si(9)–O(18) 107.0(2), O(19)–Si(10)–O(20) 109.3(2).

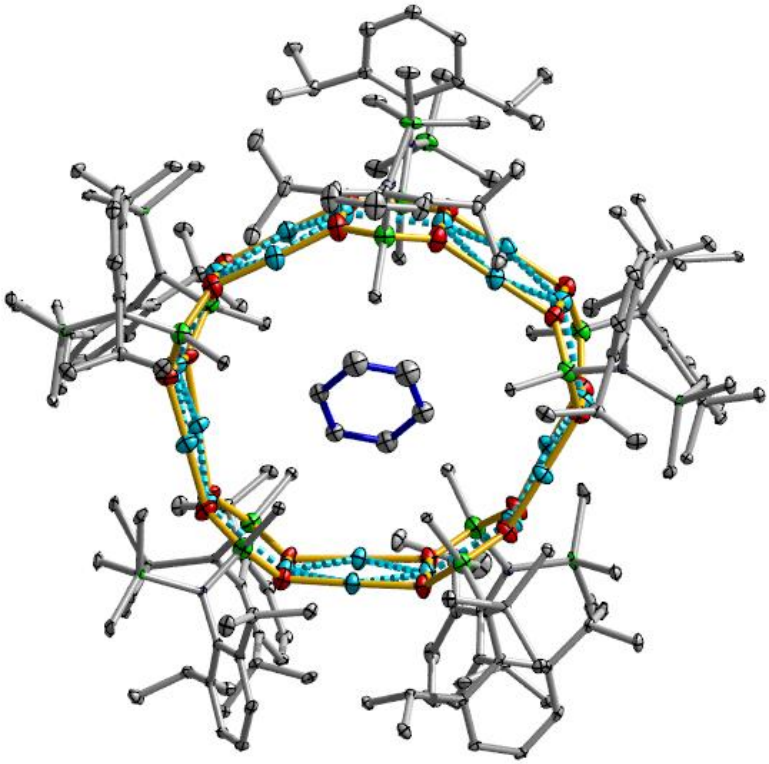

Figure S7 Crystal structure of **1b** in **1b**·C_6H_6·C_6H_{14}·0.5CH_2Cl_2 with one benzene molecule embedded in the prism core (viewed in the bc-plane direction).

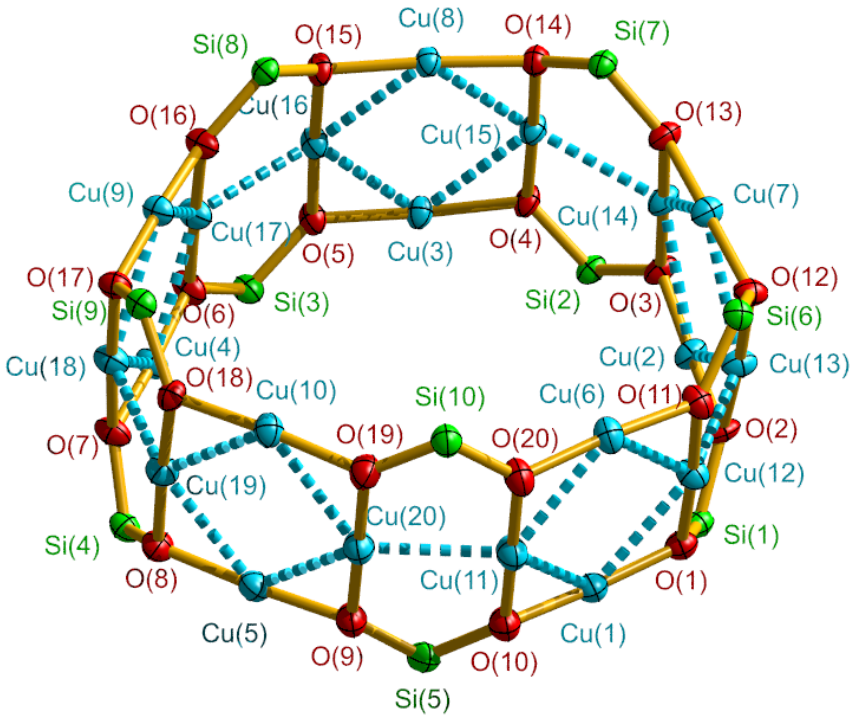

Figure S8 Crystal structure of the $Cu_{20}O_{20}Si_{10}$ core of **1b** in **1b**·C_6H_6·C_6H_{14}·0.5CH_2Cl_2 at 50% thermal ellipsoid level. Selected bond distances (Å) and angles (°): Cu(1)–O(1) 1.841(3), Cu(1)–O(10) 1.840(4), Cu(2)–O(2) 1.824(3), Cu(2)–O(3) 1.836(3), Cu(3)–O(4) 1.840(4), Cu(3)–O(5) 1.835(3), Cu(4)–O(6) 1.826(3), Cu(4)–O(7) 1.824(3), Cu(5) –O(8) 1.835(3), Cu(5)–O(9) 1.834(4), Cu(6)–O(11) 1.837(3), Cu(6)–O(20) 1.837(4), Cu(7)–O(12) 1.832(3), Cu(7)–O(13) 1.836(3), Cu(8)–O(14) 1.845(3), Cu(8)–O(15) 1.843(3), Cu(9)–O(16) 1.826(3), Cu(9)–O(17) 1.839(3), Cu(10)–O(18) 1.842(3), Cu(10)–O(19) 1.832(4), Cu(11)–O(10) 1.844(4), Cu(11)–O(20) 1.851(4), Cu(12)–O(1) 1.856(3), Cu(12)–O(11) 1.844(3), Cu(13)–O(2) 1.844(3), Cu(13)–O(12) 1.847(3), Cu(14)–O(3) 1.854(3), Cu(14)–O(13) 1.851(3), Cu(15)–O(4) 1.851(3), Cu(15)–O(14) 1.865(3), Cu(16)–O(5) 1.870(3), Cu(16)–O(15) 1.860(3), Cu(17)–O(6) 1.853(3), Cu(17)–O(16) 1.846(3), Cu(18)–O(7) 1.845(3), Cu(18)–O(17) 1.855(3), Cu(19)–O(8) 1.869(3), Cu(19)–O(18) 1.852(3), Cu(20)–O(9) 1.839(4), Cu(20)−O(19) 1.838(4), Si(1)–O(1) 1.638(4), Si(1)–O(2) 1.638(3), Si(2)–O(3) 1.643(3), Si(2)–O(4) 1.636(3), Si(3)–O(5) 1.628(3), Si(3)–O(6) 1.633(4), Si(4)–O(7) 1.634(4), Si(4)–O(8) 1.635(4), Si(5) –O(9) 1.629(4), Si(5)–O(10) 1.627(4), Si(6)–O(11) 1.636(4), Si(6)–O(12) 1.642(4), Si(7)–O(13) 1.635(4), Si(7)–O(14) 1.628(3), Si(8)–O(15) 1.633(3), Si(8)–O(16) 1.636(3), Si(9)–O(17) 1.635(4), Si(9)–O(18) 1.637(4), Si(10)–O(19) 1.637(4), Si(10)–O(20) 1.634(4), Cu(1) ··Cu(11) 2.7222(10), Cu(1) ··Cu(12) 2.6433(8), Cu(2) ··Cu(13) 2.7080(8), Cu(2) ··Cu(14) 2.6714(8), Cu(3) ··Cu(15) 2.7116(8), Cu(3) ··Cu(16) 2.6824(9), Cu(4) ··Cu(17) 2.6541(9), Cu(4) ··Cu(18) 2.7170(9), Cu(5) ··Cu(19) 2.6628(9), Cu(5) ··Cu(20) 2.7032(9), Cu(6) ··Cu(11) 2.6493(9), Cu(6) ··Cu(12) 2.7459(9), Cu(7) ··Cu(13) 2.6563(9), Cu(7) ··Cu(14) 2.7049(9), Cu(8) ··Cu(15) 2.6800(9), Cu(8) ··Cu(16) 2.6951(8), Cu(9) ··Cu(17) 2.7082(9), Cu(9) ··Cu(18) 2.6601(8), Cu(10) ··Cu(19) 2.7246(8), Cu(10) ··Cu(20) 2.6585(9), Cu(11) ··Cu(20) 2.6080(9), Cu(12) ··Cu(13) 2.6567(9), Cu(14) ··Cu(15) 2.6525(9), Cu(16) ··Cu(17) 2.6215(9), Cu(18) ··Cu(19) 2.6508(9); O(1)–Cu(1)–O(10) 175.17(15), O(2)–Cu(2)–O(3) 174.72(14), O(4)–Cu(3)–O(5) 174.65(14), O(6)–Cu(4)–O(7) 174.35(16), O(8)–Cu(5)–O(9) 175.02(16), O(11)–Cu(6)–O(20), 173.68(15), O(12)–Cu(7)–O(13) 175.39(15), O(14)–Cu(8)–O(15) 175.59(14), O(16)–Cu(9)–O(17) 174.80(15), O(18)–Cu(10)–O(19) 173.66(15),

O(10)–Cu(11)–O(20) 177.29(18), O(1)–Cu(12)–O(11) 176.74(16), O(2)–Cu(13)–O(12) 176.36(15), O(3)–Cu(14)–O(13), 176.45(16), O(4)–Cu(15)–O(14) 176.72(16), O(5)–Cu(16)–O(15) 177.63(15), O(6)–Cu(17)–O(16) 177.29(16), O(7)–Cu(18)–O(17) 176.99(15), O(8)–Cu(19)–O(18) 177.12(15), O(9)–Cu(20)–O(19) 178.10(18), O(1)–Si(1)–O(2) 110.24(18), O(3)–Si(2)–O(4) 109.03(17), O(5)–Si(3)–O(6) 109.47(18), O(7)–Si(4)–O(8) 109.20(18), O(9)–Si(5)–O(10) 106.7(2), O(11)–Si(6)–O(12) 109.52(17), O(13)–Si(7)–O(14) 110.13(18), O(15)–Si(8)–O(16) 107.35(18), O(17)–Si(9)–O(18) 109.03(19), O(19)–Si(10)–O(20) 106.51(19).

Schematic and Ortep drawing view

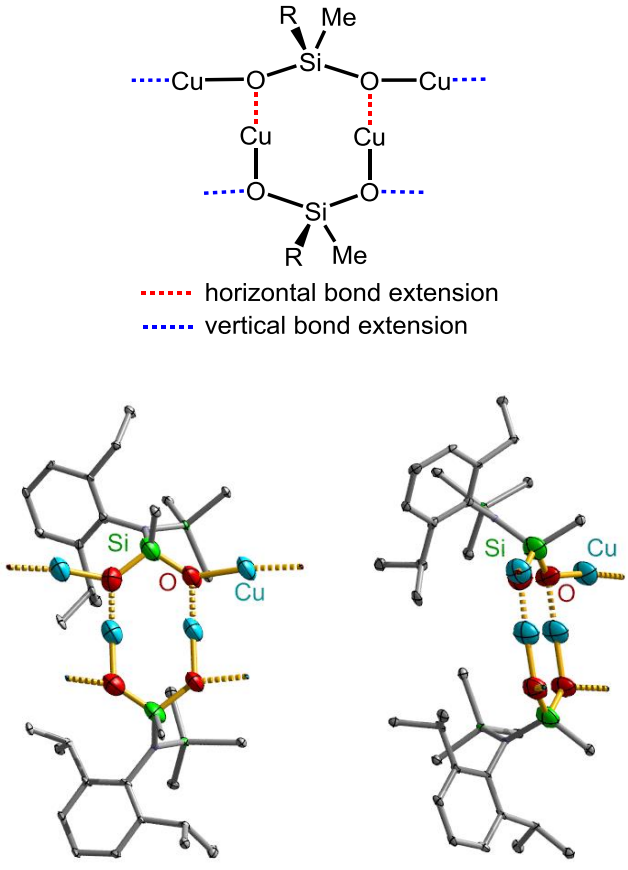

Figure S9 Schematic and Ortep drawing view of the self-assembly of the Cu–O–Si(Me)(R)–O–Cu unit by the intermolecular Cu–O bonding in both the horizontal and vertical directions for forming **1a** and **1b**. The bulk R group stands outside either the dodecagonal (**1a**) or decagonal (**1b**) prism cores whereas the Me group inward.

VI. Collected ^{1}H, ^{13}C, and ^{29}Si NMR spectra of 1

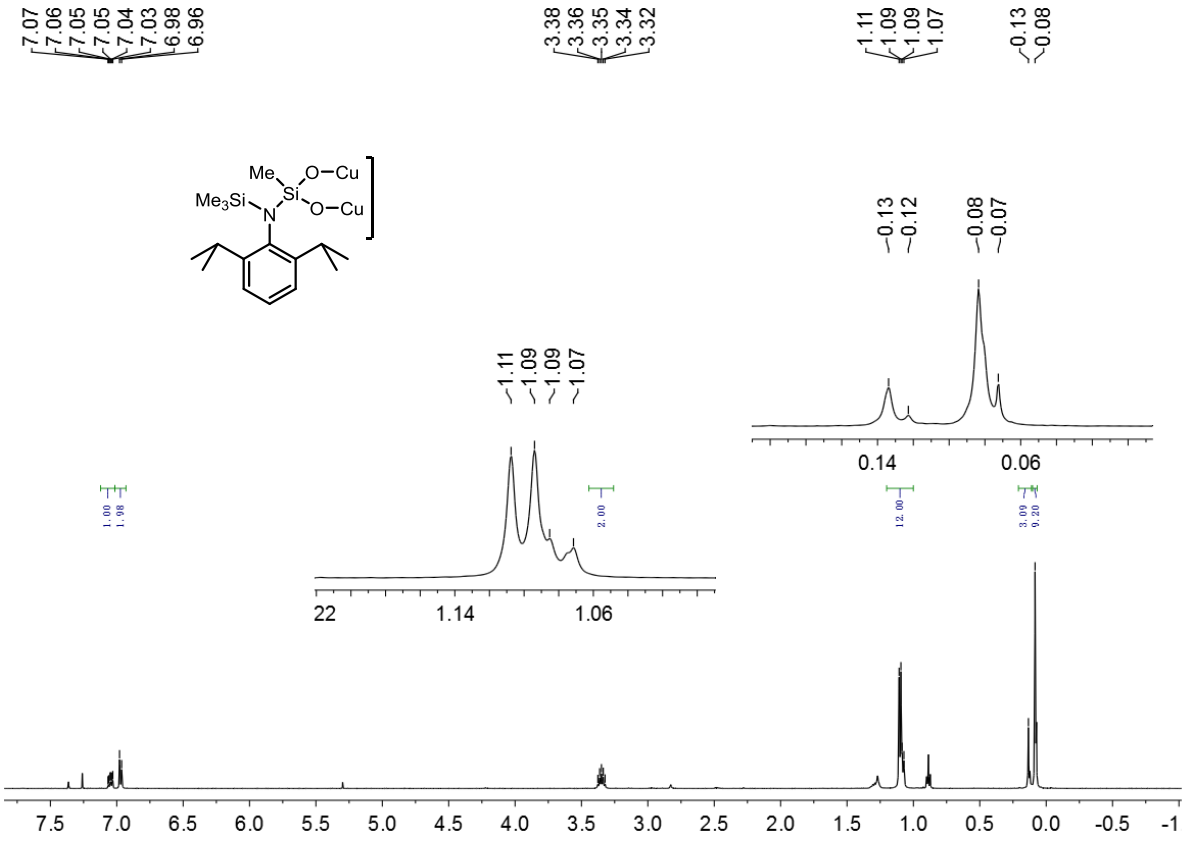

Figure S10 ^{1}H NMR spectrum of **1** in $CDCl_3$ at 298K (resonances at δ 0.08 and 1.22 ppm are from *n*-hexane; resonances at δ 7.36 ppm are probably from impurity)

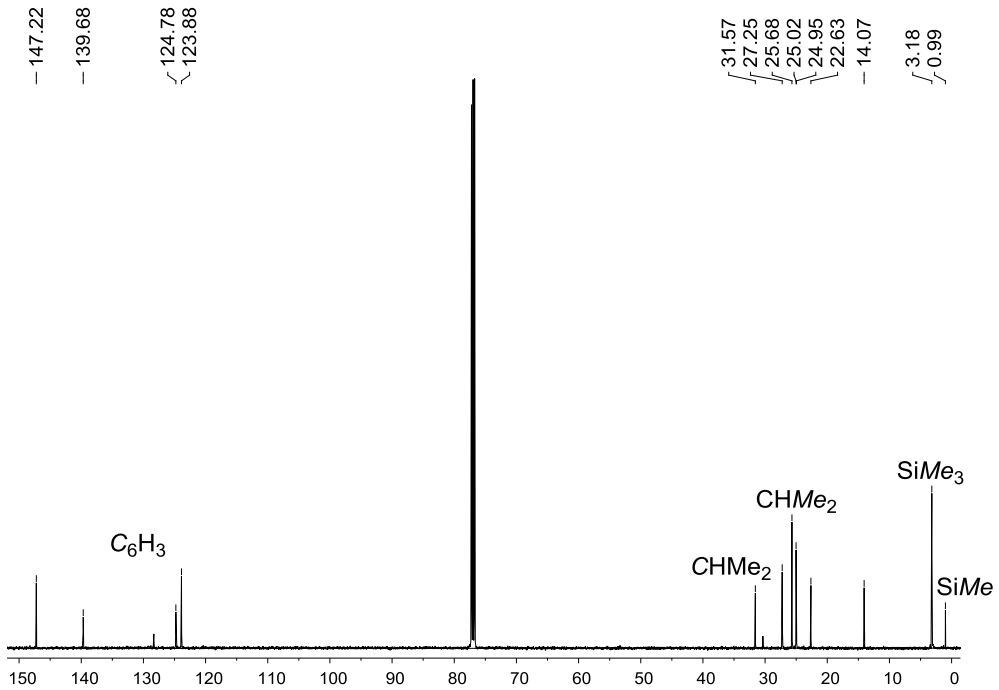

Figure S11 ^{13}C NMR spectrum of **1** in $CDCl_3$ at 298K (resonances at δ 14.07, 22.63, and 24.95 ppm are from *n*-hexane; resonance at δ 128.12 ppm is probably from the impurity)

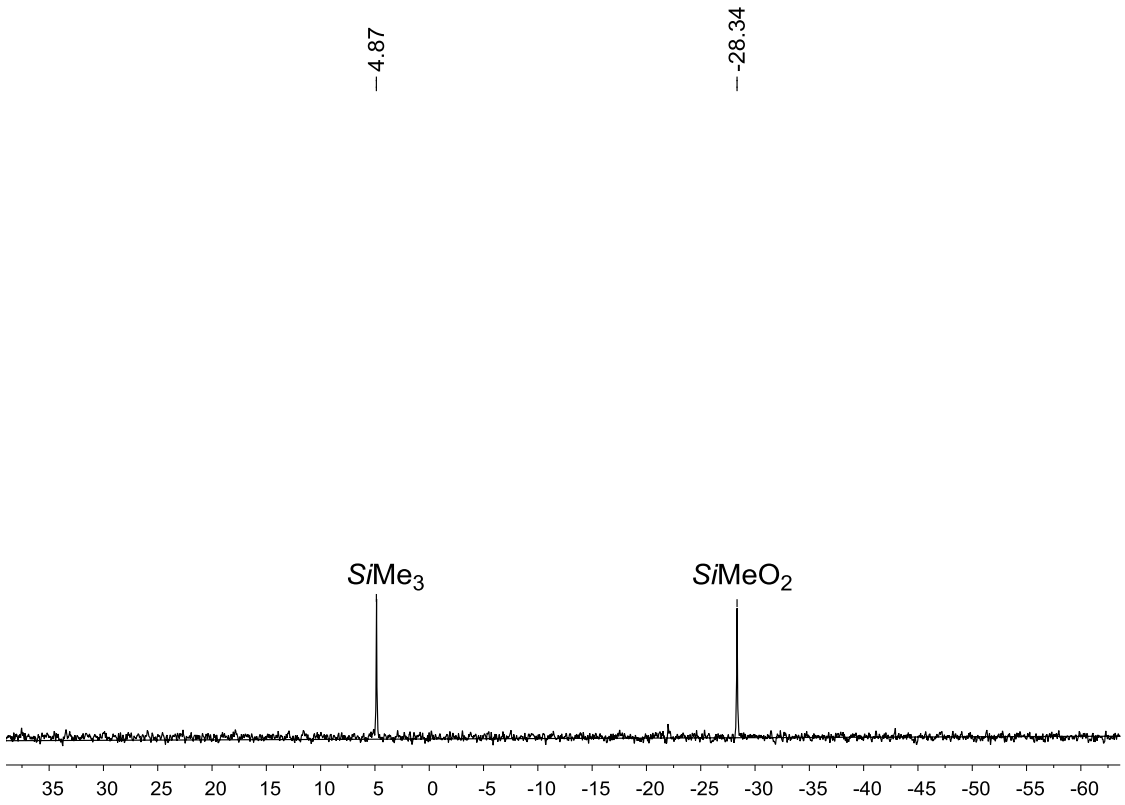

Figure S12 ^{29}Si NMR spectrum of **1** in $CDCl_3$ at 298K.

IV. General procedure for catalytic reaction and the NMR data for the products

Inside the glovebox, **1** (0.025 mmol, based on the $(CuO)_2Si(Me)R$ unit) was added in the flask. The flask was brought outside for reaction. Into this flask was added DMSO (1 mL), *H*-Phosphonates (0.5 mmol), terminal alkyne (0.6 mmol), and finally Et_3N (0.1 mmol). By stirring, a suspension was formed. Upon exposure to air, the mixture was allowed to heat to the setting temperature and further stir for a given time. Finally, a clear reaction solution was formed. All volatiles were removed under vacuum to give a residue. And then a small amount of this residue was picked up subject to the ^{31}P NMR spectral analysis to determine the yield of the product catalytically formed. By using a mixture of petroleum ether and ethyl acetate as an eluent and going through the chromatographic column filled with the commonly used silica gel (3 x 15 cm), the target product was isolated. The product was measured by ^{1}H, ^{13}C, and ^{31}P NMR spectroscopy. In the case of ethylferrocene, 1,4-diethynylbenzene, and 4,4'-diethynylbiphenyl as the respective terminal alkyne materials, O_2 was used instead.

PhC≡CP(O)(O*i*Pr)$_2$: ^{1}H NMR (400 MHz, $CDCl_3$, 298 K, ppm): δ = 1.40 (dd, $^{3}J_{HH}$ = 6.0 Hz, J_{HP} = 2.4 Hz, 12 H, CH*Me*$_2$), 4.81 (sd (septet doublet), $^{3}J_{HH}$ = 6.0 Hz, J_{HP} = 8.8 Hz, 2 H, C*H*Me$_2$), 7.30−7.56 (m, 5 H, *Ph*). ^{13}C NMR (100 MHz, $CDCl_3$, 298 K, ppm): δ = 23.6 (d, J_{CP} = 4.9 Hz), 23.9 (d, J_{CP} = 4.4 Hz) (CH*Me*$_2$), 72.4 (d, J_{CP} = 5.6 Hz, *C*HMe$_2$), 79.9 (d, J_{CP} = 296.9 Hz, ≡*C*P), 98.2 (d, J_{CP} = 52.5 Hz, PhC≡), 119.8 (d, J_{CP} = 4.6 Hz), 128.5, 130.5, 132.5 (d, J_{CP} = 2.4 Hz) (*Ph*). ^{31}P (162 MHz, $CDCl_3$, 298 K, ppm): δ = −8.56.

***n*BuC≡CP(O)(O*i*Pr)$_2$**: ^{1}H NMR (400 MHz, $CDCl_3$, 298 K, ppm): δ = 0.91 (t, 3 H), 1.42 (m, 2 H), 1.55 (m, 2 H), 2.33 (dt, 2 H) (*nBu*), 1.37 (d, $^{3}J_{HH}$ = 4.8 Hz, 12 H, CH*Me*$_2$), 4.72 (ds, $^{3}J_{HH}$ = 4.8 Hz, J_{HP} = 7.2 Hz, 2 H, C*H*Me$_2$). ^{13}C NMR (100 MHz, $CDCl_3$, 298 K, ppm): δ = 13.4, 18.8 (d, J_{CP} = 3.6 Hz), 21.9, 29.7 (*n*Bu), 23.6 (d, J_{CP} = 3.7 Hz), 23.8 (d, J_{CP} = 3.6 Hz) (CH*Me*$_2$), 71.8 (d, J_{CP} = 4.4 Hz, *C*HMe$_2$), 72.0 (d, J_{CP} = 240.4 Hz, ≡*C*P), 102.1 (d, J_{CP} = 42.0 Hz, *n*Bu*C*≡). ^{31}P ($CDCl_3$, 162 MHz, 298 K, ppm): δ = −8.55.

Cl(CH$_2$)$_3$C≡CP(O)(O*i*Pr)$_2$: ^{1}H NMR (400 MHz, $CDCl_3$, 298 K, ppm): δ = 1.35 (dd, $^{3}J_{HH}$ = 5.2 Hz, J_{HP} = 1.2 Hz, 12 H, CH*Me*$_2$), 2.03 (m, 2 H), 2.54 (dt, 2 H), 3.62 (t, 2 H) ((C*H*$_2$)$_3$), 4.72 (sd, $^{3}J_{HH}$ = 5.2 Hz, J_{HP} = 7.2 Hz, 2 H, C*H*Me$_2$). ^{13}C NMR (100 MHz, $CDCl_3$, 298 K, ppm): δ =16.6 (d, J_{CP} = 3.6 Hz), 30.1 (d, J_{CP} = 2.1 Hz), 43.1 ((*C*H$_2$)$_3$), 23.6 (d, J_{CP} = 4.0 Hz), 23.8 (d, J_{CP} = 3.6 Hz) (CH*Me*$_2$), 72.1 (d, J_{CP} = 4.4 Hz, *C*HMe$_2$), 73.1 (d, J_{CP} = 238.9 Hz, ≡*C*P), 99.5 (d, J_{CP} = 41.9 Hz, Cl(CH$_2$)$_3$*C*≡). ^{31}P ($CDCl_3$, 162 MHz, 298 K, ppm): δ = −9.16.

EtOC(O)C≡CP(O)(O*i*Pr)$_2$: ^{1}H NMR (400 MHz, $CDCl_3$, 298 K, ppm): δ = 1.33 (t, $^{3}J_{HH}$ = 5.6 Hz, 2 H, C*H*$_2$CH$_3$), 1.39 (dd, $^{3}J_{HH}$ = 5.2 Hz, J_{HP} = 2.4 Hz, 12 H, CH*Me*$_2$), 4.28 (quart, $^{3}J_{HH}$ = 5.6 Hz, 3 H, CH$_2$C*H*$_3$), 4.78 (sd, $^{3}J_{HH}$ = 5.2 Hz, J_{HP} = 4.0 Hz, 2 H, C*H*Me$_2$). ^{13}C NMR (100 MHz, $CDCl_3$, 298 K, ppm): δ = 13.9 (CH$_2$*C*H$_3$), 63.0 (*C*H$_2$CH$_3$), 23.5 (d, J_{CP} = 4.0 Hz), 23.8 (d, J_{CP} = 3.6 Hz) (CH*Me*$_2$), 73.6 (d, J_{CP} = 4.4 Hz, *C*HMe$_2$), 76.3 (d, J_{CP} = 221.8 Hz, ≡*C*P), 86.1 (d, J_{CP} = 36.7 Hz, EtOC(O)*C*≡), 151.7 (d, J_{CP} = 4.7 Hz, EtO*C*(O)). ^{31}P ($CDCl_3$, 162 MHz, 298 K, ppm): δ = −12.19.

HOCH$_2$C≡CP(O)(O*i*Pr)$_2$: ^{1}H NMR (400 MHz, $CDCl_3$, 298 K, ppm): δ =1.37 (d, $^{3}J_{HH}$ = 6.0 Hz, 12 H, CH*Me*$_2$), 4.37 (br, 2 H, C*H*$_2$), 4.75 (sd, $^{3}J_{HH}$ = 6.0 Hz, J_{HP} = 1.6 Hz, 2 H, C*H*Me$_2$). ^{13}C NMR (100 MHz, $CDCl_3$, 298 K, ppm): δ = 23.6 (d, J_{CP} = 5.0 Hz), 23.8 (d, J_{CP} = 4.5 Hz) (CH*Me*$_2$), 50.7 (d, J_{CP} = 4.7 Hz, *C*H$_2$), 72.6 (d, J_{CP} = 5.7 Hz, *C*HMe$_2$), 76.2 (d, J_{CP} = 294.8 Hz, ≡*C*P), 98.3 (d, J_{CP} = 49.7 Hz, HOCH$_2$*C*≡). ^{31}P ($CDCl_3$,162 MHz, 298 K, ppm): δ = −9.55.

FcC≡CP(O)(O*i*Pr)$_2$: ^{1}H NMR (400 MHz, $CDCl_3$, 298 K, ppm): δ = 1.40 (dd, $^{3}J_{HH}$ = 4.8 Hz, J_{CP} = 4.8 Hz,

12 H, CH*Me*$_2$), 4.24 (s, 5 H, Fc-C$_5$*H*$_5$), 4.30 (m, 2 H), 4.55 (m, 2 H) (Fc-C$_5$*H*$_4$), 4.82 (sd, $^3J_{HH}$ = 4.8 Hz, J_{CP} = 7.2 Hz, 2 H, C*H*Me$_2$). ^{13}C NMR (100 MHz, CDCl$_3$, 298 K, ppm): δ = 23.6 (d, J_{CP} = 4.0 Hz), 23.9 (d, J_{CP} = 3.6 Hz) (CH*Me*$_2$), 70.0, 70.3, 72.4 (d, J_{CP} = 1.8 Hz) (Fc-*C*$_5$H$_5$ and *C*$_5$H$_4$), 71.9 (d, J_{CP} = 4.3 Hz, *C*HMe$_2$), 76.4 (d, J_{CP} = 240.7 Hz, ≡*C*P), 99.6 (d, J_{CP} = 43.6 Hz, Fc*C*≡). ^{31}P (CDCl$_3$,162 MHz, 298 K, ppm): δ = −8.02.

1,4-[(*i*PrO)$_2$(O)PC≡C]$_2$C$_6$H$_4$: ^{1}H NMR (400 MHz, CDCl$_3$, 298 K, ppm): δ = 1.41 (dd, $^3J_{HH}$ = 5.2 Hz, J_{HP} = 2.0 Hz, 24 H, CH*Me*$_2$), 4.82 (sd, $^3J_{HH}$ = 5.2 Hz, J_{HP} = 6.4 Hz, 4 H, C*H*Me$_2$), 7.27 (s, 2 H), 7.54 (s, 2 H) (C$_6$*H*$_4$). ^{13}C NMR (100 MHz, CDCl$_3$, 298 K, ppm): δ = 23.6 (d, J_{CP} = 3.7 Hz), 23.9 (d, J_{CP} = 3.7 Hz) (CH*Me*$_2$), 72.6 (d, J_{CP} = 4.6 Hz, *C*HMe$_2$), 82.8 (d, J_{CP} = 235.5 Hz, P*C*≡), 96.3 (d, J_{CP} = 41.4 Hz, ≡*C*C$_6$H$_4$), 121.9 (d, J_{CP} = 4.6 Hz), 128.8, 130.9, 132.5 (d, J_{CP} = 1.8 Hz) (*C*$_6$H$_4$). ^{31}P (CDCl$_3$,162 MHz, 298 K, ppm): δ = −9.30.

PhC≡CP(O)(OEt)$_2$: ^{1}H NMR (400 MHz, CDCl$_3$, 298 K, ppm): δ = 1.41 (t, $^3J_{HH}$ = 7.2 Hz, 6 H, CH$_2$C*H*$_3$), 4.24 (m, $^3J_{HH}$ = 7.2 Hz, 4 H, C*H*$_2$CH$_3$), 7.34−7.59 (m, 5 H, *Ph*). ^{13}C NMR (100 MHz, CDCl$_3$, 298 K, ppm): δ = 16.3 (d, J_{CP} = 6.0 Hz, CH$_2$*C*H$_3$), 63.4 (d, J_{CP} = 5.3 Hz, *C*H$_2$CH$_3$), 78.8 (d, J_{CP} = 264.1 Hz, ≡*C*P), 99.3 (d, J_{CP} = 52.6 Hz, Ph*C*≡), 119.8 (d, J_{CP} = 5.8 Hz), 128.8, 130.9, 132.9 (d, J_{CP} = 2.0 Hz) (*Ph*). ^{31}P (CDCl$_3$,162 MHz, 298 K, ppm): δ = −5.98.

***n*BuC≡CP(O)(OEt)$_2$**: ^{1}H NMR (400 MHz, CDCl$_3$, 298 K, ppm): δ = 0.93 (t, 3 H), 1.44 (m, 2 H), 1.57 (m, 2 H), 2.36 (dt, 2 H) (*nBu*), 1.39 (t, $^3J_{HH}$ = 5.6 Hz, 6 H, CH$_2$C*H*$_3$), 4.15 (td, $^3J_{HH}$ = 5.6 Hz, J_{HP} = 6.8 Hz, 4 H, C*H*$_2$CH$_3$). ^{13}C NMR (100 MHz, CDCl$_3$, 298 K, ppm): δ = 13.4, 16.1 (d, J_{CP} = 5.6 Hz), 18.9 (d, J_{CP} = 3.6 Hz), 21.9 (*nBu*), 29.5 (CH$_2$*C*H$_3$), 62.9 (d, J_{CP} = 4.3 Hz, *C*H$_2$CH$_3$), 70.5 (d, J_{CP} = 241.0 Hz, ≡*C*P), 103.1 (d, J_{CP} = 42.0 Hz, *n*Bu*C*≡). ^{31}P (CDCl$_3$, 162MHz, 298 K, ppm): δ = −6.08.

Cl(CH$_2$)$_3$C≡CP(O)(OEt)$_2$: ^{1}H NMR (400 MHz, CDCl$_3$, 298 K, ppm): δ = 1.37 (t, $^3J_{HH}$ = 5.6 Hz, 6 H, CH$_2$C*H*$_3$), 2.04 (m, 2 H), 2.57 (m, 2 H), 3.64 (t, 2 H) ((C*H*$_2$)$_3$), 4.11–4.17 (td, $^3J_{HH}$ = 5.6 Hz, J_{HP} = 8.0 Hz, 4 H). ^{13}C NMR (100 MHz, CDCl$_3$, 298 K, ppm): δ = 16.3 (d, J_{CP} = 5.6 Hz), 16.9 (d, J_{CP} = 3.6 Hz), 30.3 (d, J_{CP} = 1.8 Hz) ((*C*H$_2$)$_3$), 43.3 (CH$_2$*C*H$_3$), 63.2 (d, J_{CP} = 4.4 Hz, *C*H$_2$CH$_3$), 71.9 (d, J_{CP} = 239.5 Hz, ≡*C*P), 100.8 (d, J_{CP} = 41.9 Hz, Cl(CH$_2$)$_3$*C*≡). ^{31}P (CDCl$_3$, 162MHz, 298 K, ppm): δ = −6.67.

PhC≡CP(O)(O*n*Bu)$_2$: ^{1}H NMR (400 MHz, CDCl$_3$, 298 K, ppm): δ = 0.95 (t, 6 H), 1.46 (m, 4 H), 1.73 (m, 4 H), 4.15 (m, 4 H) (*nBu*), 7.30–7.60 (m, 5 H, *Ph*). ^{13}C NMR (100 MHz, CDCl$_3$, 298 K, ppm): δ = 13.6, 18.7, 32.2 (d, J_{CP} = 7.1 Hz), 66.9 (d, J_{CP} = 5.8 Hz) (*nBu*), 78.5 (d, J_{CP} = 259.7 Hz, ≡*C*P), 99.1 (d, J_{CP} = 52.3 Hz, Ph*C*≡), 119.6 (d, J_{CP} = 5.2 Hz), 128.6, 130.7, 132.6 (d, J_{CP} = 2.4 Hz) (*Ph*). ^{31}P (CDCl$_3$,162 MHz, 298 K, ppm): δ = −5.74.

***n*BuC≡CP(O)(O*n*Bu)$_2$**: ^{1}H NMR (400 MHz, CDCl$_3$, 298 K, ppm): δ = 0.93 (t, 6 H), 1.41 (m, 4 H), 1.55 (m, 2 H), 1.68 (m, 2 H), 2.34 (m, 2 H), 4.05 (quart, 2 H) (*nBu*C and O*nBu*). ^{13}C NMR (100 MHz, CDCl$_3$, 298 K, ppm): δ = 13.4, 18.9 (d, J_{CP} = 3.6 Hz), 21.9, 29.4 (*nBu*C), 13.5, 18.7, 32.2 (d, J_{CP} = 5.6 Hz), 66.5 (d, J_{CP} = 4.5 Hz) (O*nBu*), 70.5 (d, J_{CP} = 240.5 Hz, ≡*C*P), 103.0 (d, J_{CP} = 41.9 Hz, *n*Bu*C*≡). ^{31}P (CDCl$_3$, 162 MHz, 298 K, ppm): δ = −6.43.

Cl(CH$_2$)$_3$C≡CP(O)(O*n*Bu)$_2$: ^{1}H NMR (400 MHz, CDCl$_3$, 298 K, ppm): δ = 0.94 (t, 6 H), 1.43 (m, 4 H), 1.69 (m, 4 H), 4.07 (m, 4 H) (*nBu*), 2.04 (m, 2 H), 2.55 (m, 2 H), 3.64 (t, 2 H) ((C*H*$_2$)$_3$). ^{13}C NMR (100 MHz, CDCl$_3$, 298 K, ppm): δ = 13.5, 32.2 (d, J_{CP} = 5.6 Hz), 43.1, 66.6 (d, J_{CP} = 4.7 Hz) (*nBu*), 16.6 (d, J_{CP} = 3.7 Hz), 18.7, 30.1 (d, J_{CP} = 1.7 Hz) ((*C*H$_2$)$_3$), 71.7 (d, J_{CP} = 239.4 Hz, P*C*≡), 100.5 (d, J_{CP} = 41.7 Hz, ≡*C*(CH$_2$)$_3$Cl). ^{31}P (CDCl$_3$, 162 MHz, 298 K, ppm): δ = −6.29.

PhC≡CP(O)(OCH$_2$Ph)$_2$: ^{1}H NMR (400 MHz, $CDCl_3$, 298 K, ppm): δ = 5.18 (d, J_{HP} = 7.2 Hz, 4 H, C*H*$_2$), 7.30−7.55 (m, 15 H, Ph). ^{13}C NMR (100 MHz, $CDCl_3$, 298 K, ppm): δ = 68.7 (d, J_{CP} = 5.1 Hz, *C*H$_2$), 78.5 (d, J_{CP} = 236.9 Hz, P*C*≡), 100.1 (d, J_{CP} = 43.6 Hz, ≡*C*Ph), 119.5 (d, J_{CP} = 5.7 Hz), 128.2, 128.7 (m), 131.0, 132.9 (d, J_{CP} = 2.4 Hz), 135.7 (d, J_{CP} = 7.1 Hz) (*Ph*). ^{31}P ($CDCl_3$, 162 MHz,): δ = −5.47.

***n*BuC≡CP(O)(OCH$_2$Ph)$_2$**: ^{1}H NMR (400 MHz, $CDCl_3$, 298 K, ppm): δ = 0.91 (t, 3 H), 1.40 (m, 2 H), 1.53 (m, 2 H), 2.32 (td, J_{HP} = 4.8 Hz, 2 H) (*nBu*), 5.09 (d, J_{HP} = 8.8 Hz, 4 H, C*H*$_2$Ph), 7.30−7.40 (m, 10 H, *Ph*). ^{13}C NMR (100 MHz, $CDCl_3$, 298 K, ppm): δ = 13.4, 18.9 (d, J_{CP} = 4.4 Hz), 21.9, 29.3 (d, J_{CP} = 2.1 Hz) (*nBu*), 68.2 (d, J_{CP} = 4.9 Hz, *C*H$_2$Ph), 70.5 (d, J_{C-P} = 246.7 Hz, P*C*≡), 104.1 (d, J_{CP} = 53.7 Hz, ≡*Cn*Bu), 127.9, 128.4, 128.5, 135.7 (d, J_{CP} = 7.4 Hz) (*Ph*). ^{31}P ($CDCl_3$, 162 MHz, 298 K, ppm): δ = −5.64.

Cl(CH$_2$)$_3$C≡CP(O)(OCH$_2$Ph)$_2$: ^{1}H NMR (400 MHz, $CDCl_3$, 298 K, ppm): δ = 1.97 (m, 2 H), 2.51 (tb, 2 H), 3.56 (t, 2 H) ((C*H*$_2$)$_3$), 5.08 (d, J_{H-P} = 7.2 Hz, 4 H, C*H*$_2$), 7.31−7.38 (m, 10 H, *Ph*). ^{13}C NMR (100 MHz, $CDCl_3$, 298 K, ppm): δ = 16.6 (d, J_{CP} = 3.7 Hz), 30.0, 43.0 ((*C*H$_2$)$_3$), 68.4 (d, J_{CP} = 4.3 Hz, *C*H$_2$Ph), 71.4 (d, J_{CP} = 244.0 Hz, ≡*C*P), 101.5 (d, J_{CP} = 42.7 Hz, Cl(CH$_2$)$_3$*C*≡), 127.1, 128.5, 128.6, 135.5 (d, J_{CP} = 5.6 Hz) (*Ph*). ^{31}P ($CDCl_3$, 162 MHz, 298 K, ppm): δ = −6.26.

VII. Collected ^{1}H, ^{13}C, and ^{31}P NMR spectra of the product compounds

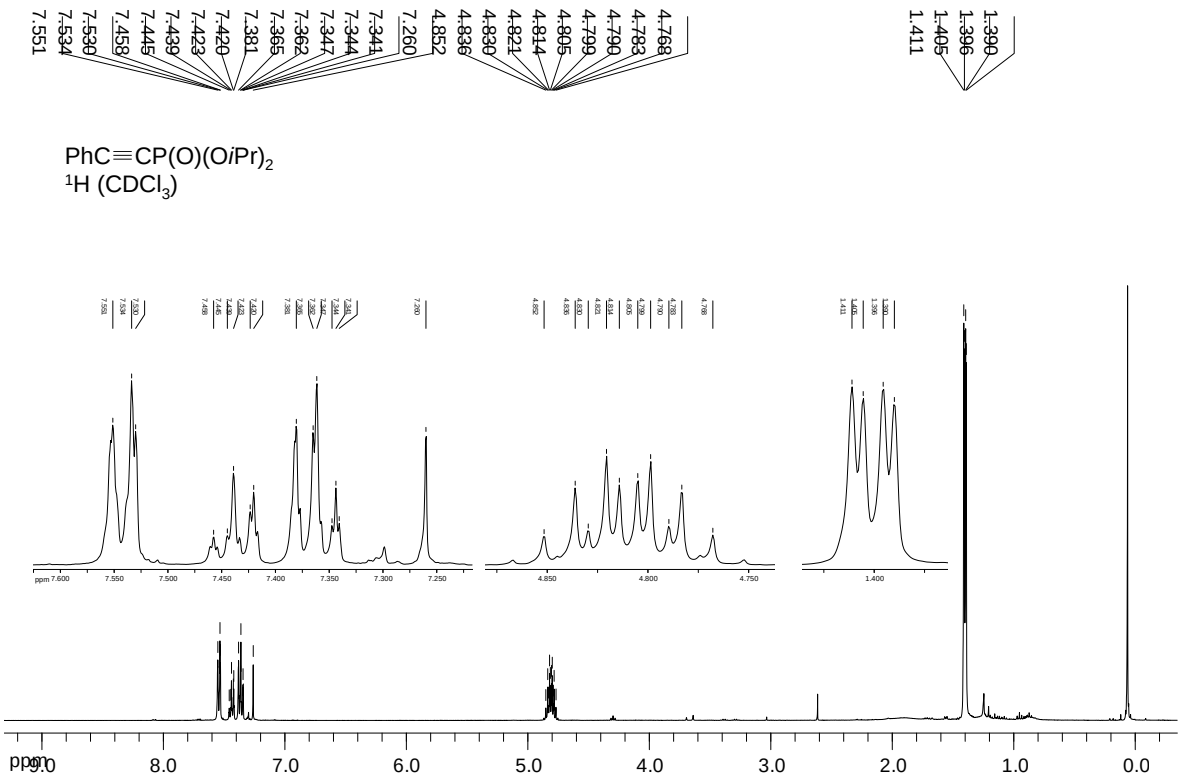

Figure S13 ^{1}H NMR spectrum of PhC≡CP(O)(O*i*Pr)$_2$ in $CDCl_3$ at 298K.

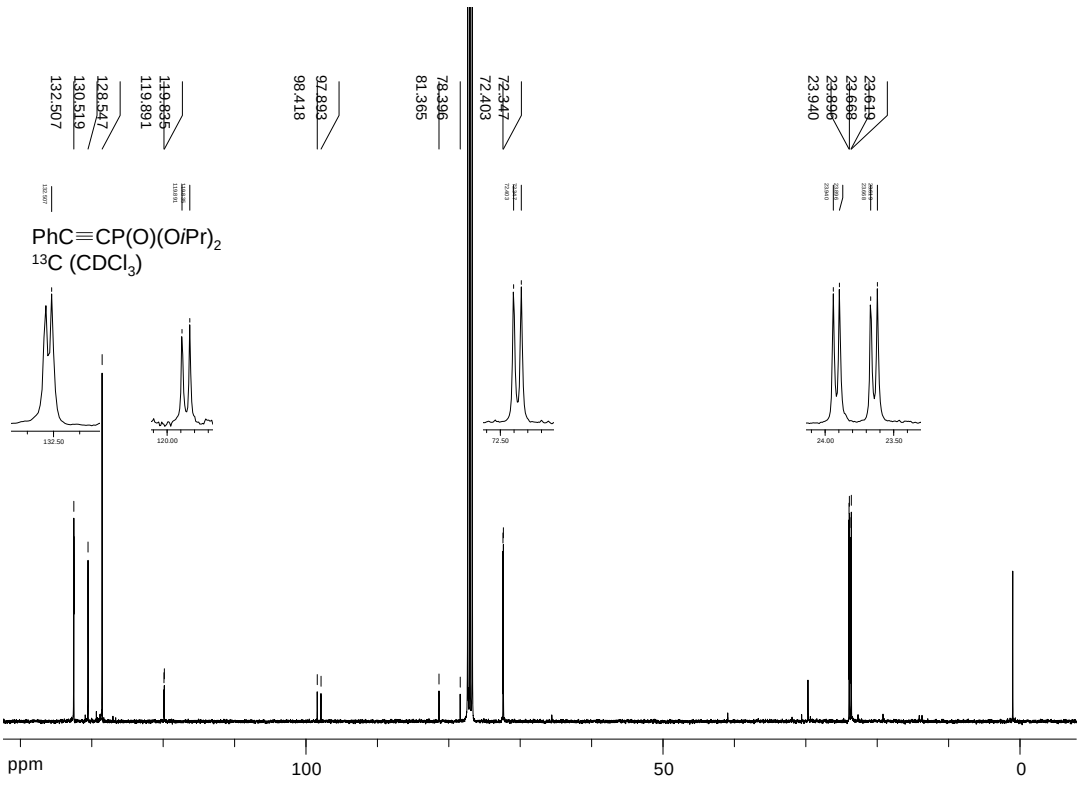

Figure S14 ^{13}C NMR spectrum of PhC≡CP(O)(O*i*Pr)$_2$ in $CDCl_3$ at 298K.

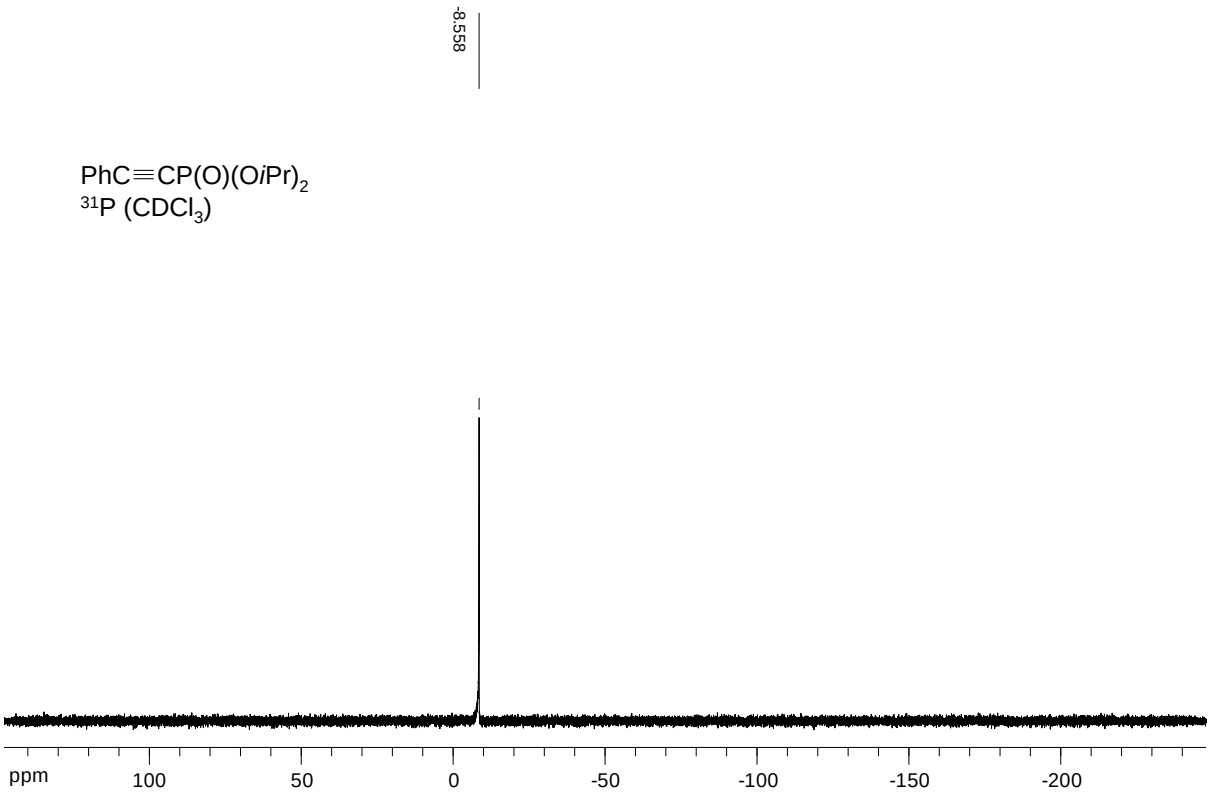

Figure S15 ^{31}P NMR spectrum of PhC≡CP(O)(O*i*Pr)$_2$ in $CDCl_3$ at 298K.

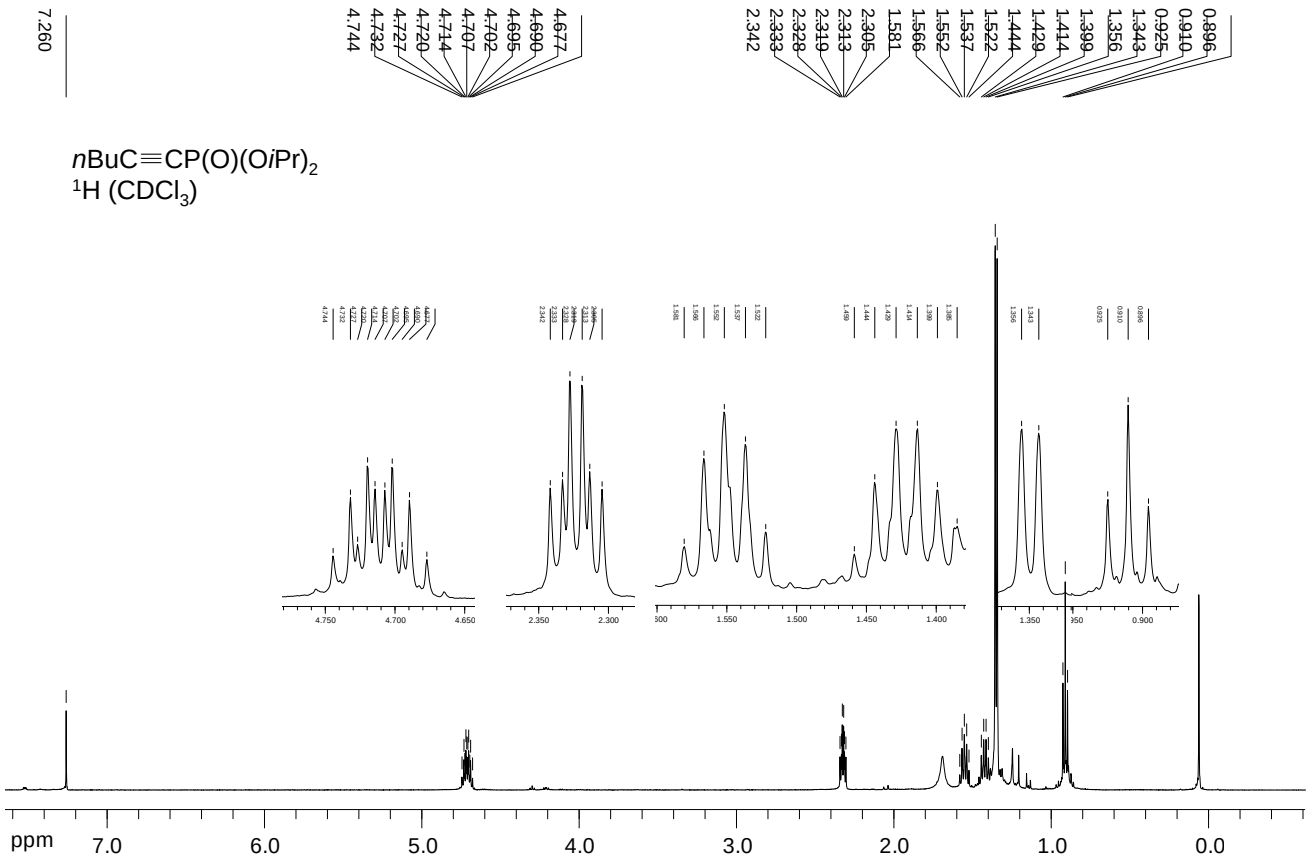

Figure S16 ^{1}H NMR spectrum of *n*BuC≡CP(O)(O*i*Pr)$_2$ in $CDCl_3$ at 298K.

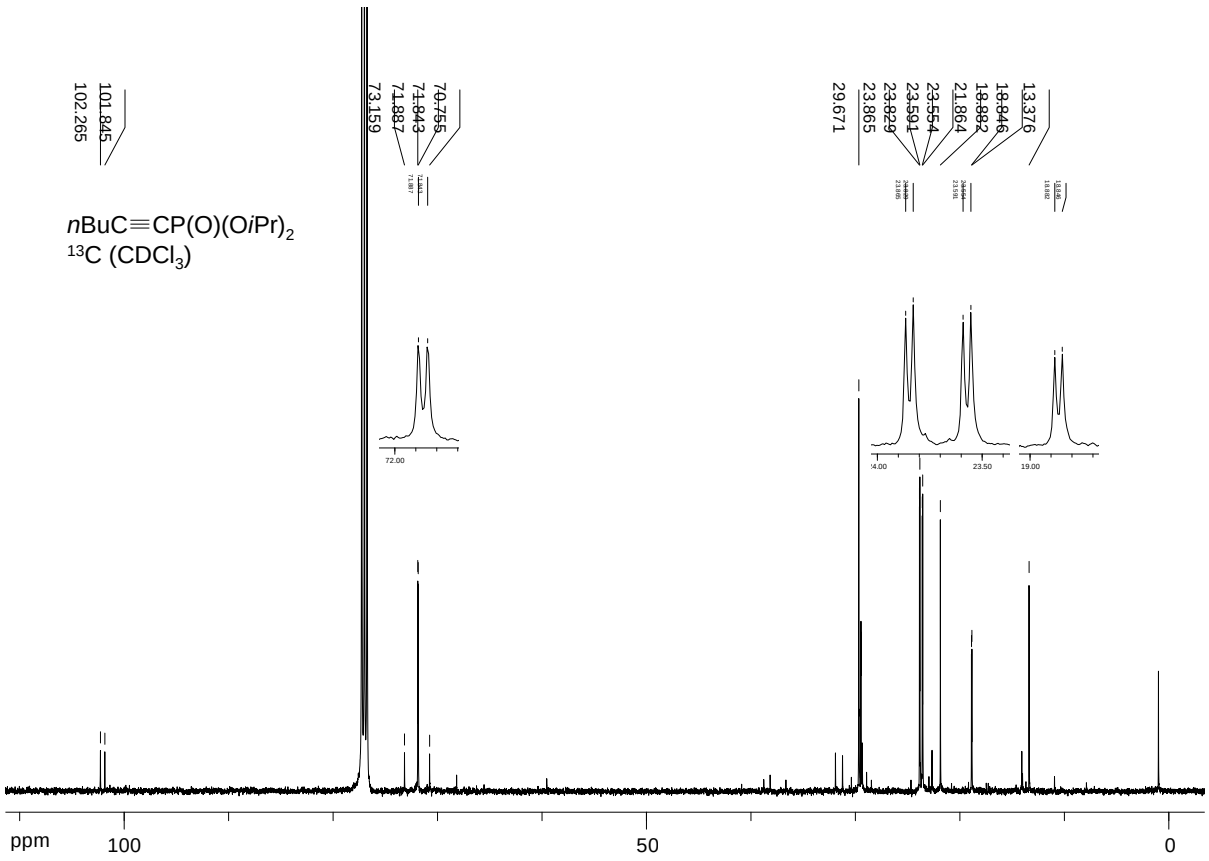

Figure S17 ^{13}C NMR spectrum of *n*BuC≡CP(O)(O*i*Pr)$_2$ in $CDCl_3$ at 298K.

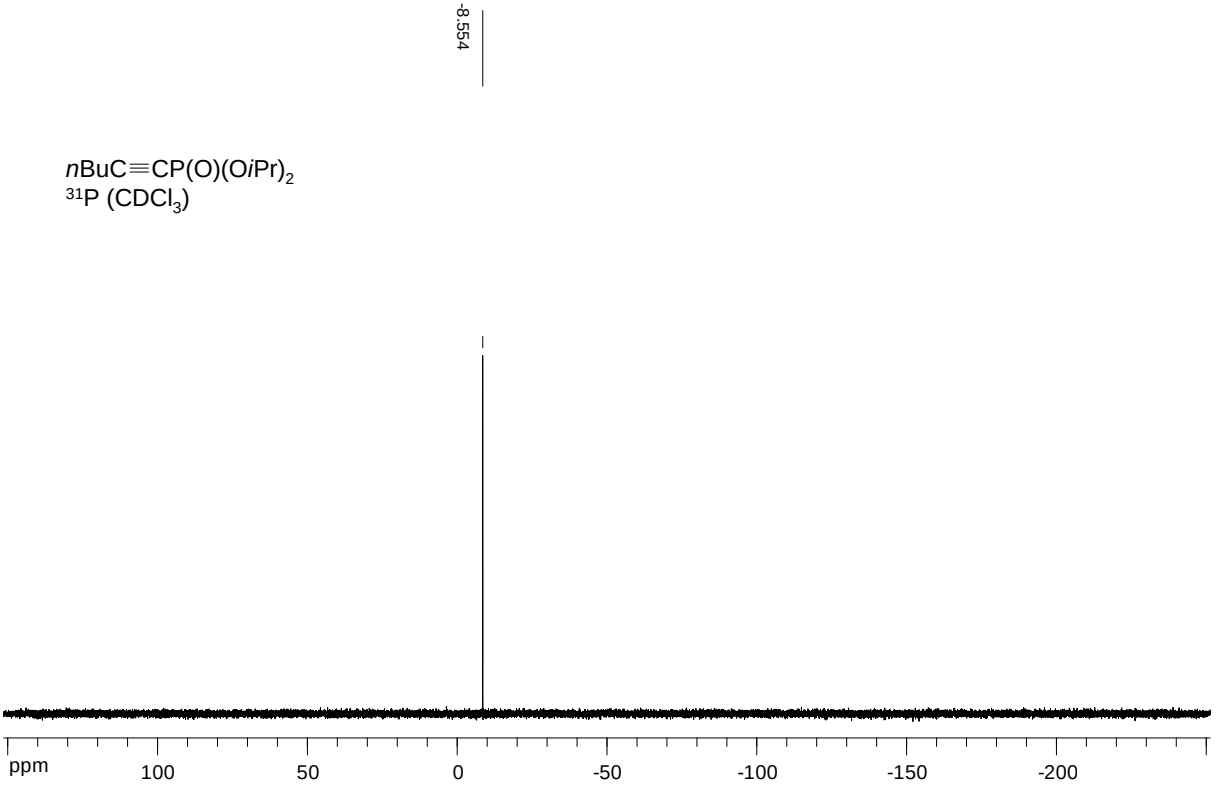

Figure S18 ^{31}P NMR spectrum of *n*BuC≡CP(O)(O*i*Pr)$_2$ in $CDCl_3$ at 298K.

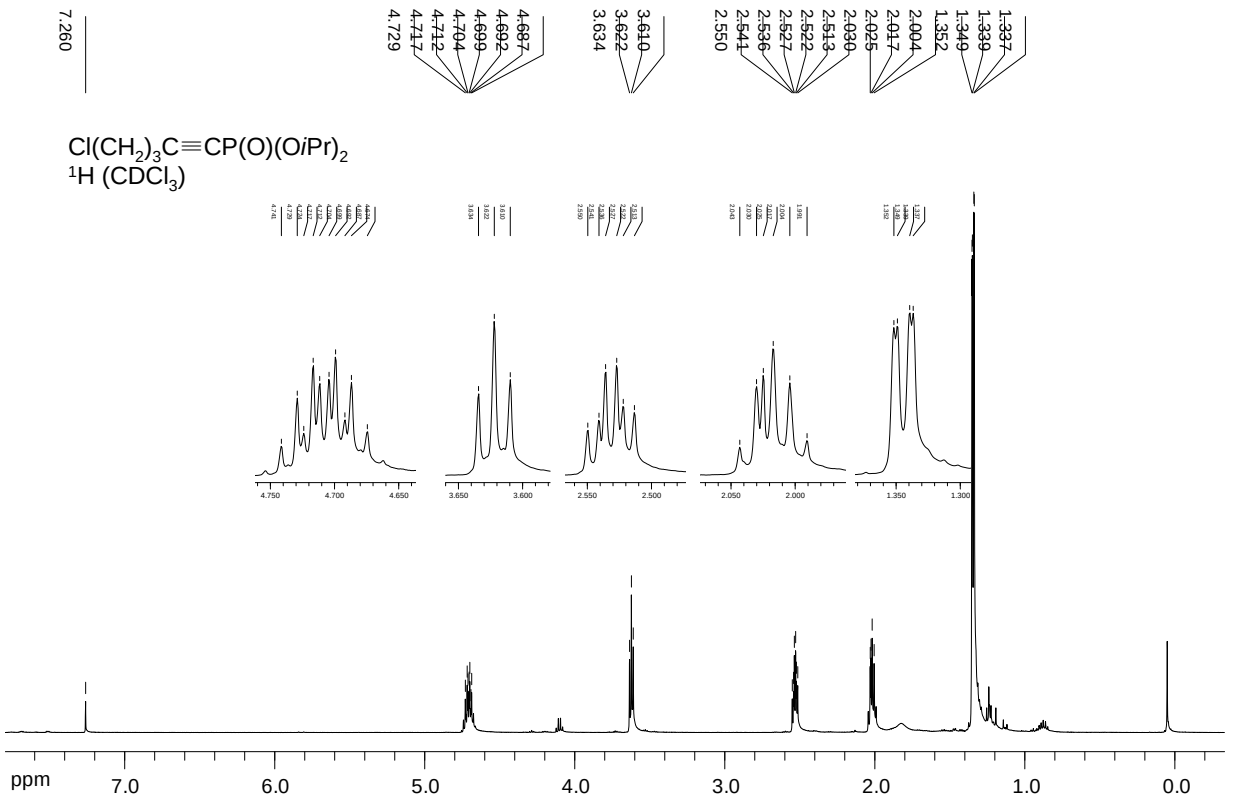

Figure S19 ^{1}H NMR spectrum of $Cl(CH_2)_3C{\equiv}CP(O)(O\textit{i}Pr)_2$ in $CDCl_3$ at 298K.

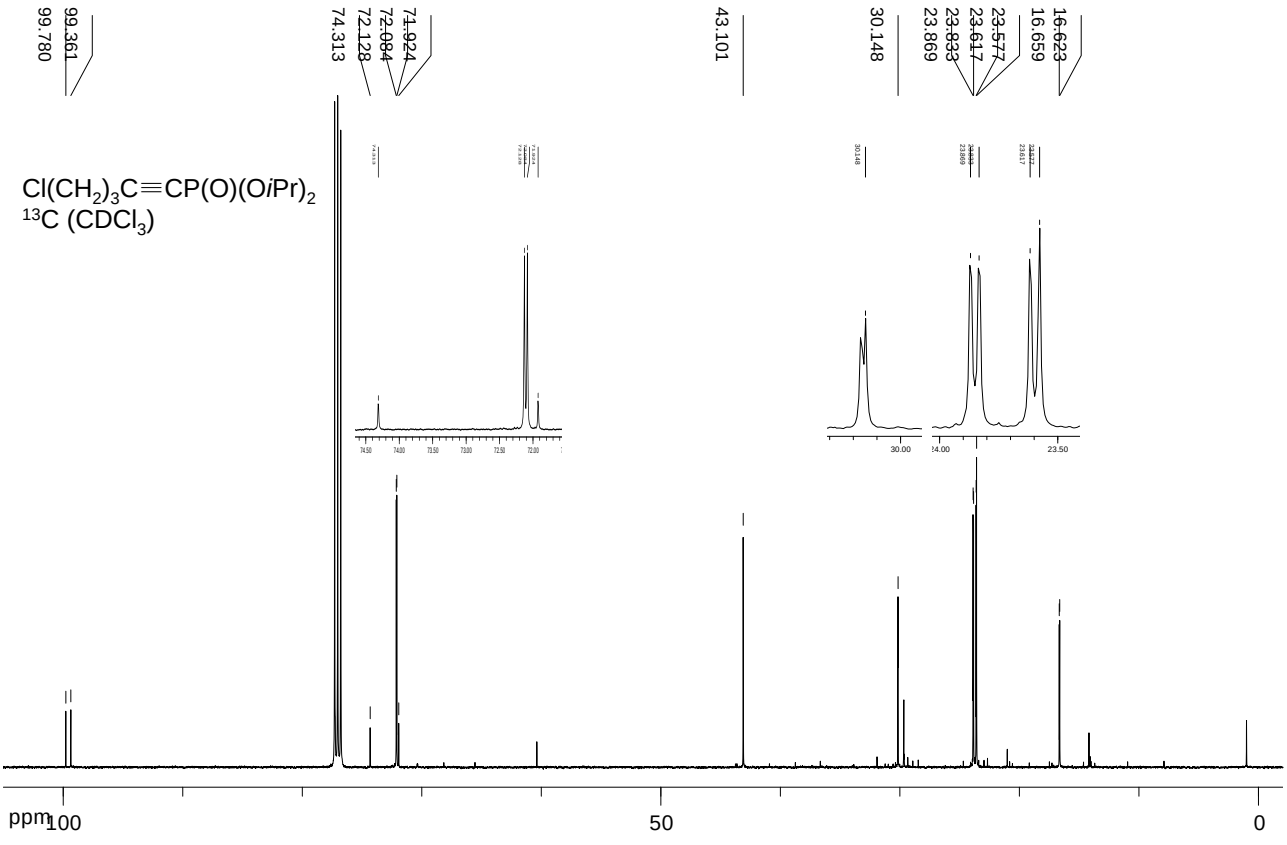

Figure S20 ^{13}C NMR spectrum of $Cl(CH_2)_3C{\equiv}CP(O)(O\textit{i}Pr)_2$ in $CDCl_3$ at 298K.

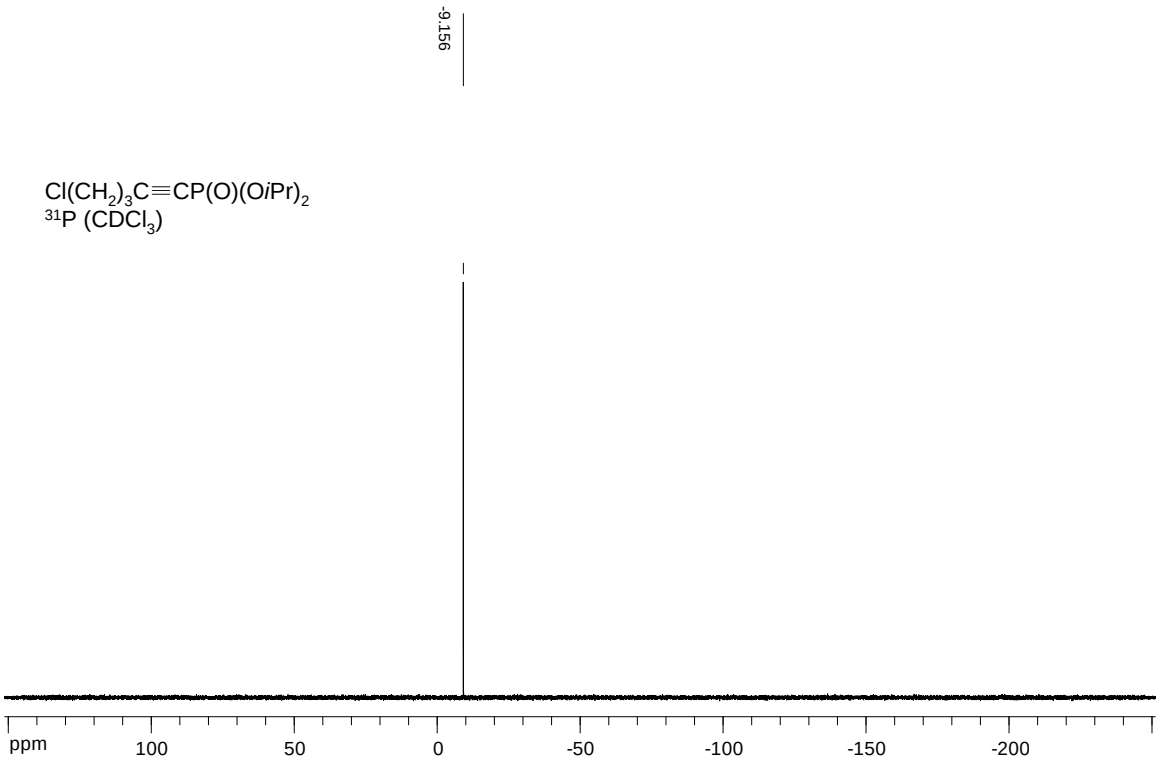

Figure S21 ^{31}P NMR spectrum of $Cl(CH_2)_3C{\equiv}CP(O)(O\textit{i}Pr)_2$ in $CDCl_3$ at 298K.

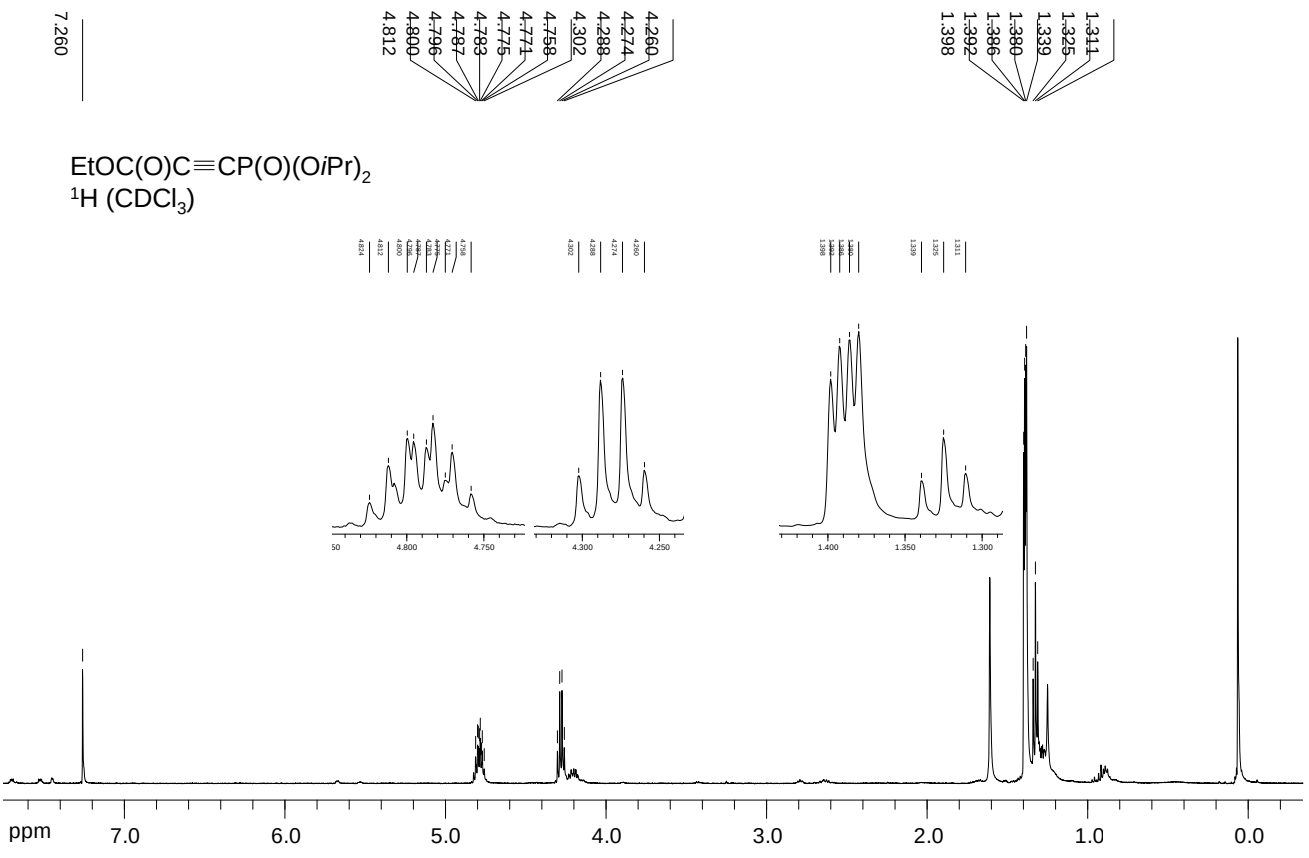

Figure S22 ^{1}H NMR spectrum of $EtOC(O)C{\equiv}CP(O)(O\textit{i}Pr)_2$ in $CDCl_3$ at 298K.

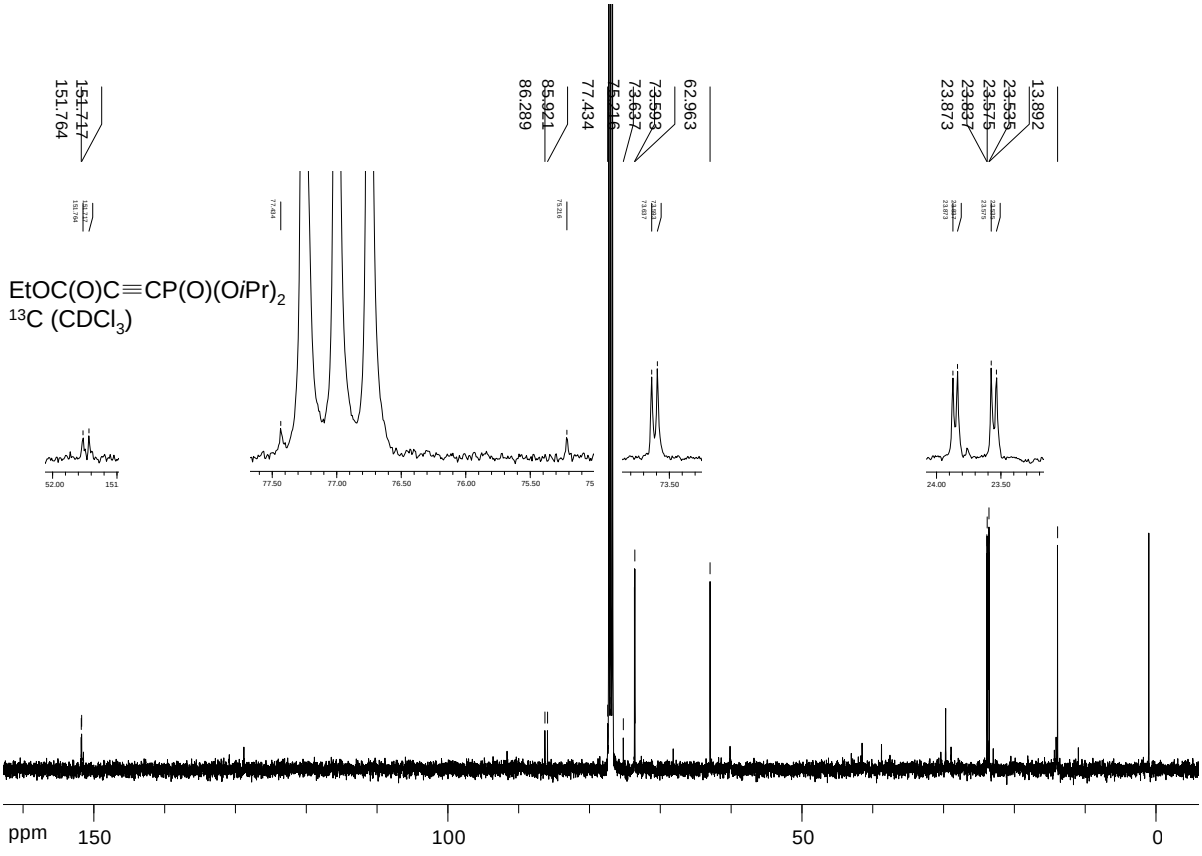

Figure S23 ^{13}C NMR spectrum of EtOC(O)C≡CP(O)(O*i*Pr)$_2$ in $CDCl_3$ at 298K.

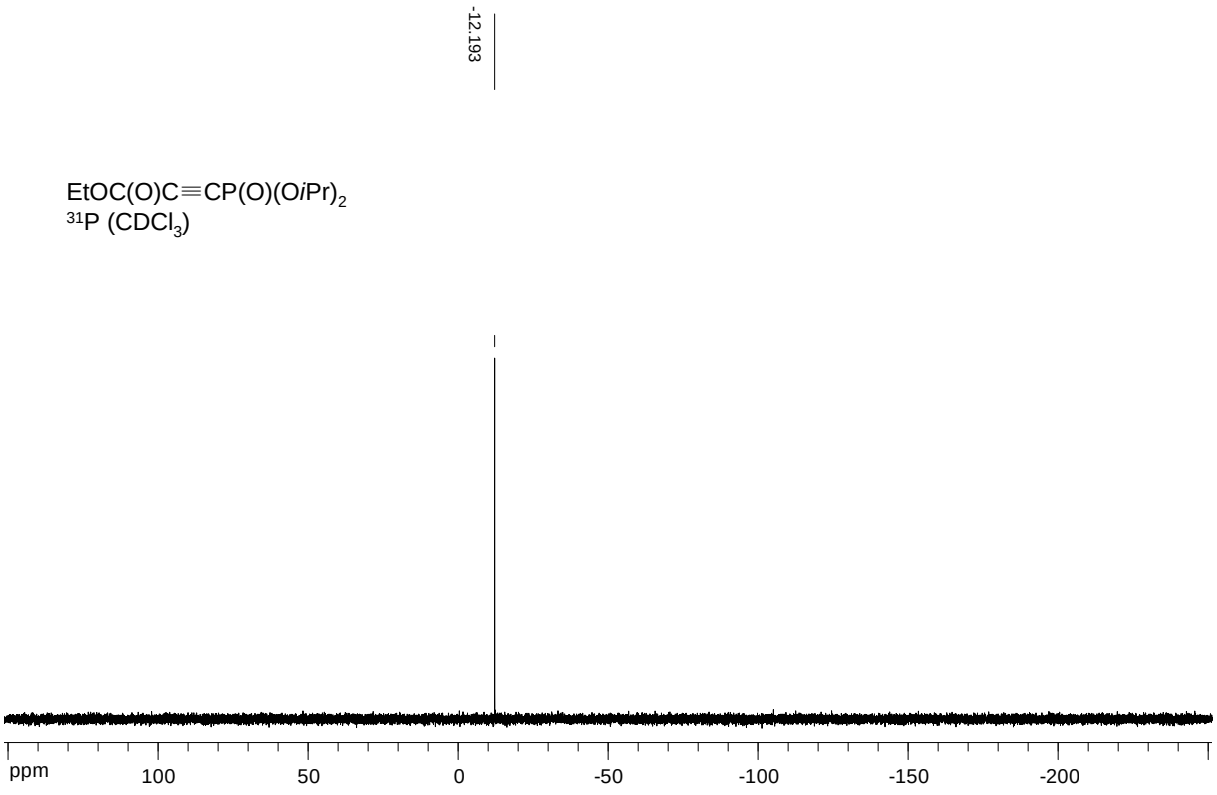

Figure S24 ^{31}P NMR spectrum of EtOC(O)C≡CP(O)(O*i*Pr)$_2$ in $CDCl_3$ at 298K.

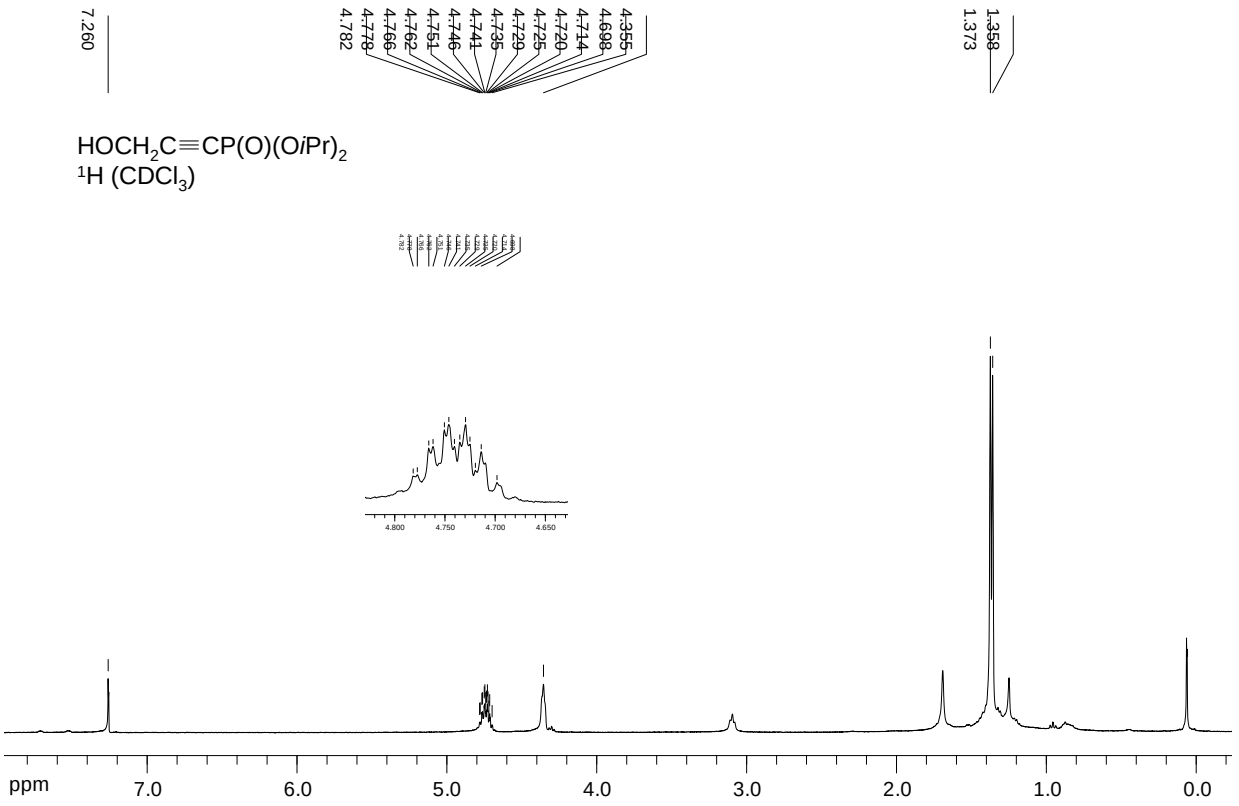

Figure S25 ^{1}H NMR spectrum of $HOCH_2C{\equiv}CP(O)(OiPr)_2$ in $CDCl_3$ at 298K.

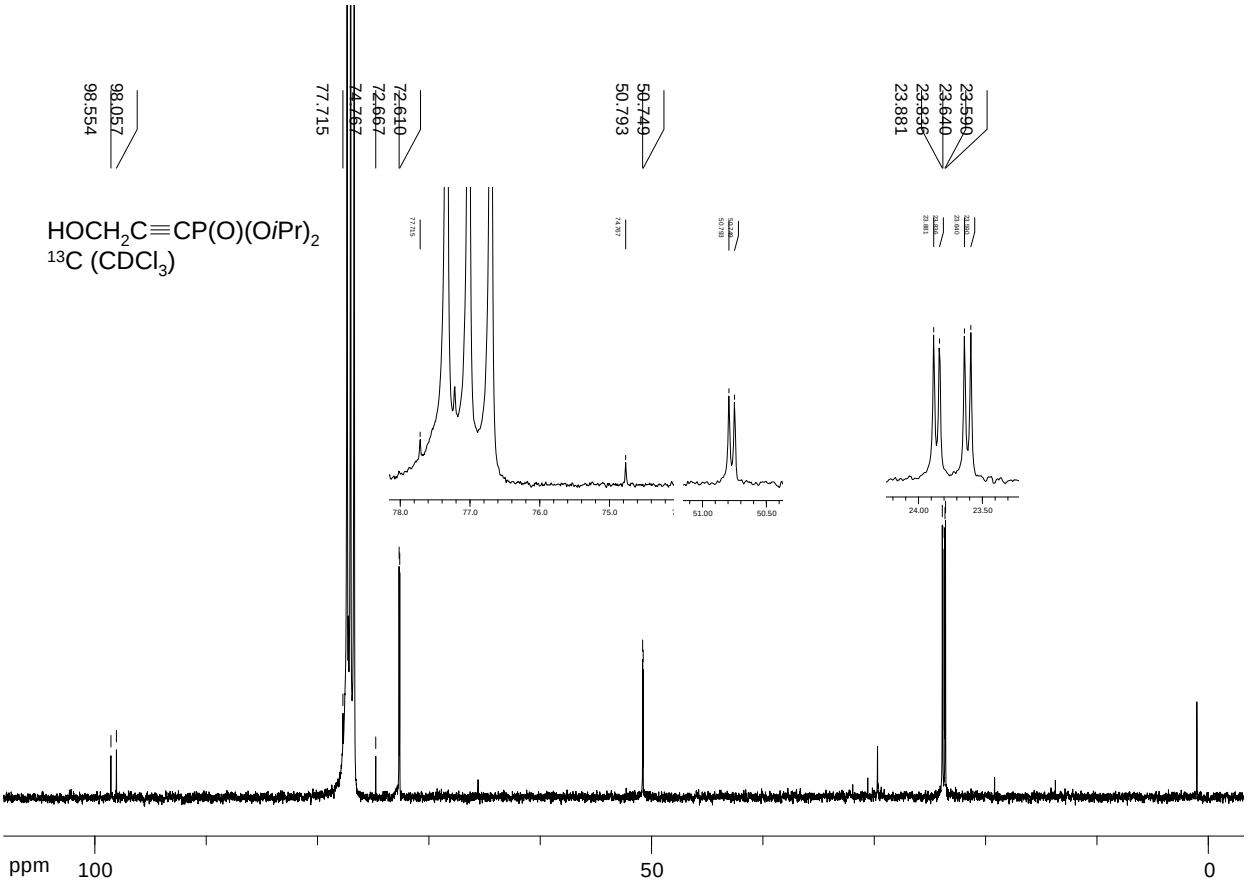

Figure S26 ^{13}C NMR spectrum of $HOCH_2C{\equiv}CP(O)(OiPr)_2$ in $CDCl_3$ at 298K.

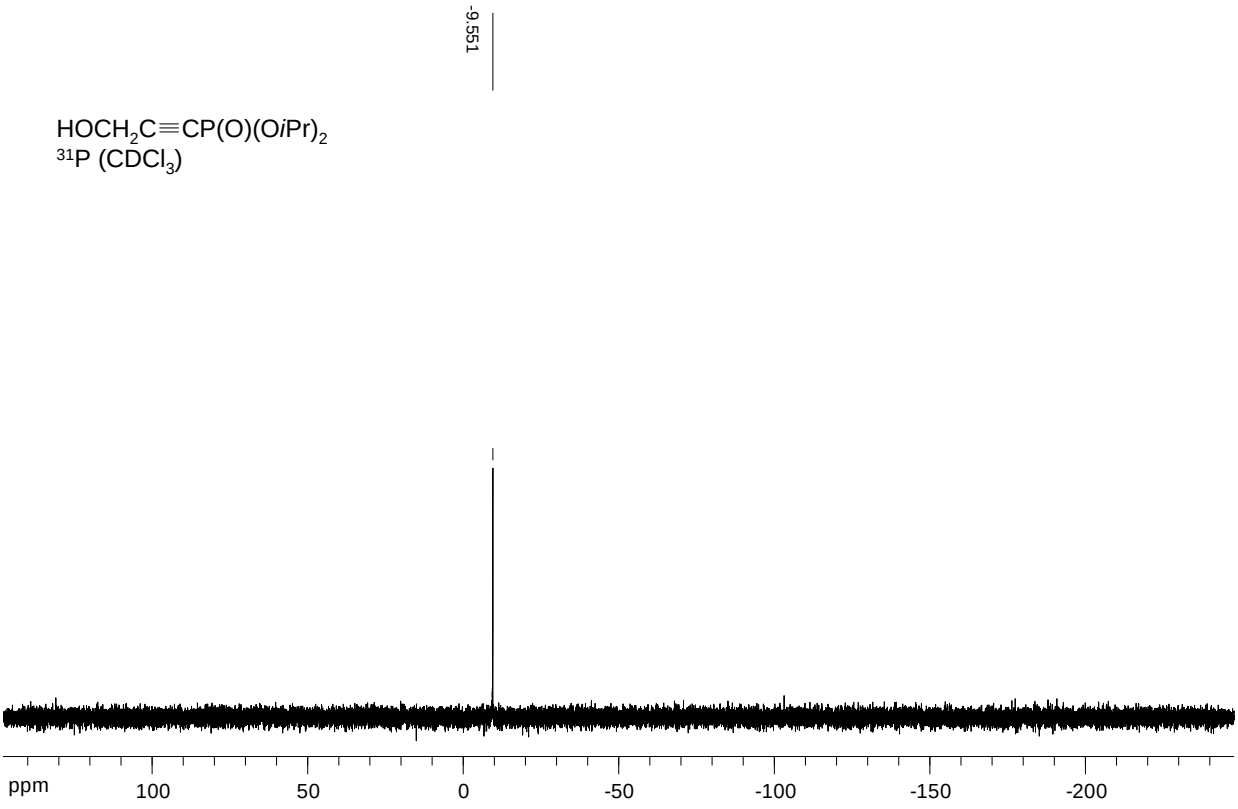

Figure S27 ^{31}P NMR spectrum of $HOCH_2C{\equiv}CP(O)(OiPr)_2$ in $CDCl_3$ at 298K.

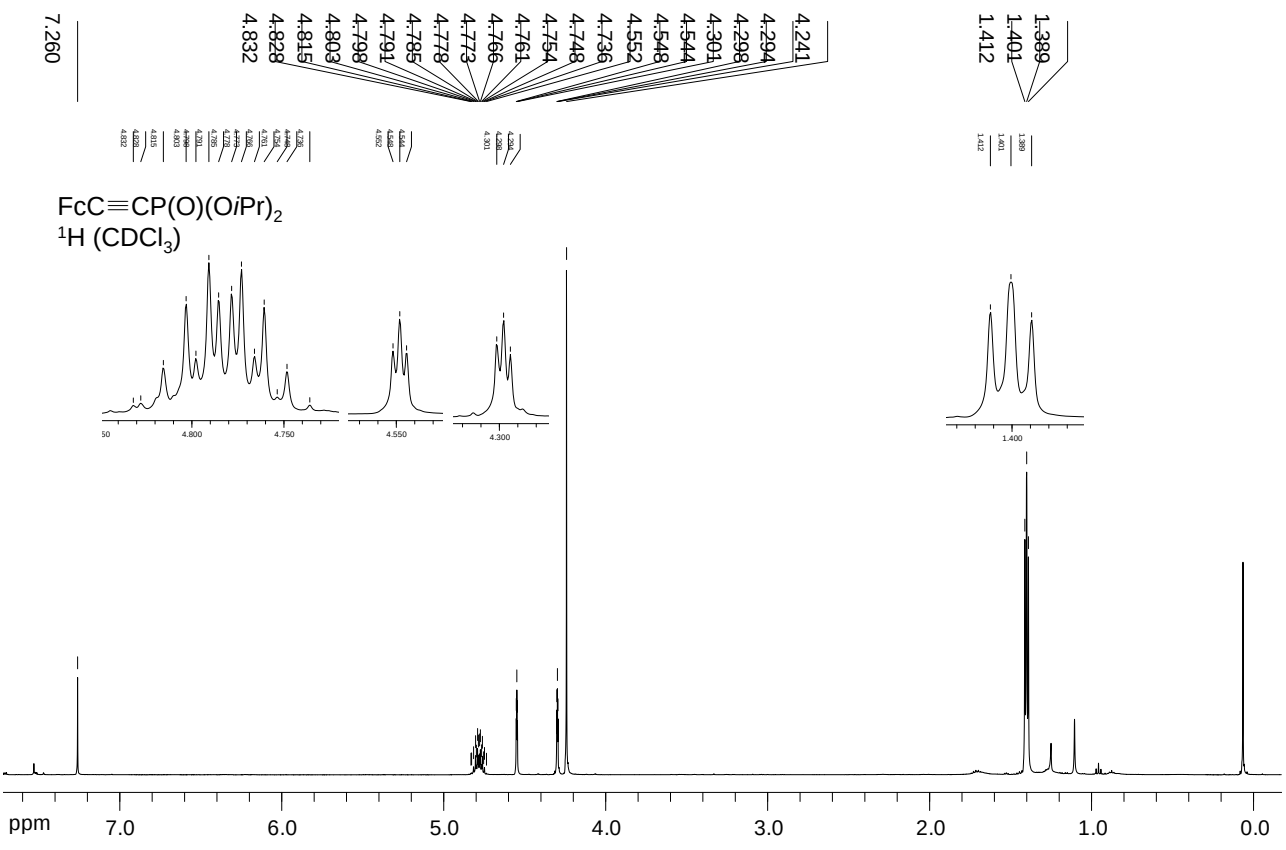

Figure S28 ^{1}H NMR spectrum of $FcC{\equiv}CP(O)(OiPr)_2$ in $CDCl_3$ at 298K.

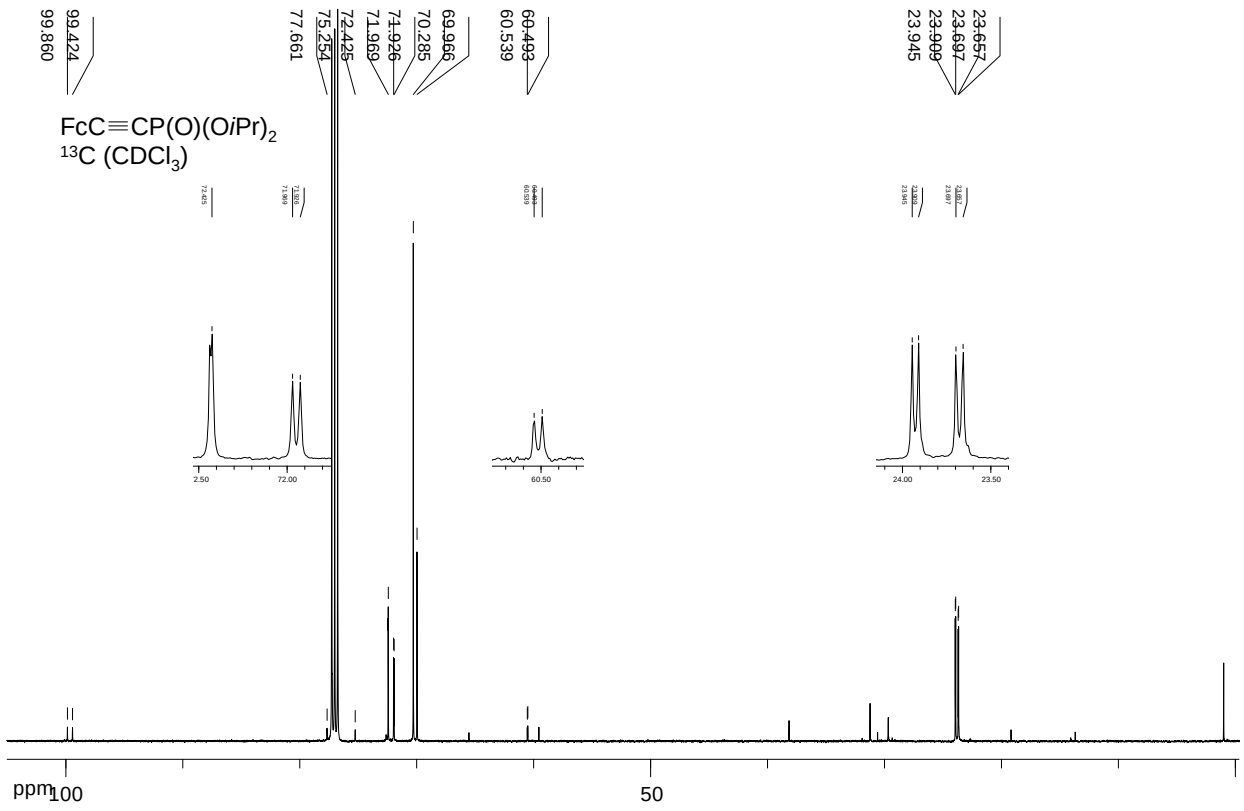

Figure S29 ^{13}C NMR spectrum of FcC≡CP(O)(O*i*Pr)$_2$ in $CDCl_3$ at 298K.

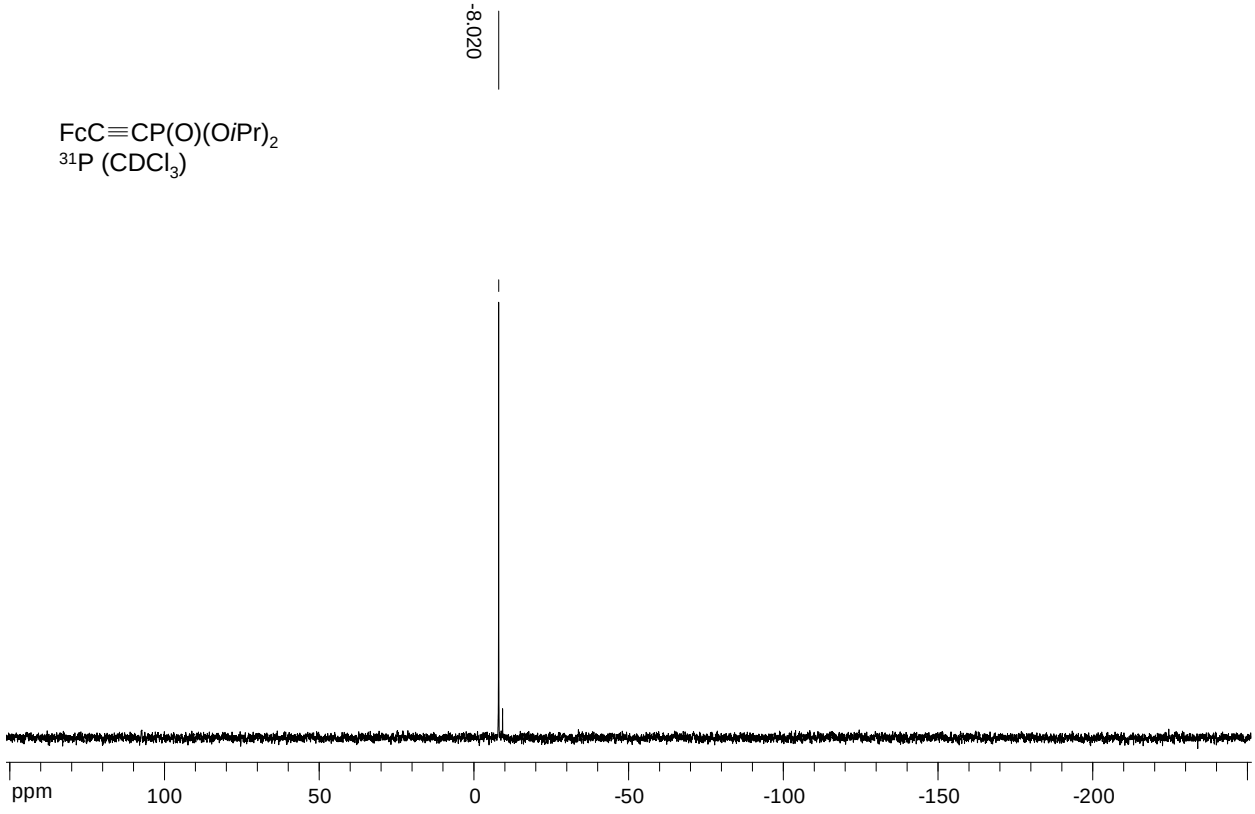

Figure S30 ^{31}P NMR spectrum of FcC≡CP(O)(O*i*Pr)$_2$ in $CDCl_3$ at 298K.

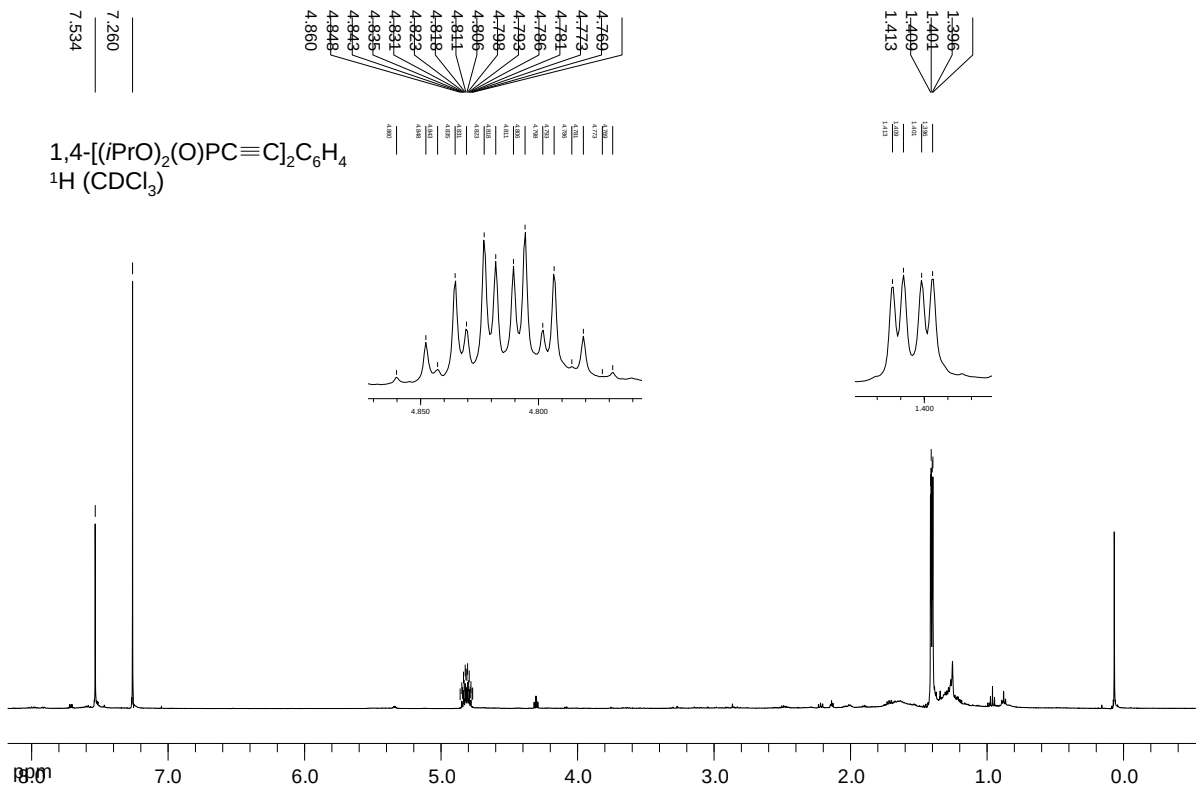

Figure S31 ^{1}H NMR spectrum of 1,4-[(*i*PrO)$_2$(O)PC≡C]$_2$C$_6$H$_4$ in $CDCl_3$ at 298K.

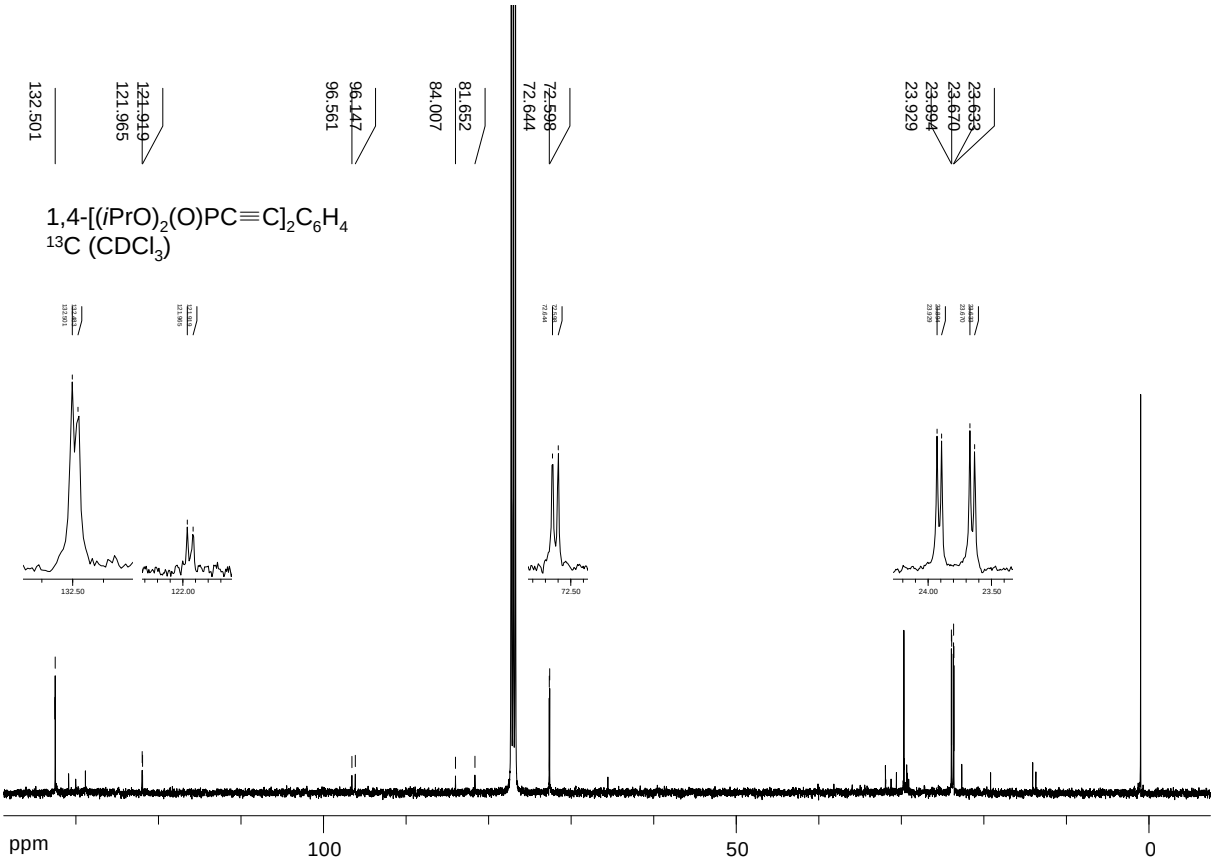

Figure S32 ^{13}C NMR spectrum of 1,4-[(*i*PrO)$_2$(O)PC≡C]$_2$C$_6$H$_4$ in $CDCl_3$ at 298K.

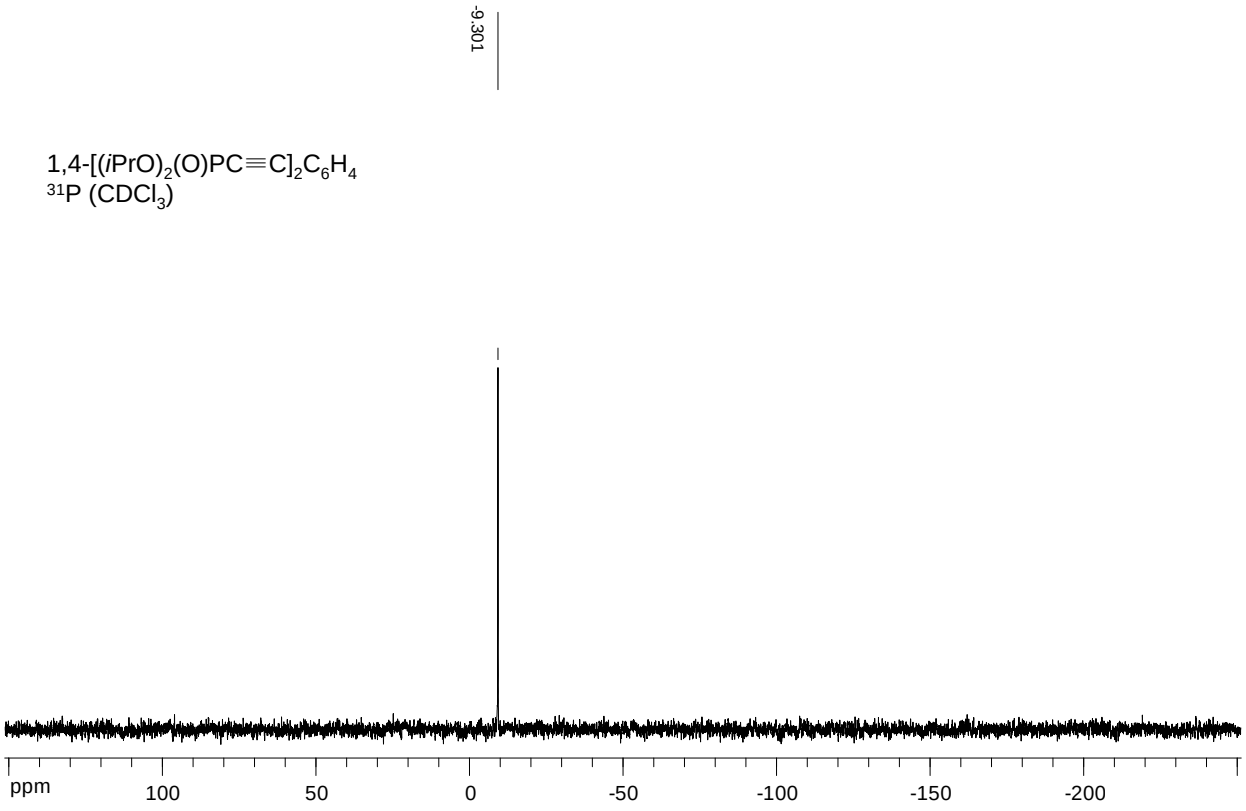

Figure S33 ^{1}H NMR spectrum of 1,4-[(*i*PrO)$_2$(O)PC≡C]$_2$C$_6$H$_4$ in $CDCl_3$ at 298K.

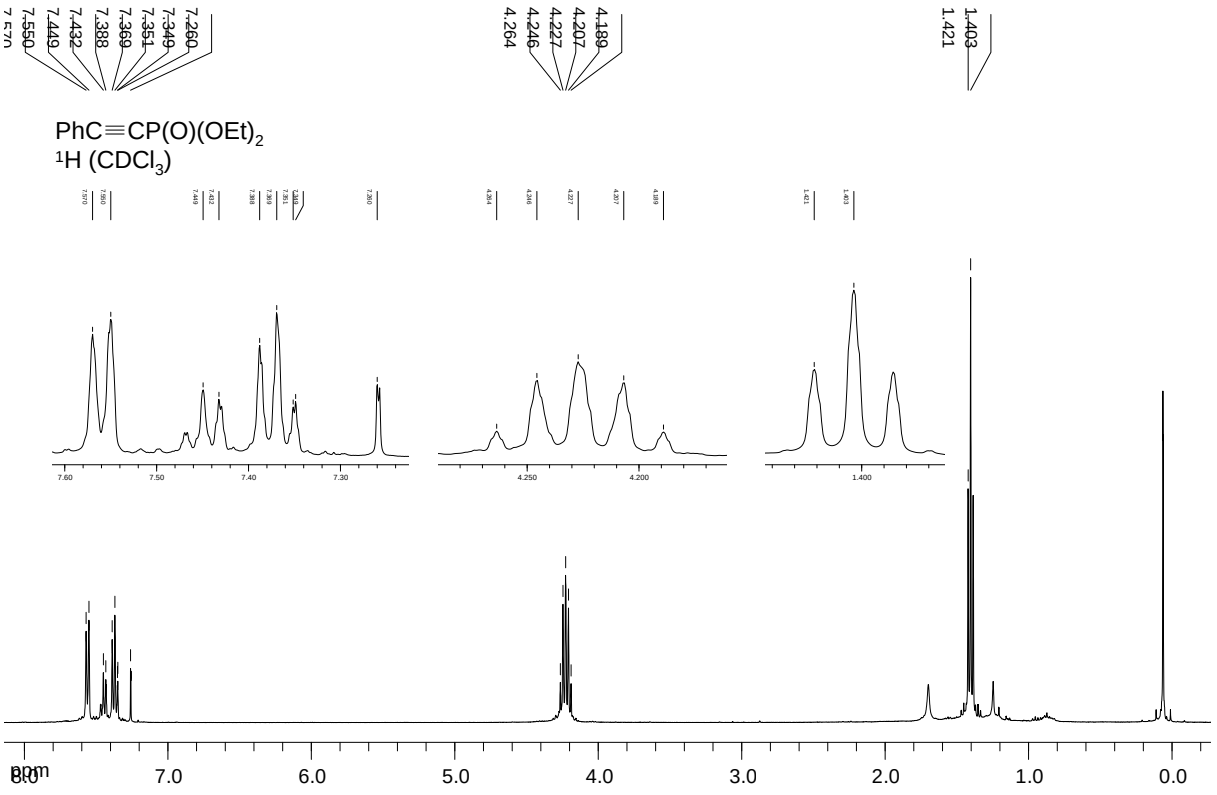

Figure S34 ^{1}H NMR spectrum of PhC≡CP(O)(OEt)$_2$ in $CDCl_3$ at 298K.

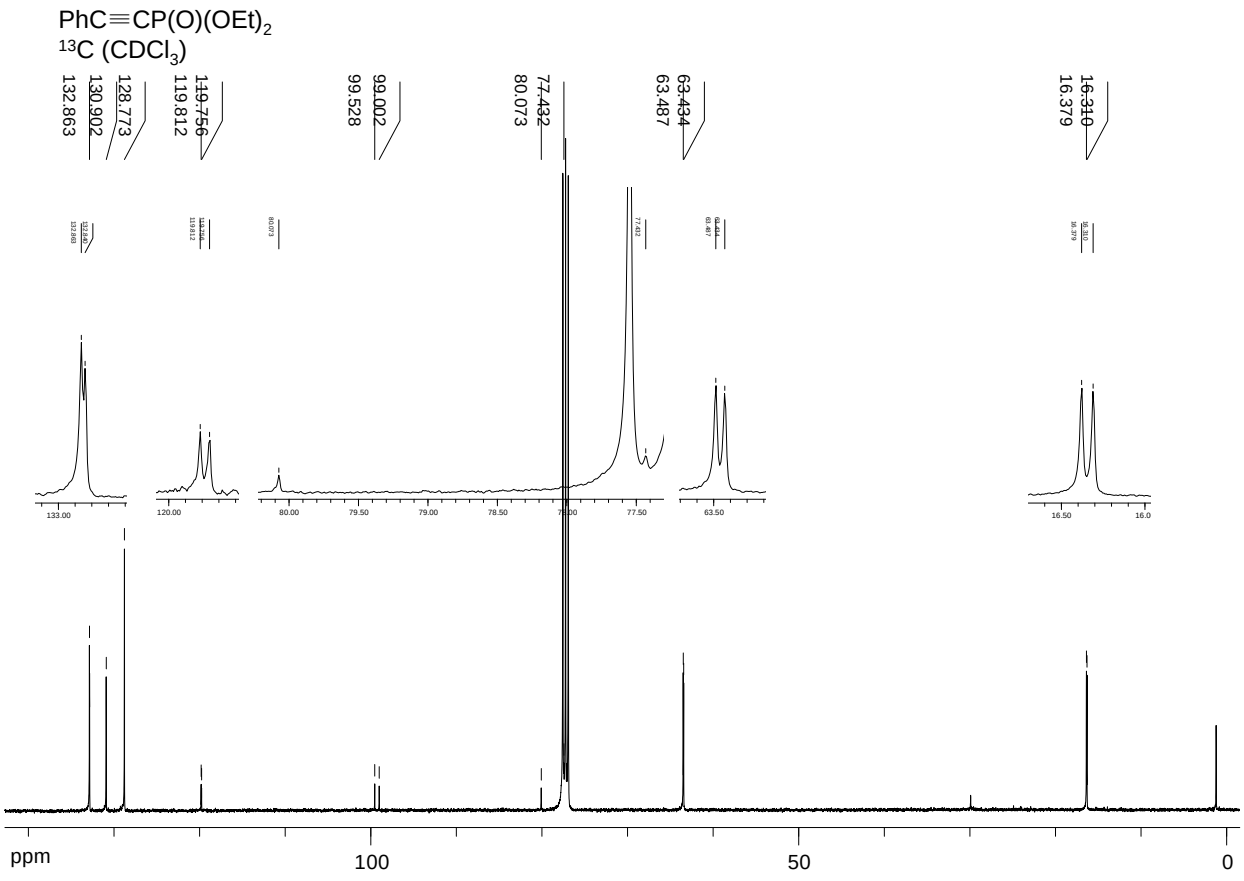

Figure S35 ^{13}C NMR spectrum of PhC≡CP(O)$(OEt)_2$ in $CDCl_3$ at 298K.

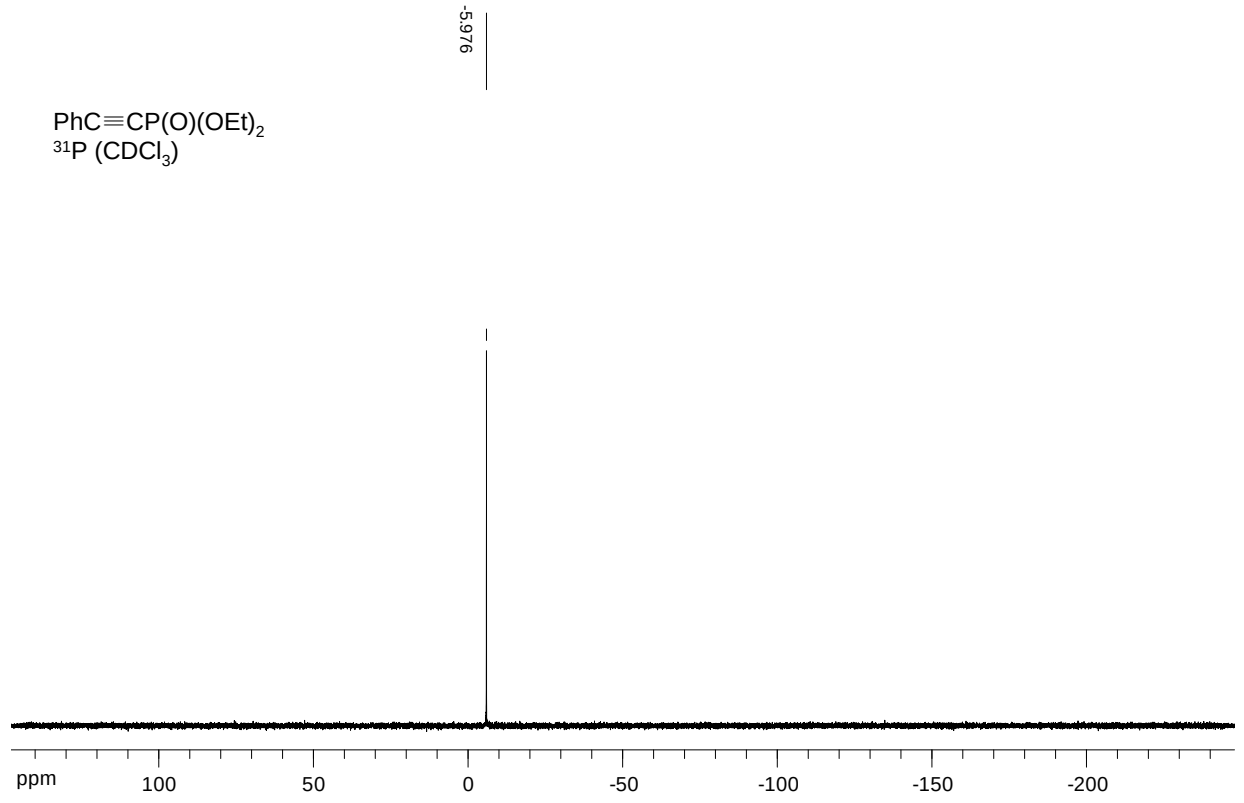

Figure S36 ^{31}P NMR spectrum of PhC≡CP(O)$(OEt)_2$ in $CDCl_3$ at 298K.

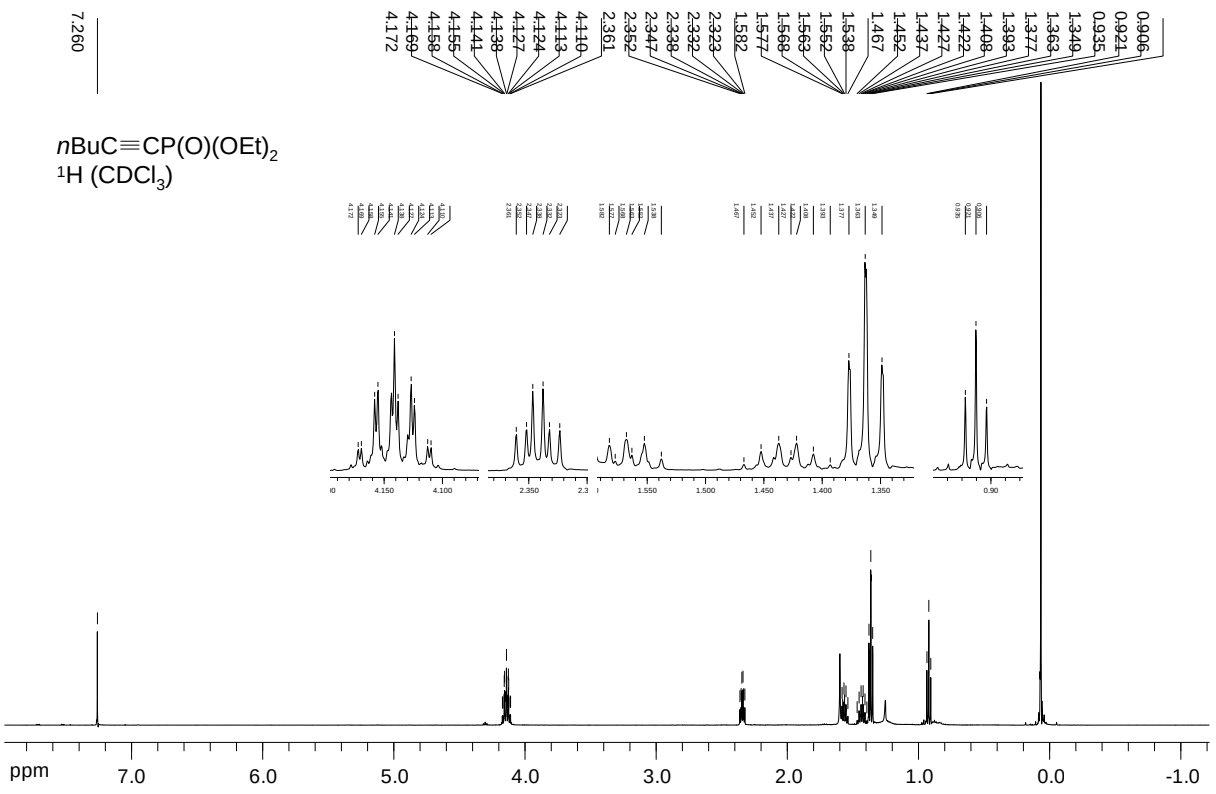

Figure S37 ^{1}H NMR spectrum of *n*BuC≡CP(O)(OEt)$_2$ in $CDCl_3$ at 298K.

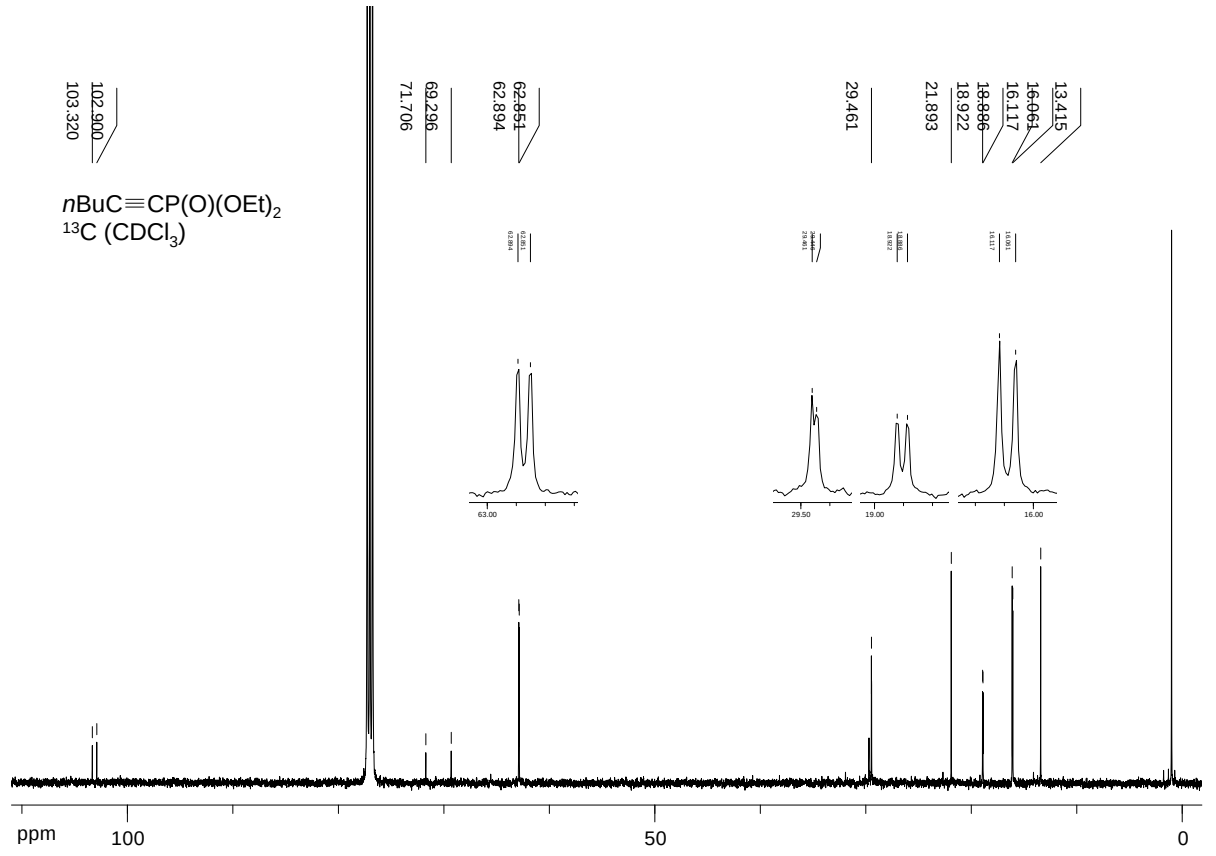

Figure S38 ^{13}C NMR spectrum of *n*BuC≡CP(O)(OEt)$_2$ in $CDCl_3$ at 298K.

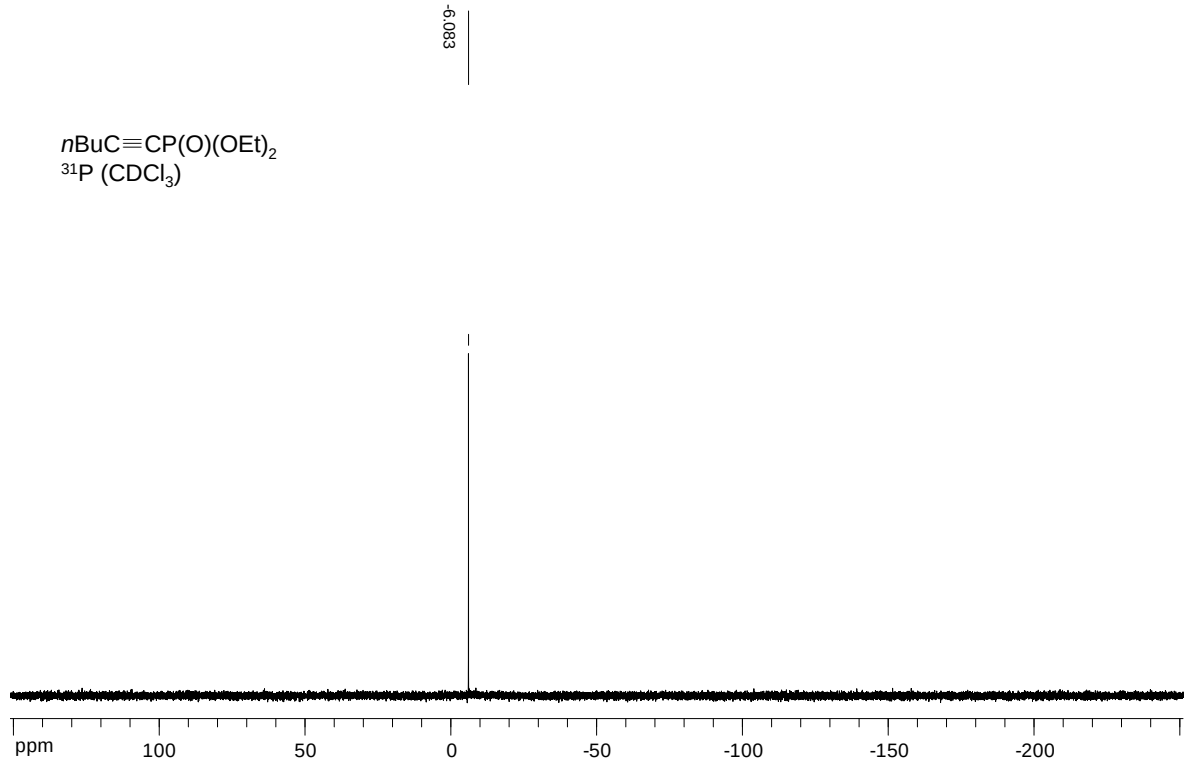

Figure S39 ^{31}P NMR spectrum of *n*BuC≡CP(O)(OEt)$_2$ in $CDCl_3$ at 298K.

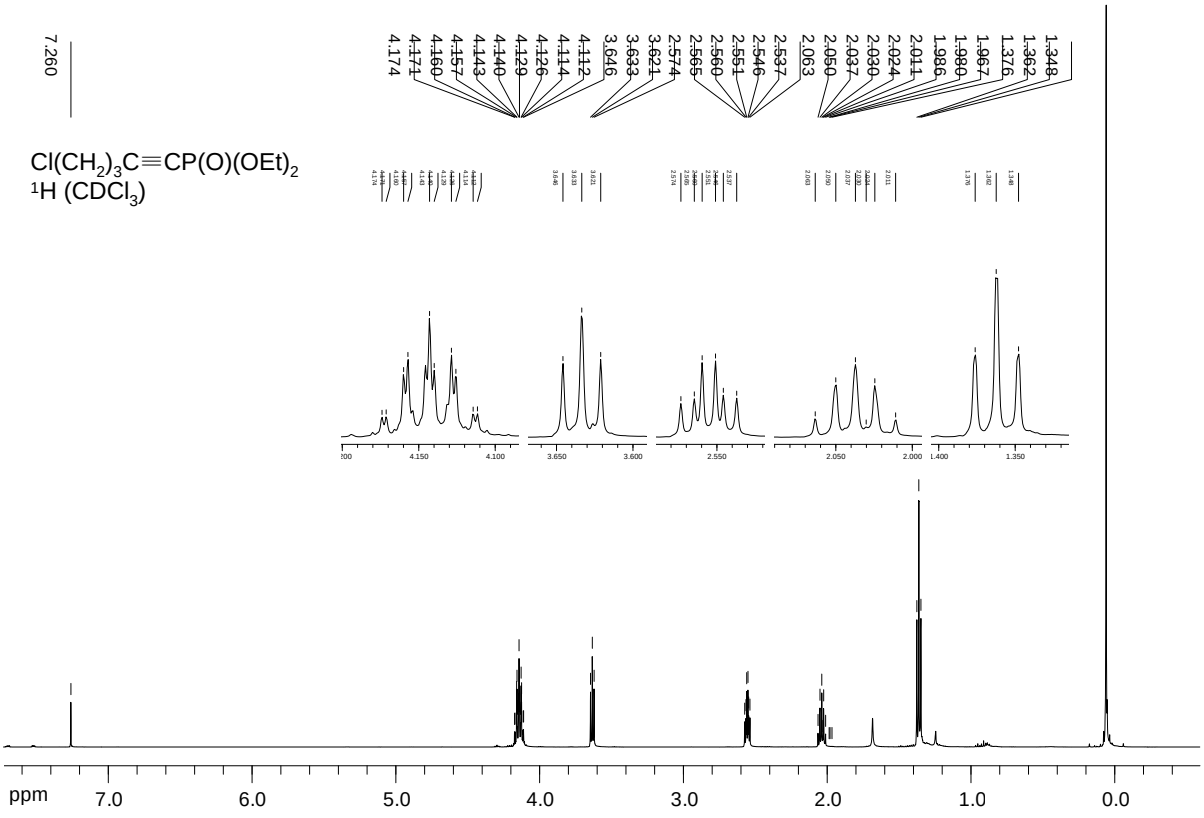

Figure S40 ^{1}H NMR spectrum of $Cl(CH_2)_3C{\equiv}CP(O)(OEt)_2$ in $CDCl_3$ at 298K.

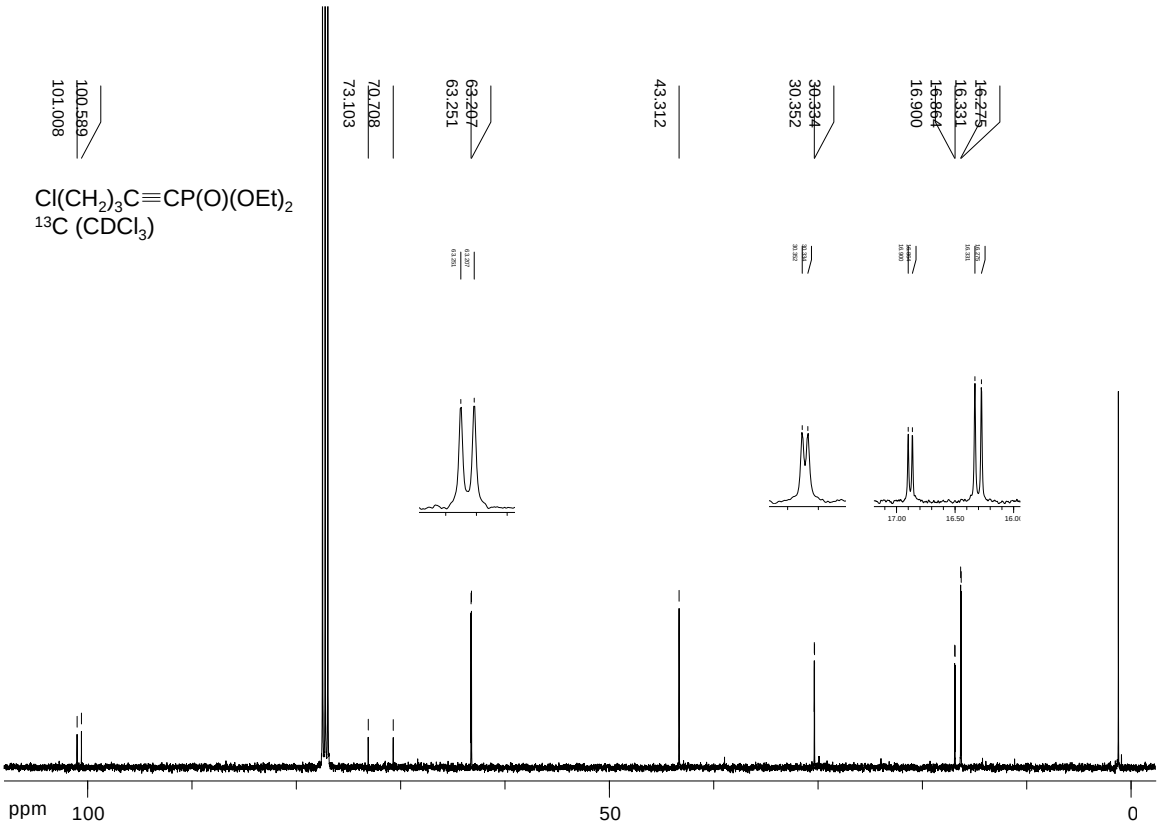

Figure S41 ^{13}C NMR spectrum of $Cl(CH_2)_3C{\equiv}CP(O)(OEt)_2$ in $CDCl_3$ at 298K.

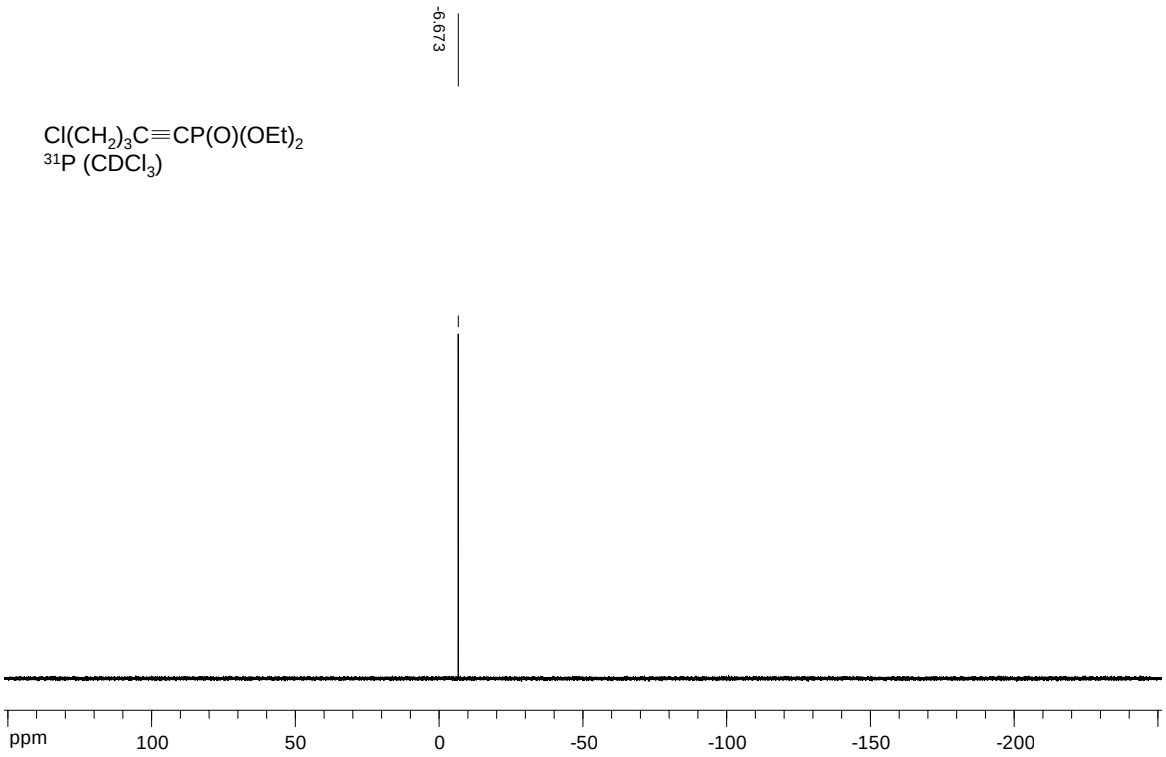

Figure S42 ^{31}P NMR spectrum of $Cl(CH_2)_3C{\equiv}CP(O)(OEt)_2$ in $CDCl_3$ at 298K.

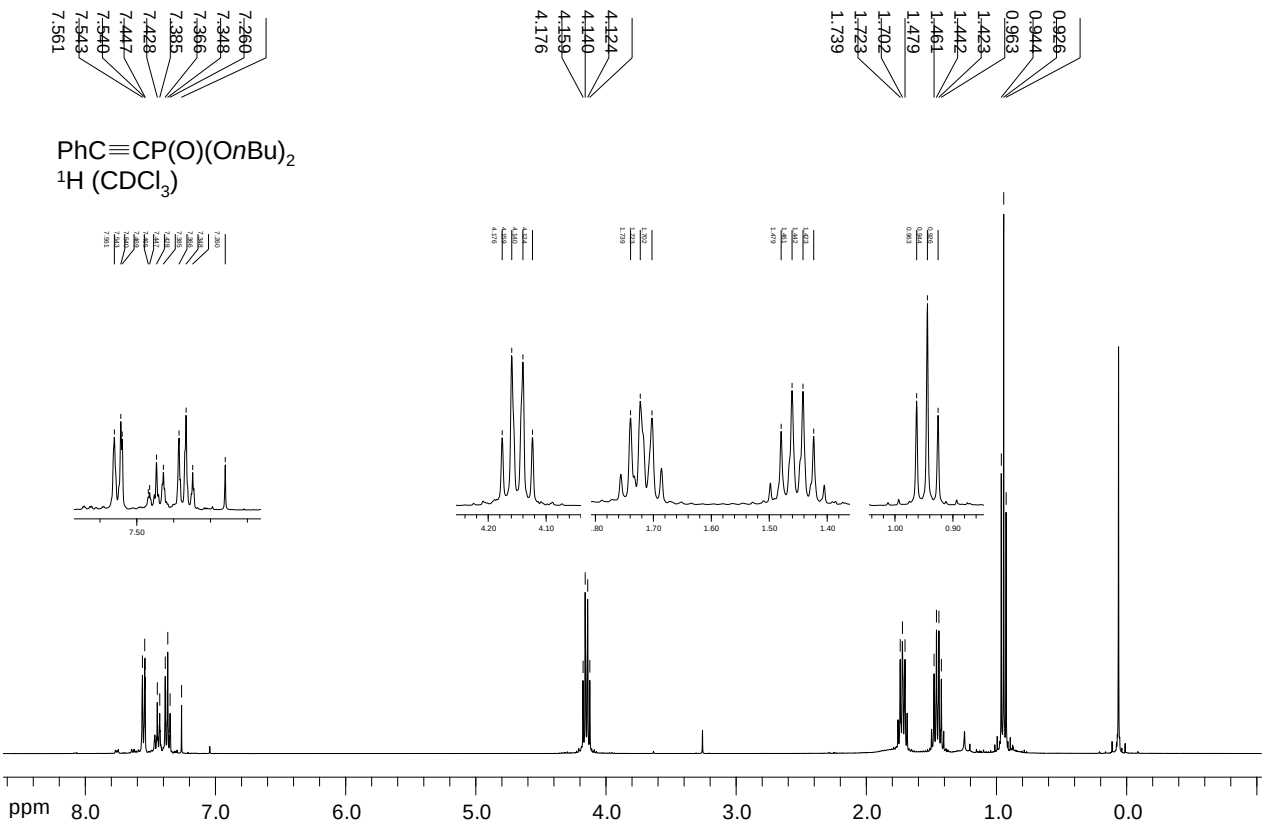

Figure S43 ^{1}H NMR spectrum of PhC≡CP(O)(O*n*Bu)$_2$ in $CDCl_3$ at 298K.

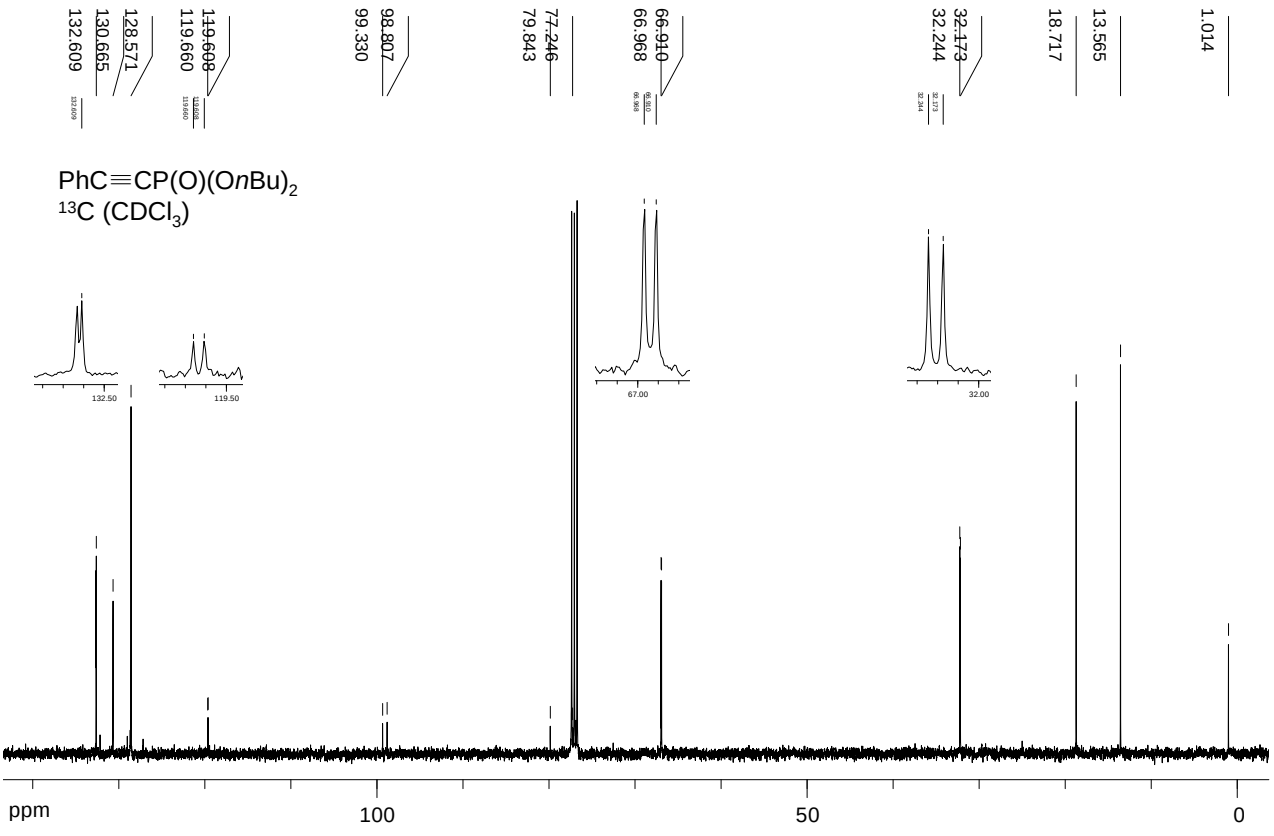

Figure S44 ^{13}C NMR spectrum of PhC≡CP(O)(O*n*Bu)$_2$ in $CDCl_3$ at 298K.

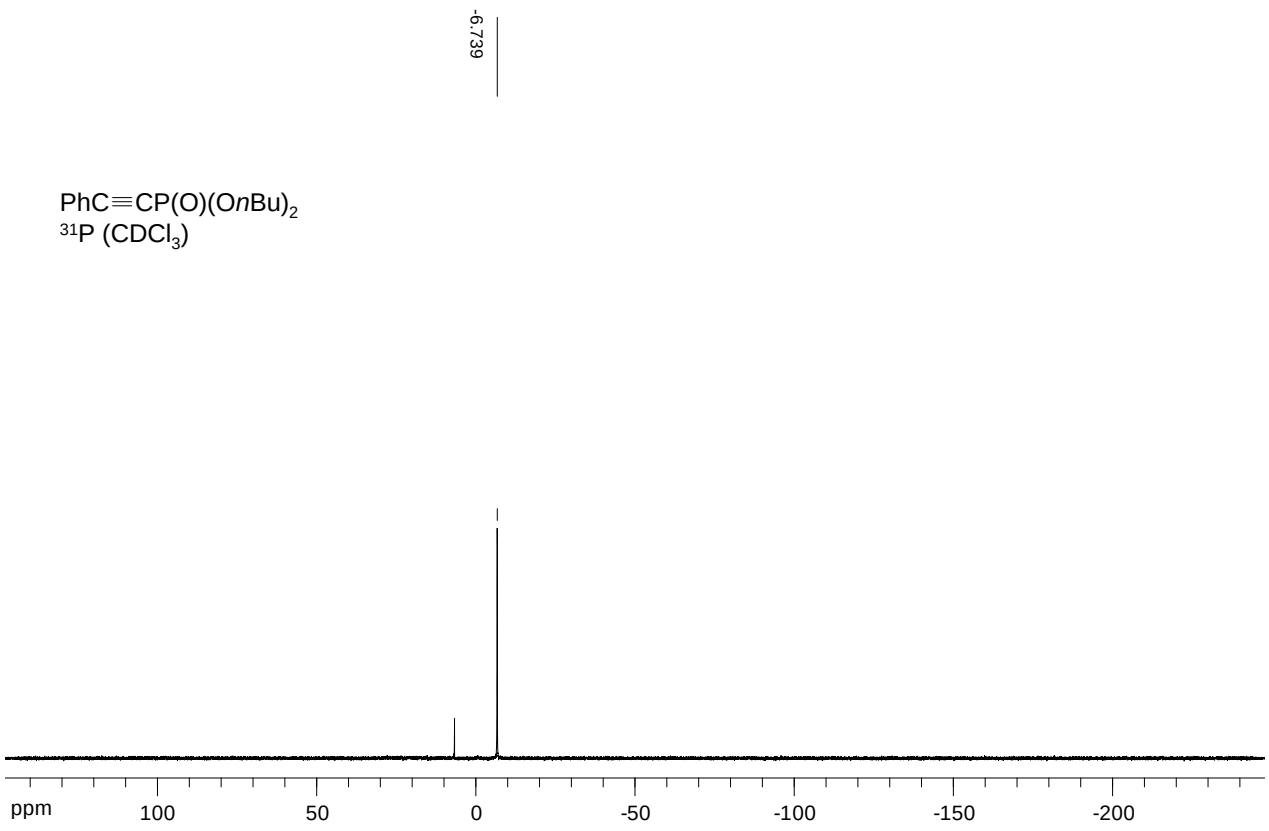

Figure S45 ^{31}P NMR spectrum of PhC≡CP(O)(O*n*Bu)$_2$ in $CDCl_3$ at 298K.

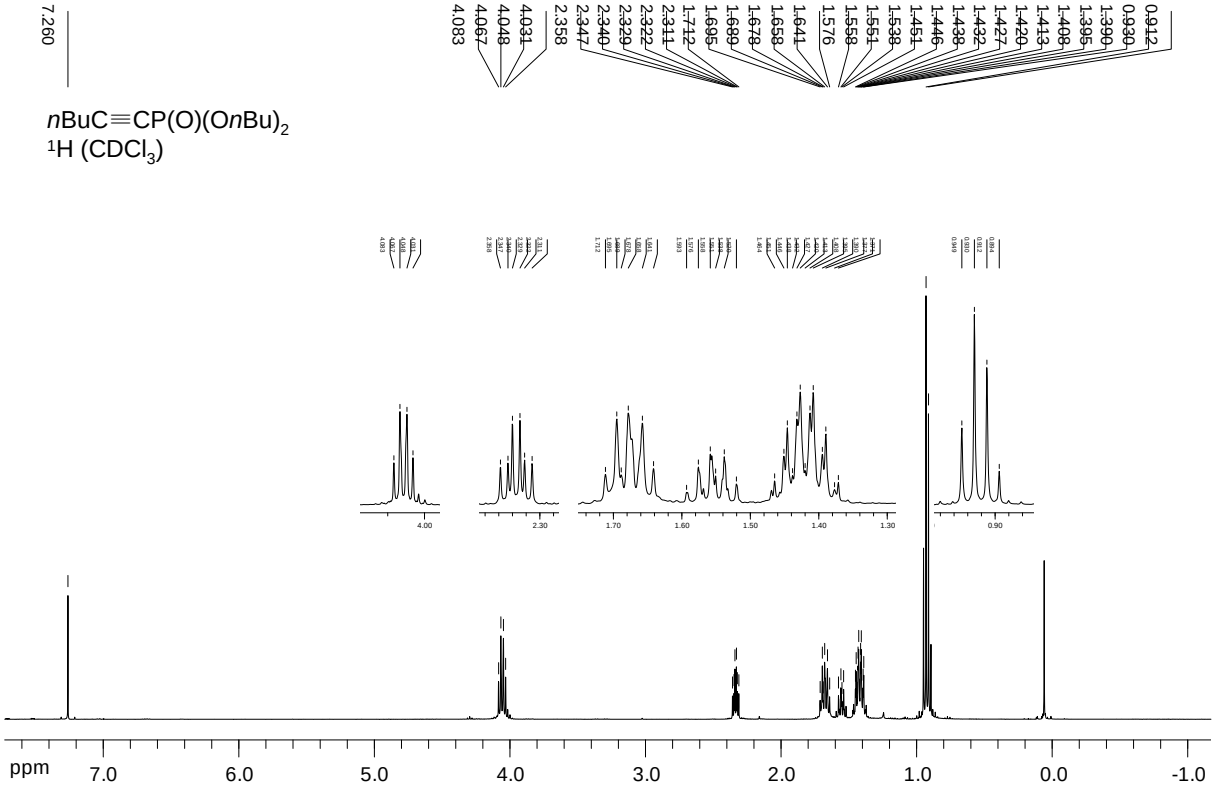

Figure S46 ^{1}H NMR spectrum of *n*BuC≡CP(O)(O*n*Bu)$_2$ in $CDCl_3$ at 298K.

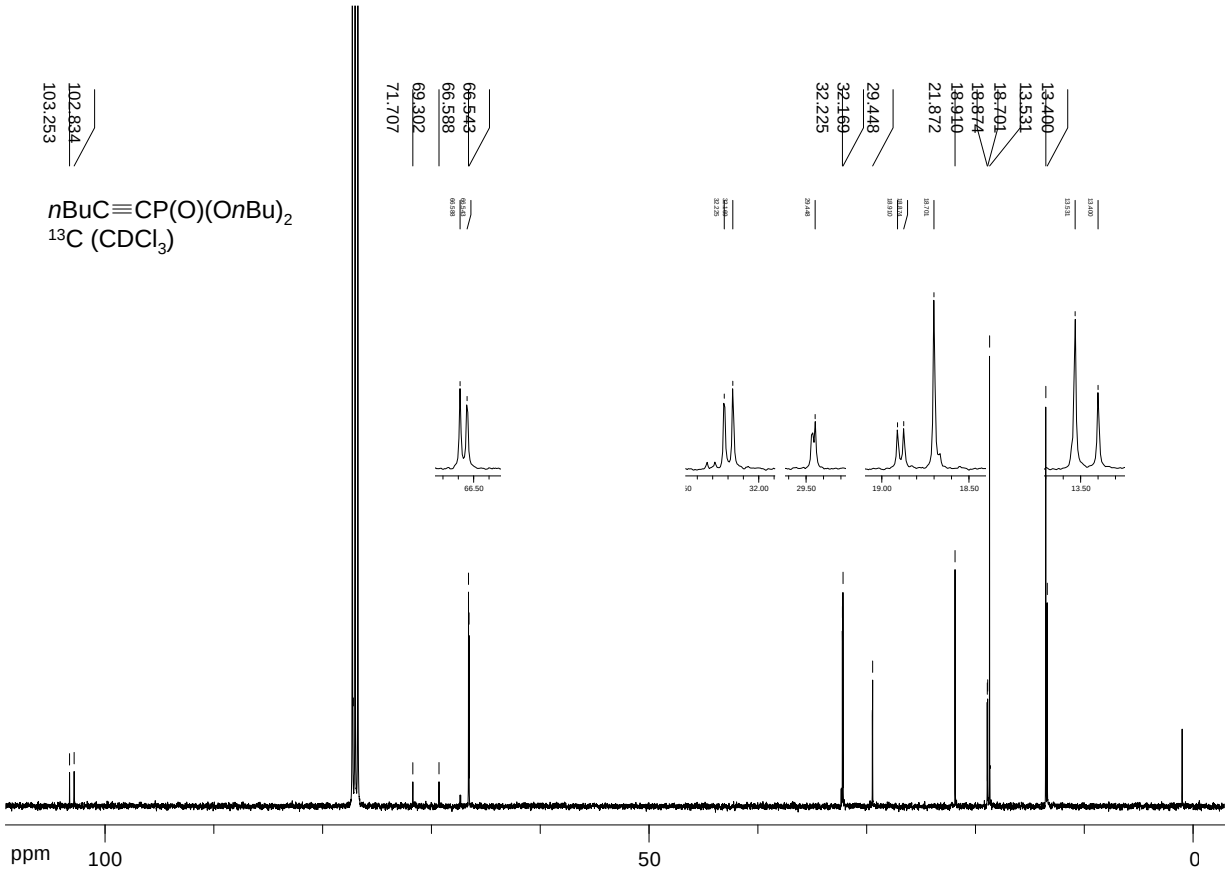

Figure S47 ^{13}C NMR spectrum of *n*BuC≡CP(O)(O*n*Bu)$_2$ in $CDCl_3$ at 298K.

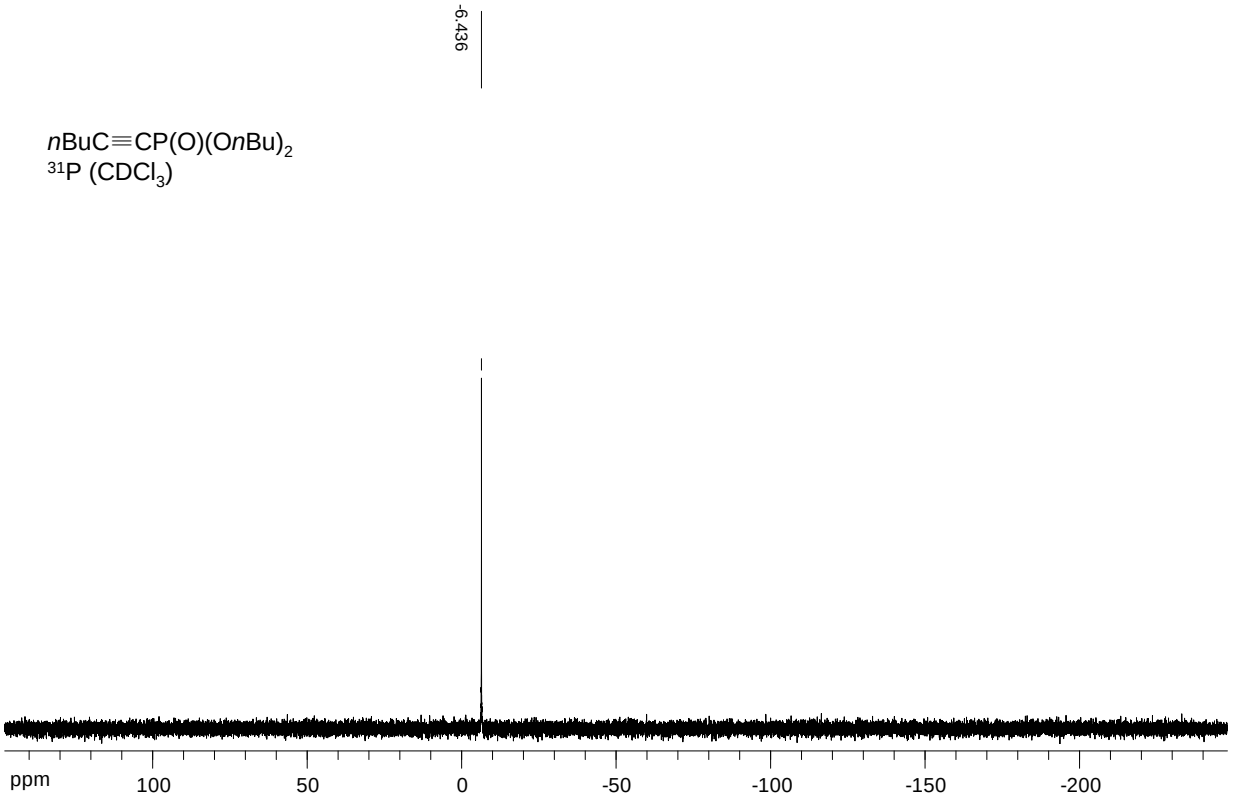

Figure S48 ^{31}P NMR spectrum of *n*BuC≡CP(O)(O*n*Bu)$_2$ in $CDCl_3$ at 298K.

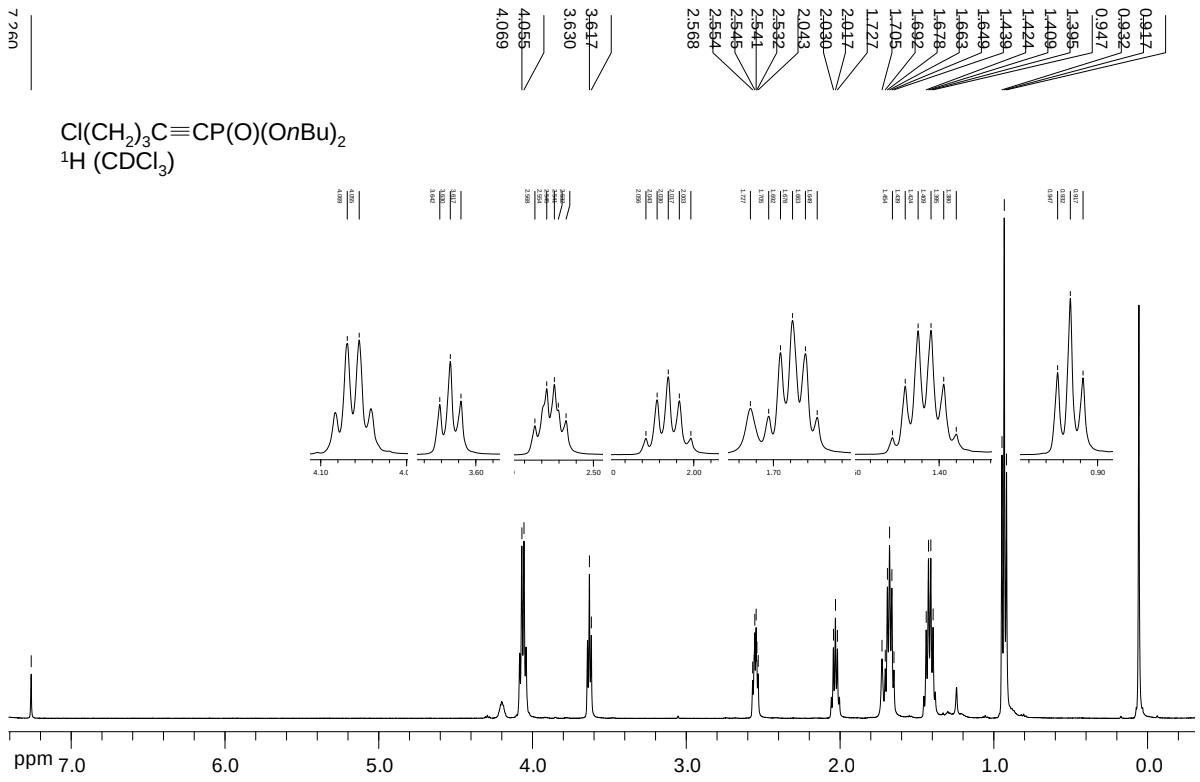

Figure S49 ^{1}H NMR spectrum of $Cl(CH_2)_3C{\equiv}CP(O)(O\mathit{n}Bu)_2$ in $CDCl_3$ at 298K.

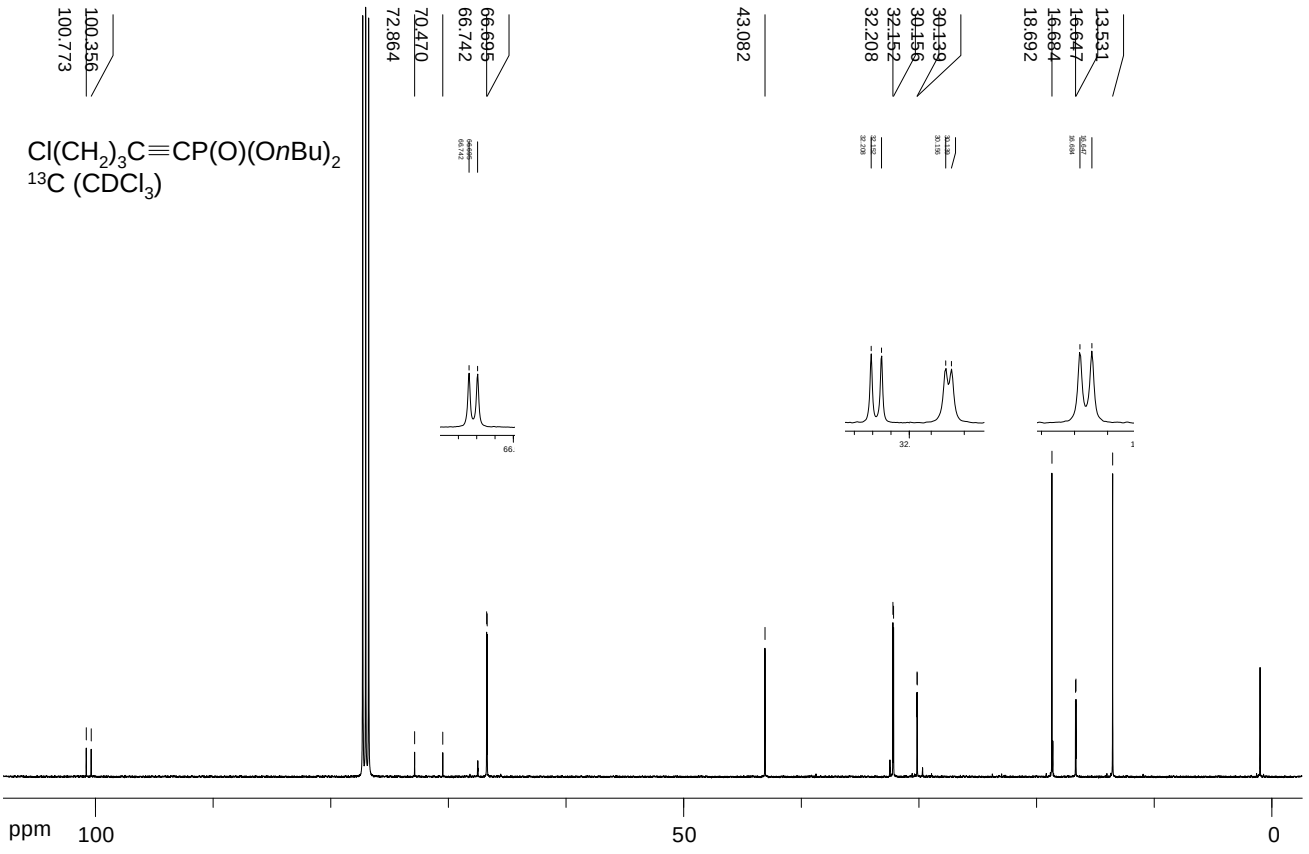

Figure S50 ^{13}C NMR spectrum of $Cl(CH_2)_3C{\equiv}CP(O)(O\mathit{n}Bu)_2$ in $CDCl_3$ at 298K.

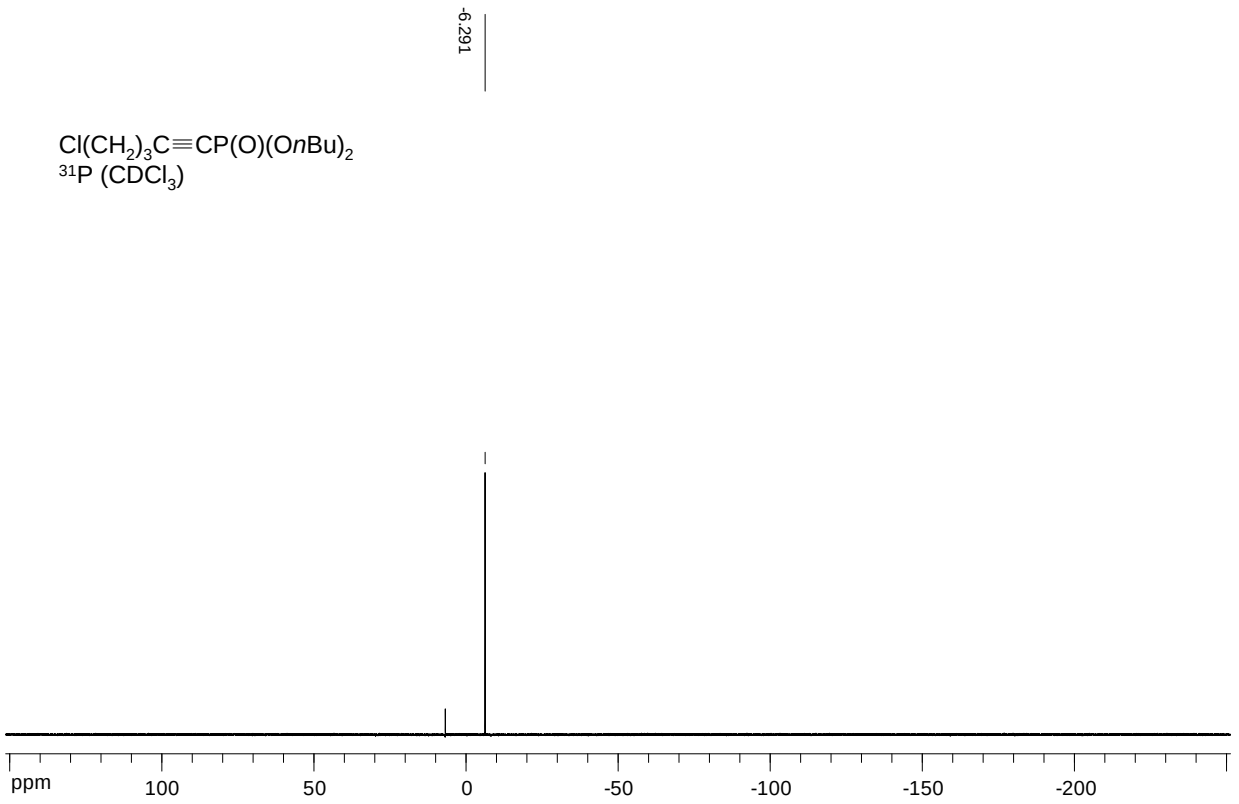

Figure S51 ^{31}P NMR spectrum of $Cl(CH_2)_3C{\equiv}CP(O)(O\textit{n}Bu)_2$ in $CDCl_3$ at 298K.

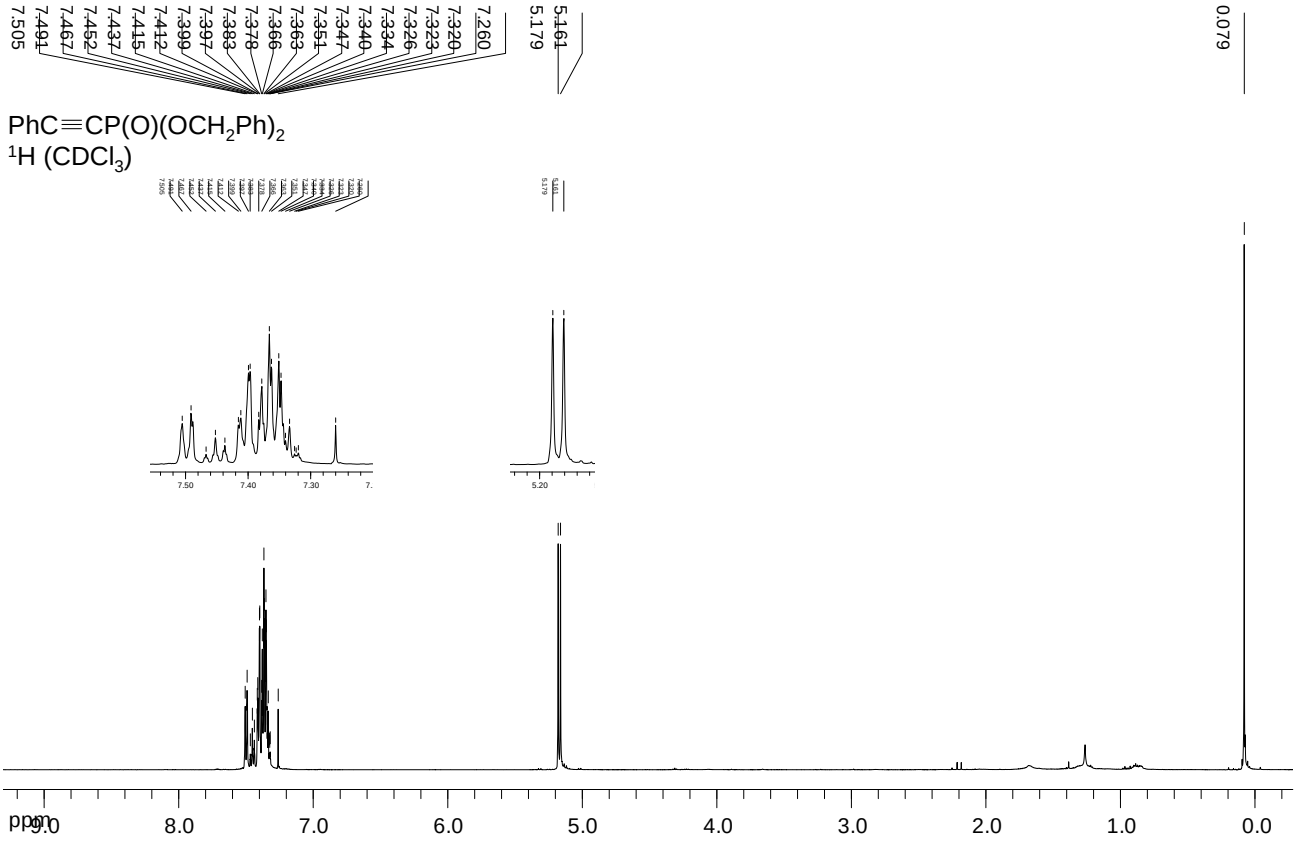

Figure S52 ^{1}H NMR spectrum of $PhC{\equiv}CP(O)(OCH_2Ph)_2$ in $CDCl_3$ at 298K.

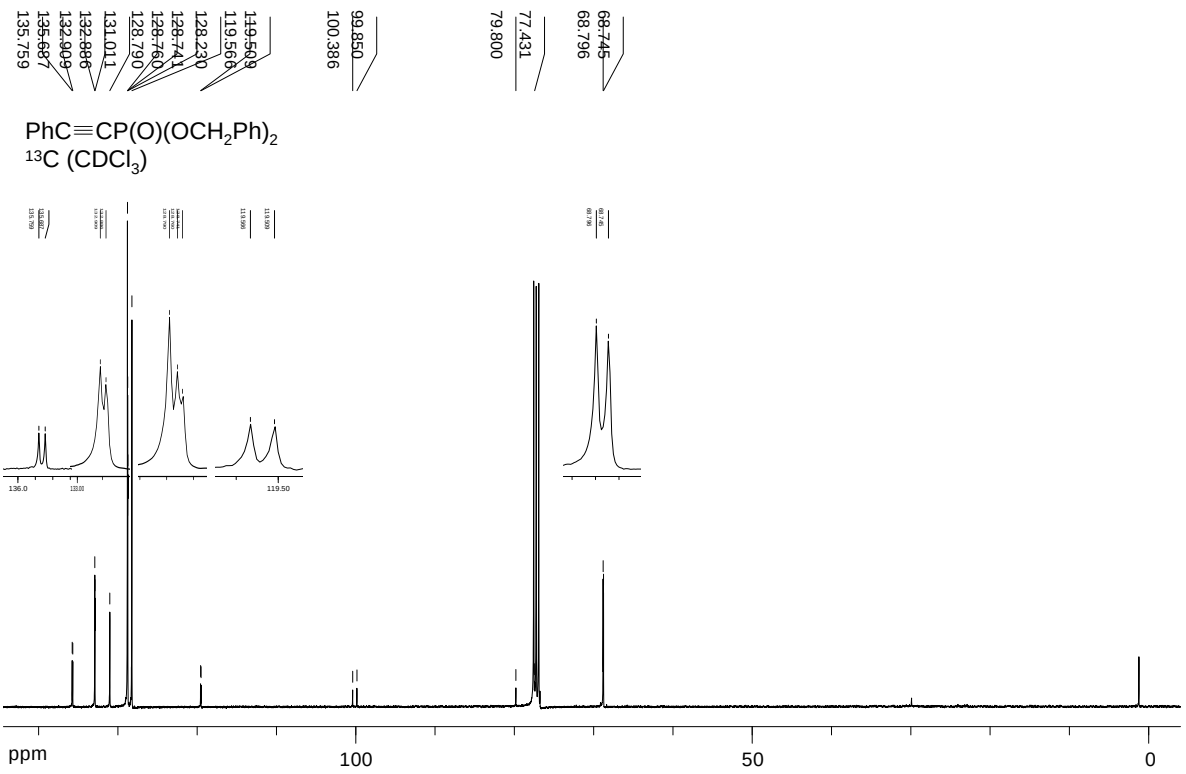

Figure S53 ^{13}C NMR spectrum of PhC≡CP(O)$(OCH_2Ph)_2$ in $CDCl_3$ at 298K.

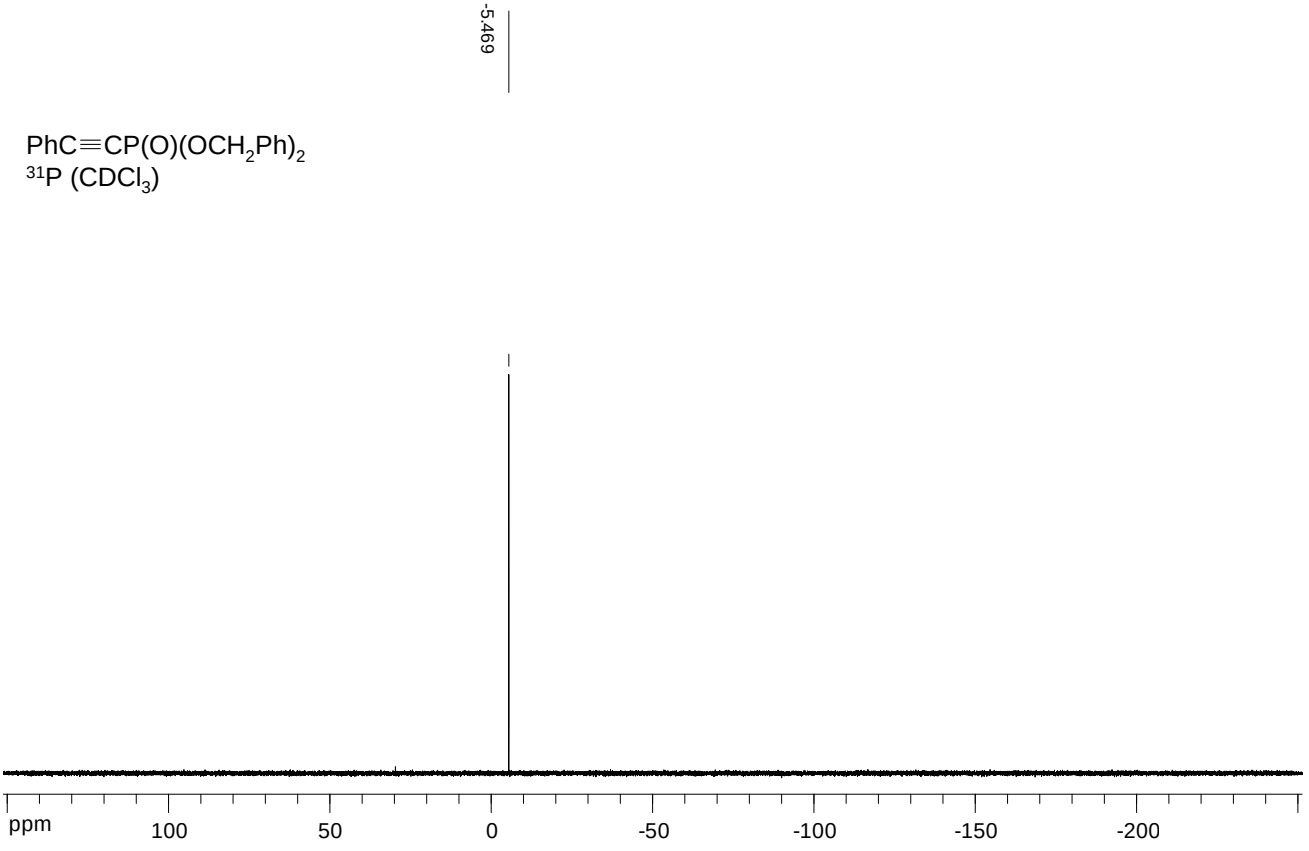

Figure S54 ^{31}P NMR spectrum of PhC≡CP(O)$(OCH_2Ph)_2$ in $CDCl_3$ at 298K.

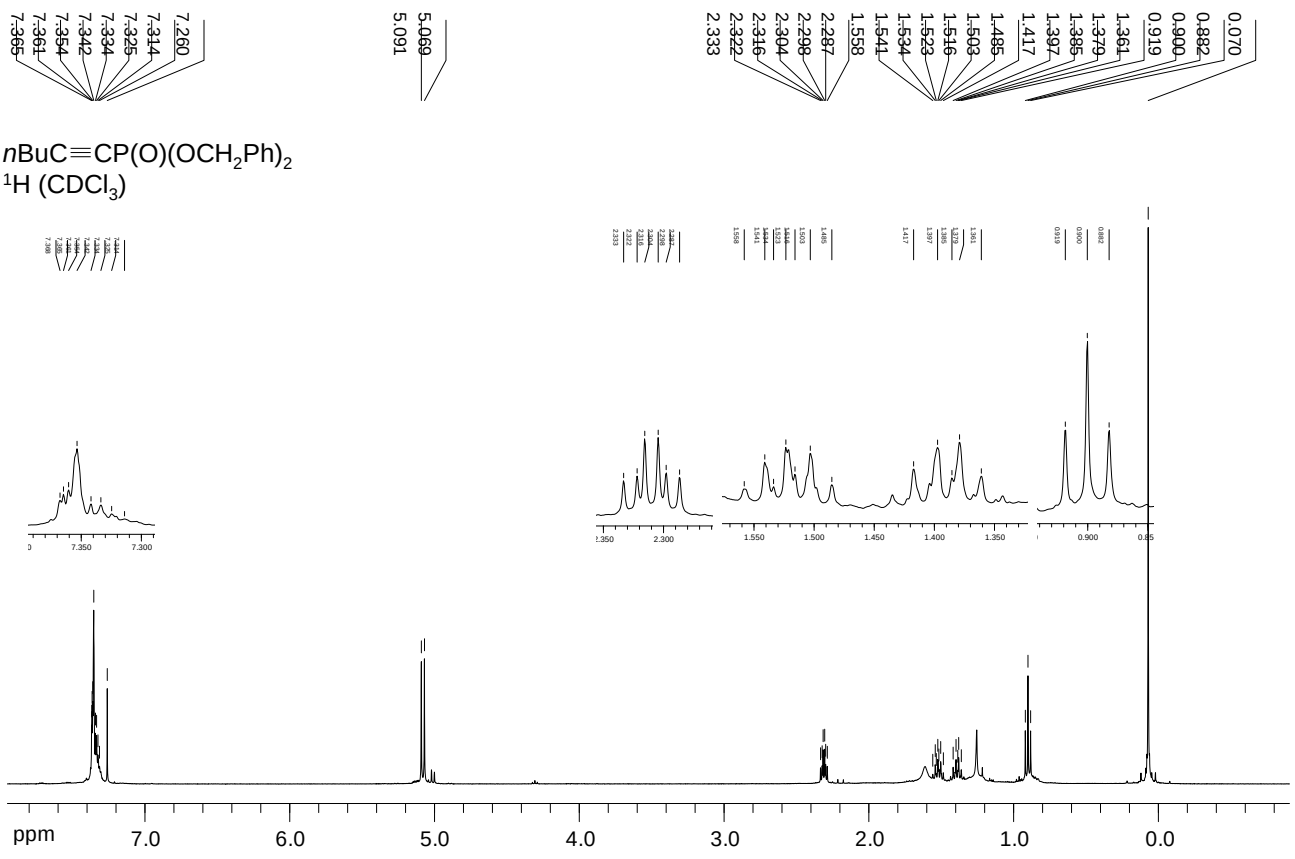

Figure S55 ^{1}H NMR spectrum of *n*BuC≡CP(O)(OCH$_2$Ph)$_2$ in CDCl$_3$ at 298K.

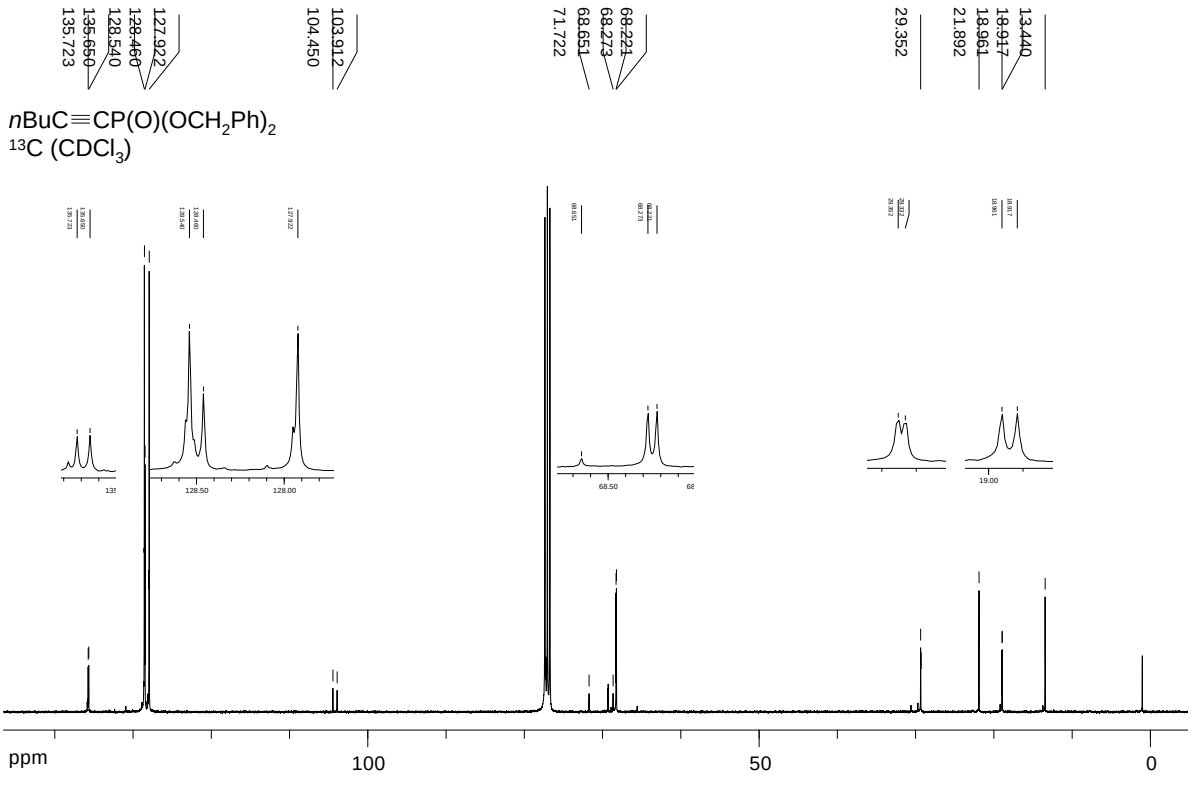

Figure S56 ^{13}C NMR spectrum of *n*BuC≡CP(O)(OCH$_2$Ph)$_2$ in CDCl$_3$ at 298K.

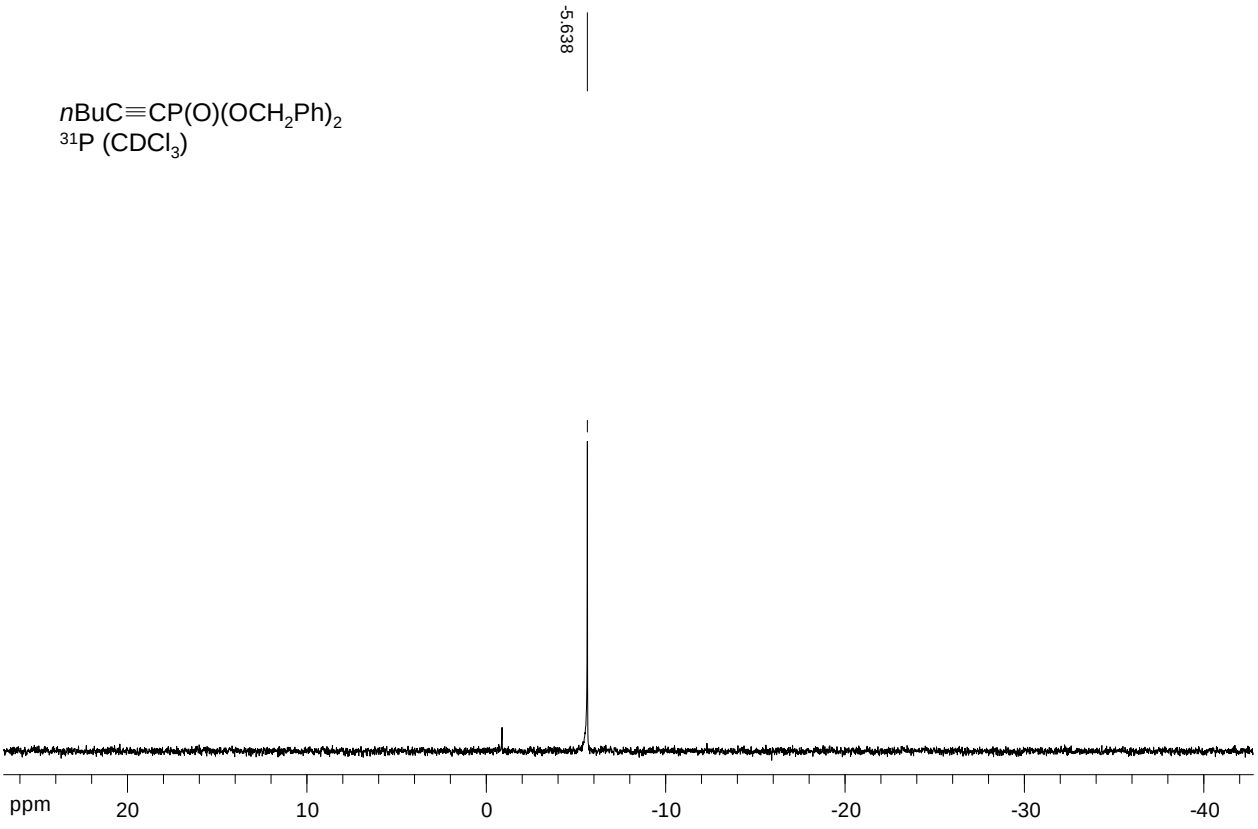

Figure S57 ^{31}P NMR spectrum of *n*BuC≡CP(O)(OCH$_2$Ph)$_2$ in CDCl$_3$ at 298K.

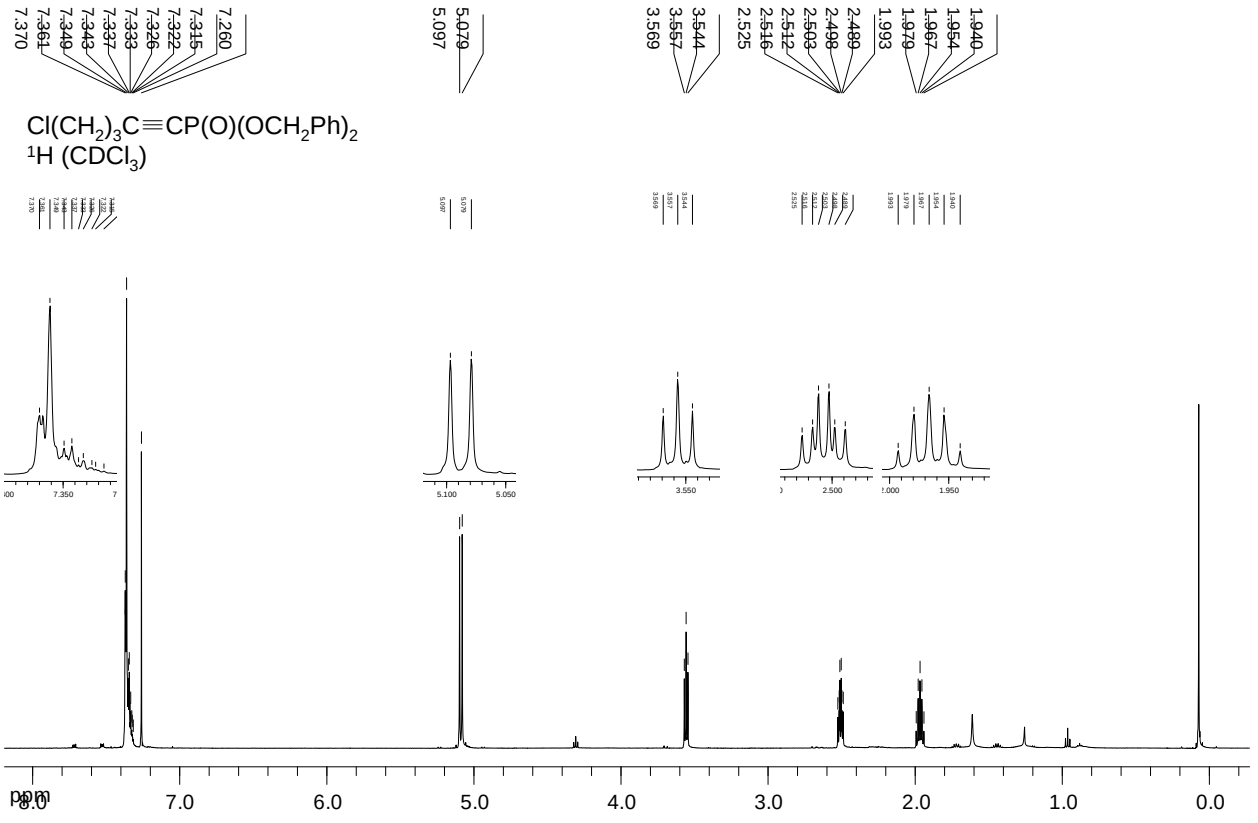

Figure S58 ^{1}H NMR spectrum of Cl(CH$_2$)$_3$C≡CP(O)(OCH$_2$Ph)$_2$ in CDCl$_3$ at 298K.

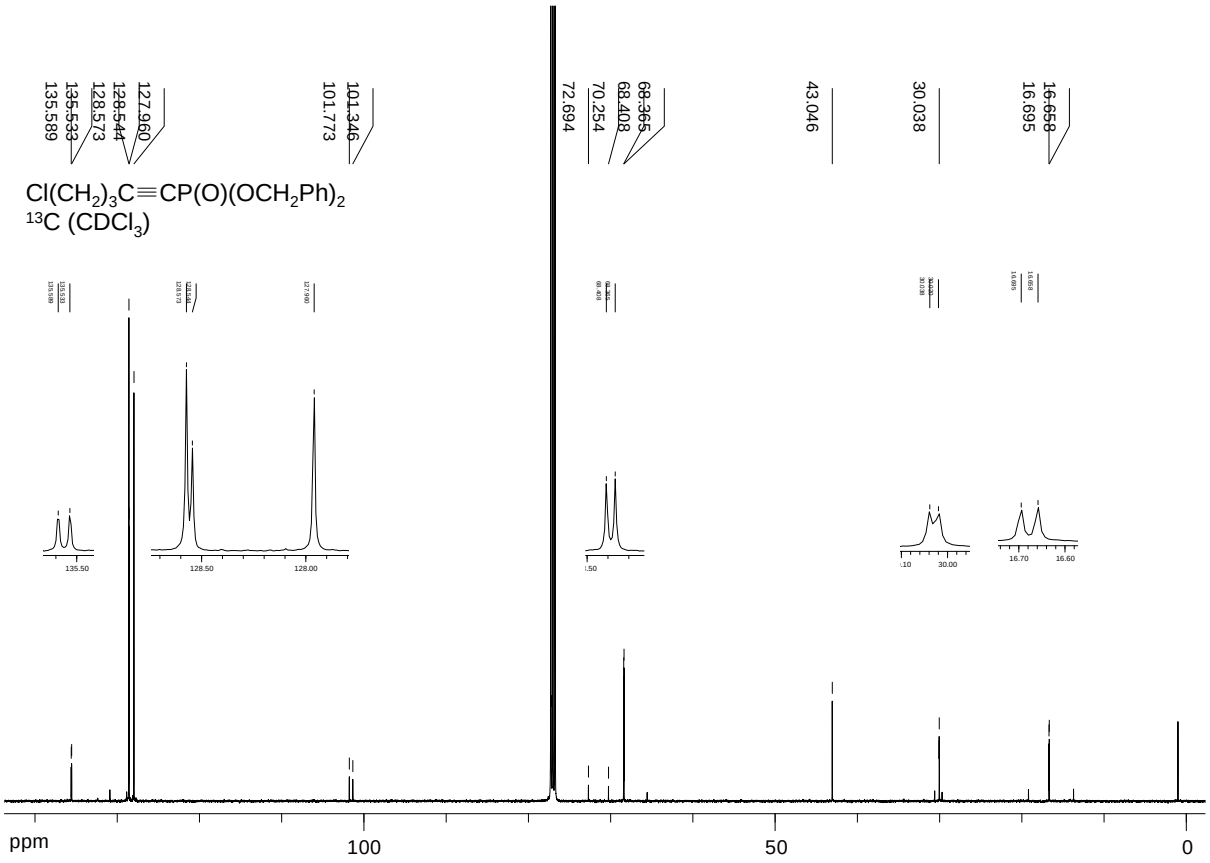

Figure S59 ^{13}C NMR spectrum of $Cl(CH_2)_3C{\equiv}CP(O)(OCH_2Ph)_2$ in $CDCl_3$ at 298K.

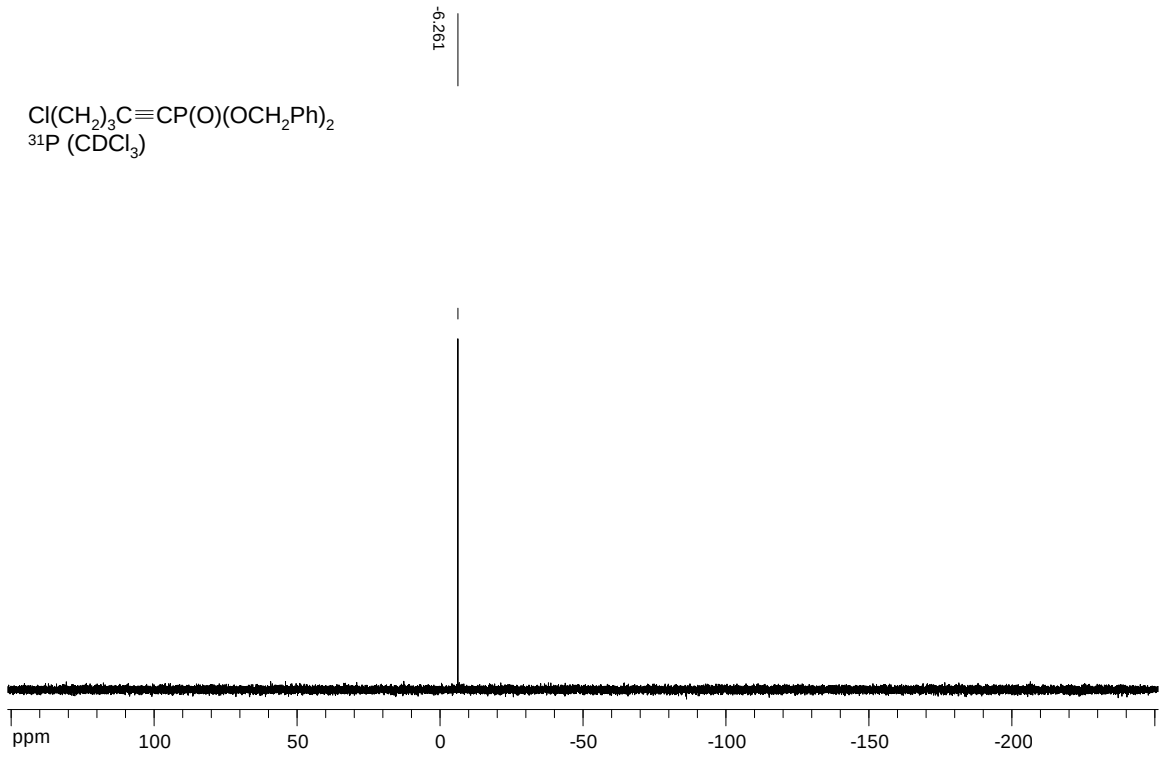

Figure S60 ^{31}P NMR spectrum of $Cl(CH_2)_3C{\equiv}CP(O)(OCH_2Ph)_2$ in $CDCl_3$ at 298K.